UNIVERSITÀ DEGLI STUDI DI PADOVA

SAFE OPERATIONAL BANDWIDTH OF GAS STORAGE RESERVOIRS
WP5 - WP6 REPORT

Pietro Teatini
Claudia Zoccarato
Massimiliano Ferronato
Andrea Franceschini
Matteo Frigo
Giovanni Isotton
Carlo Janna

Padova, January 2019

DIPARTIMENTO DI INGEGNERIA CIVILE, EDILE E AMBIENTALE - I C E A
DEPARTMENT OF CIVIL, ENVIRONMENTAL AND ARCHITECTURAL ENGINEERING

Contents

1. Introduction

The project “Safe operational bandwidth of gas storage reservoirs” is aimed at investigating the geomechanical hazards and risks associated with gas storage in Underground Gas Storage (UGS) reservoirs. In particular, the aim of the research activities is to investigate how possible drivers of fault reactivation can combine in UGS to increase the hazard of (significant) seismic events and/or even induced "un-expected" (micro-) seismicity.

At the end of the project “Safe Operational Bandwidth of Gas Storage Reservoir”, Phase 1, it was realized that the assumption of sealing faults, i.e. the pressure change does not propagate from the reservoir blocks into the surrounding/intercepting faults, represents a worst case in relation to the possibility of fault activation.

The present Phase 2 of the research aims to relax this assumption, investigating which are the mechanisms and the critical factors that are responsible for fault activation during the various stages of UGS when a part of the pore pressure change occurring in the reservoirs is simultaneously experienced by the fault too.

The report summarizes the activities and the results obtained in WP5 and WP6. WP5 presents the outcomes obtained with geomechanical code M3E_GEPS3D to test the effect of the pressure change propagation from the reservoir blocks into the faults. The model is applied to the "reference case" defined in WP3. At the same time, the properties of the salt caprock layer, in particular its thickness and stiffness, have been updated to represent in more resemblance the setting typical of the UGS reservoirs in The Netherlands. Moreover, the reference case has been used to evaluate the possibility of computing the criticality index $\chi = \tau/\tau_L$, which represents the ratio between actual tangential stress τ acting on a fault and the limit tangential stress τ_L according with the Mohr-Coulomb criterion, on the grid elements rather than on the nodes. It is to recall that when χ=1.0 the fault starts sliding. Notice that stress regime on the faults are computed at the node level.

The scenarios investigated in WP3 have been re-evaluated in WP6 taking into account the pressure change within the faults and the updated features of the salt caprock. A few more combined mechanisms have been investigated as required by the request to offer “Extra work on the generic study on safe operational bandwidth of gas storage reservoirs”.

The report is organised as follows. In Section 2 we briefly introduce the model implementation to account for pressure changes within the faults and summarize the outcomes related to the so-called “reference” test case (Scenario 1 in our "Technical and economical proposal, Phase 2"). Section 3 presents the results obtained through a sensitivity analysis carried out with the reference and varying a single (geometric, geomechanical, stress regime) parameter at a time (Scenarios 2 to 7 in our "Technical and economical proposal, Phase 2"). Mechanisms 4 and 5 (Scenarios 8 and 9) and combination scenarios (Scenarios 10 to 14) are discussed in Section 4.

Finally, notice that P refers to a pressure value and ΔP to pressure change throughout WP6 and WP7. This choice partially differs from the convention used in WP3, but allows avoiding possible misunderstandings.

2. Propagation of pressure change into faults

The simulations carried out in WP3 were run under the assumption that the faults are impermeable, i.e. the faults hold their initial fluid pressure while the adjacent reservoir depletes. Under this assumption, faults get lubricated as the high initial pressures of reservoir are maintained in the fault. Therefore, the WP3 model results display worst-case scenarios: the original (high) pressure is maintained in the faults that then load them easily to a critical failure state.

In this Phase 2, a more realistic assumption is considered for the fluid pressures in the faults to better signify the role of other model parameters on the safe operational bandwidth. Specifically, the faults experience a pore pressure change ΔPf that varies according to reservoir compartments so that, if different ΔP1 and ΔP2 pressure changes develop at the opposite sides of fault, then ΔPf = 0.5·(ΔP1 + ΔP2).

The implementation in M3E_GEPS3D of the fault Interface Element (IE) approximation has been updated to account for ΔPf $\neq 0$.

2.1 Model implementation

Using the total stress formulation, the equilibrium equation can be written as (Gambolati et al., 2001):

$$\int_{\Omega} \varepsilon^T \hat{\sigma} dV = \int_{\Sigma} u^T \hat{t} dS$$

where $\hat{\sigma}$ and ϵ are the symmetric total stress and deformation tensor in Voigt notation, respectively, u and $\hat{t}$ the displacement and traction force, respectively, Ω is the 3D domain and Σ its 2D boundary (Garipov et al., 2016). In this case, the 2D boundary contains also the fault surfaces. Using Terzaghi's principle, it can be written:

$$\hat{\sigma} = \sigma - i\alpha p \qquad \hat{t} = t - np$$

where α is the Biot coefficient, σ the effective stress tensor in Voigt notation, *p* the pore pressure, *i* = $[1; 1; 1; 0; 0; 0]^T$ the vectorial form of the Kronecker delta, *t* the effective traction, and *n* the outward vector normal to Σ.

Substituting Terzaghi's principle into the equilibrium equation, we obtain:

$$\int_{\Omega} \varepsilon^T (\sigma - i\alpha p) dV = \int_{\Sigma} u^T (t - np) dS$$

i.e.:

$$\int_{\Omega} \varepsilon^T \sigma dV = \int_{\Omega} \varepsilon^T i\alpha p dV + \int_{\Sigma} u^T t dS - \int_{\Sigma} u^T np dS \qquad (1)$$

Note that in $\int_{\Sigma} u^T np dS$, *p* is the pressure acting on the 2D boundary, i.e. the faults in the case of interest. Whenever we are working with an equilibrated reference state and quantity variations, σ

represents the effective stress change, and *p* must be substituted with ΔPf, i.e. the pressure change acting within the fault.

Considering a 3D computational grid of n_e elements (tetrahedra are used in the following for simplicity) such that $\Omega = \bigcup_{i=1}^{n_e} \Omega_i^e$, with Ω_i^e nonoverlapping tetrahedral elements of order 1, the displacement shape function for a finite element Ω_i^e reads:

$$N_u = \begin{bmatrix} \xi_1 & 0 & 0 & \xi_2 & 0 & 0 & \xi_3 & 0 & 0 & \xi_4 & 0 & 0 \\ 0 & \xi_1 & 0 & 0 & \xi_2 & 0 & 0 & \xi_3 & 0 & 0 & \xi_4 & 0 \\ 0 & 0 & \xi_1 & 0 & 0 & \xi_2 & 0 & 0 & \xi_3 & 0 & 0 & \xi_4 \end{bmatrix}$$

Using piece-wise constant pressure, the shape function is simply:

$$N_p = [1]$$

Using the symbol $\bar{\blacksquare}$ to indicate the nodal values, the displacement u inside the finite element and the pressure *p* on its surface (i.e. the fault) read:

$$u = N_u \bar{u} \qquad p = N_p \bar{p}$$

Using these relationships, the last term of the integral expression (1) becomes:

$$\int_\Sigma u^T n p dS = \bar{u}^T \left(\int_\Sigma N_u^T n N_p dS \right) \bar{p} \tag{2}$$

Developing the integral term in (2) with the selected interpolation functions, results:

$$\int_\Sigma N_u^T n N_p dS = \int_\Sigma \begin{bmatrix} \xi_1 n \\ \xi_2 n \\ \xi_3 n \\ \xi_4 n \end{bmatrix} dS$$

where every term $\xi_i n$ is a 3×1 column matrix:

$$\xi_i n = \begin{bmatrix} \xi_i n_x \\ \xi_i n_y \\ \xi_i n_z \end{bmatrix}$$

Assuming that Σ is the face that does not contain node *j*, we have:

$$\int_\Sigma \xi_i dS = \begin{cases} \Sigma/3 & \text{if } \; i \neq j \\ 0 & \text{if } \; i = j \end{cases}$$

where Σ also represents the areal measure of this face. In the case *j* = 4, the integral is:

$$\int_{\Sigma} N_u^T n N_p dS = \frac{\Sigma}{3}\begin{bmatrix} n_x \\ n_y \\ n_z \\ n_x \\ n_y \\ n_z \\ n_x \\ n_y \\ n_z \\ 0 \\ 0 \\ 0 \end{bmatrix}$$

Therefore, the forcing term reads (Figure 1):

$$f = \int_{\Sigma} N_u^T n N_p dS \bar{p} = \frac{\Sigma \bar{p}}{3}\begin{bmatrix} n_x \\ n_y \\ n_z \\ n_x \\ n_y \\ n_z \\ n_x \\ n_y \\ n_z \\ 0 \\ 0 \\ 0 \end{bmatrix}$$

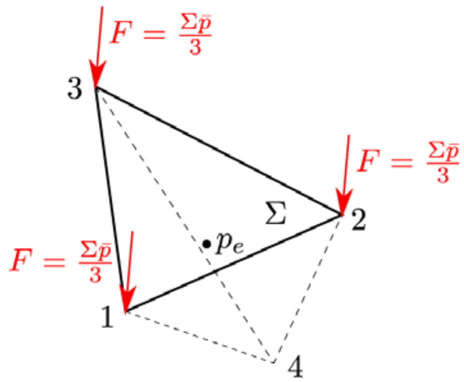

Figure 1 Distribution of forces on a triangular face **Σ**. p_e is the pressure inside the finite element. Whenever we are working with an equilibrated reference state and quantity variations p_e must be substituted with Δp_e and $\bar{\boldsymbol{p}}$ with $\Delta\bar{\boldsymbol{p}}$.

2.2 Testing the model on the reference case (Scenario 1)

A first set of simulations has been carried out with the reference case. The analysis is mainly aimed at investigating the effect on the possible fault activation of the two updates implemented in Phase 2, i.e.:

1. each fault experiences a pore pressure change ΔPf that is the average of the pressure variation within the two portions of the domain facing the discontinuity;

2. the Zechstein formation is stiffer than the reservoir. In particular, E = 20 GPa below -1800 m depth and E = 33 GPa for the depth range from -1500 m and -1800 m.

All the other parameters remain unchanged, see Section 2.3, WP3 Report.

Moreover, a critical review of the Phase 1 outcome has suggested the use of a criticality index χ evaluated at the grid element level. Indeed, in a number of scenarios it was obtained that only the fault nodes located in correspondence of the top/bottom of reservoir were activated. This is due to the abrupt change of the pore pressure that sharply decreases within the reservoir and keeps the initial value within the caprock. This generates an infinite pressure gradient, and consequently a shear stress concentration, that is unphysical as in nature the pressure variation penetrates to a certain extent into the caprock. Working at the element level, which means averaging the values at the nodes forming an element, reduces this effect without the need of vertically refining the mesh discretization in proximity of the reservoir/caprock bound. Therefore, we believe the post-processing of the model outcome along this line provides a more realistic evaluation of the likely occurrence of fault reactivation.

Based on the above considerations, the following sub-scenarios have been run to analyse in-depth the effects of the implemented variations:

1a) $E_{Zechstein}$ = 10 GPa and no pressure change within the faults, i.e. $\Delta Pf = 0$. This corresponds to the WP3 "reference" and allows us to highlight the effect of the χ evaluation at the element level;

1b) $E_{Zechstein}$ = 10 GPa and the actual pressure change ΔPf within the faults as defined above;

1c) $E_{Zechstein}$ = 20 GPa / 35 GPa and no pressure change within the faults, i.e. $\Delta Pf = 0$;

1d) $E_{Zechstein}$ = 20 GPa / 35 GPa and the actual pressure change ΔPf within the faults. This will represent the "reference" in the sensitivity that follows.

The same pressure history used in Phase 1 has been used in the Phase 2 analyses (Figure 2). A 10-year primary production with a pressure depletion of 200 bar is followed by a cushion gas injection phase lasting 2 years during which the initial pressure is recovered and one (or more) UGS cycle, with a 6-month production and a 6-month injection phases and a maximum pressure drops amounting to 100 bar.

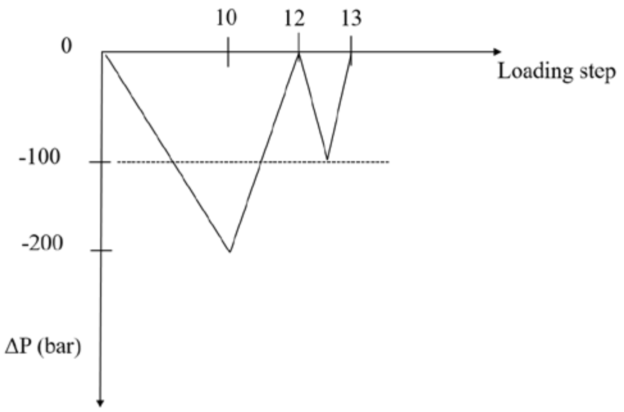

Figure 2 Pore pressure change ΔP in the reservoir compartments 1 and 2.

The modelling results are provided in the subsections that follow in terms of time behaviour of maximum criticality index χ_{max} and maximum sliding δ_{max}. Moreover, the 3D representations of the $|\tau|$ and χ at the end of primary production (l.s. = 10) and the values of t_a, t_{80}, and t_{50} (i.e., the fault thickness with χ = 1 (t_a), χ > 0.8 (t_{80}), and χ > 0.5 (t_{50})) are provided in Annex I and Annex II, respectively. Notice that χ distributions and values in both Annexes are the direct outcome of the geomechanical simulator, i.e. refer to a node-based computation. Therefore, they cannot be straightforward compared with the element-based χ_{max} pictures shown in the main text of the report. Moreover, the stress path $|\tau|$ vs the effective normal stress σ acting on fault F2 has been provided for node 2665 (or node 1920 when an offset between the two reservoir blocks are accounted for). These nodes are located at the reservoir top (Figure 3), i.e. in the most critical condition concerning fault activation because of their shallowest depth and consequently smallest normal stress component.

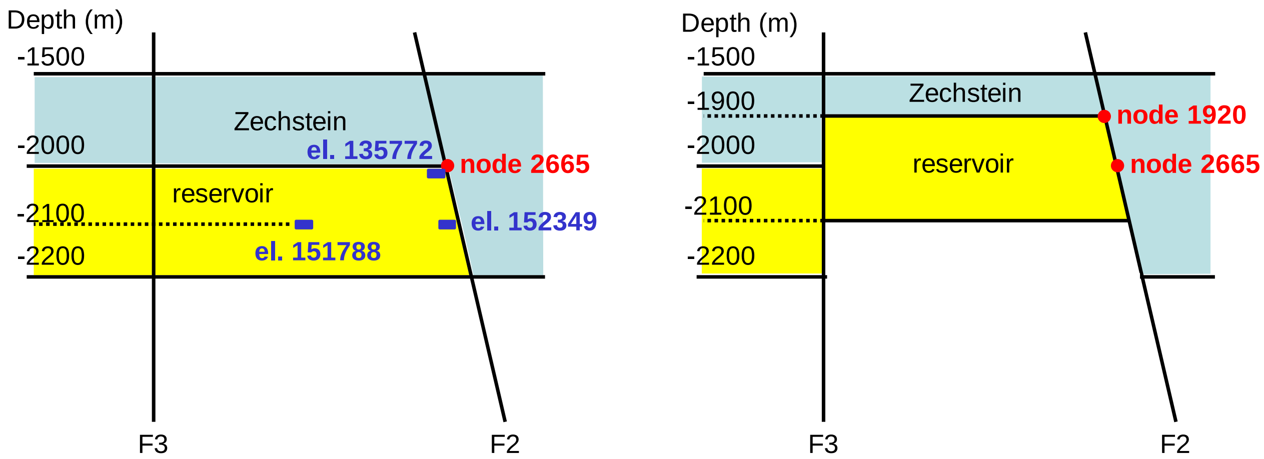

Figure 3 Location and number of nodes and elements used to represent the stress path without (left) and with (right) an offset of the two reservoir blocks.

Sub-scenario 1a

This is the reference case of the WP3 analyses. Figure 4 provides the behaviour vs time of χ_{max} for each of the F1 - F5 faults. The values obtained by post-processing the model outcomes on the nodes and elements of the IE discretization are compared. The node-based behaviour coincides with that provided by Figure 13 in the WP3 Report. The comparison clearly shows that the element-based analysis provides smaller χ values. The index approaches the critical value $\chi = 1.0$ only at the end of the primary production, with a maximum value equal to $\cong 0.9$. During UGS, $\chi_{max} < 0.6$, with the highest value at the end of the injection phase when P=Pi.

Figure 5 shows the stress path for node 2665 located on fault F2. The actual stress state touches the yield bound at loading step (l.s.) #6 and remains on the yield surface till the end of primary production (l.s. #10). During cushion gas, the stress state initially departs from the yield condition but returns close to it during the last part of the phase when the pressure recovers to the initial value. UGS behaves elastically over the path experienced during the last part of the CG phase.

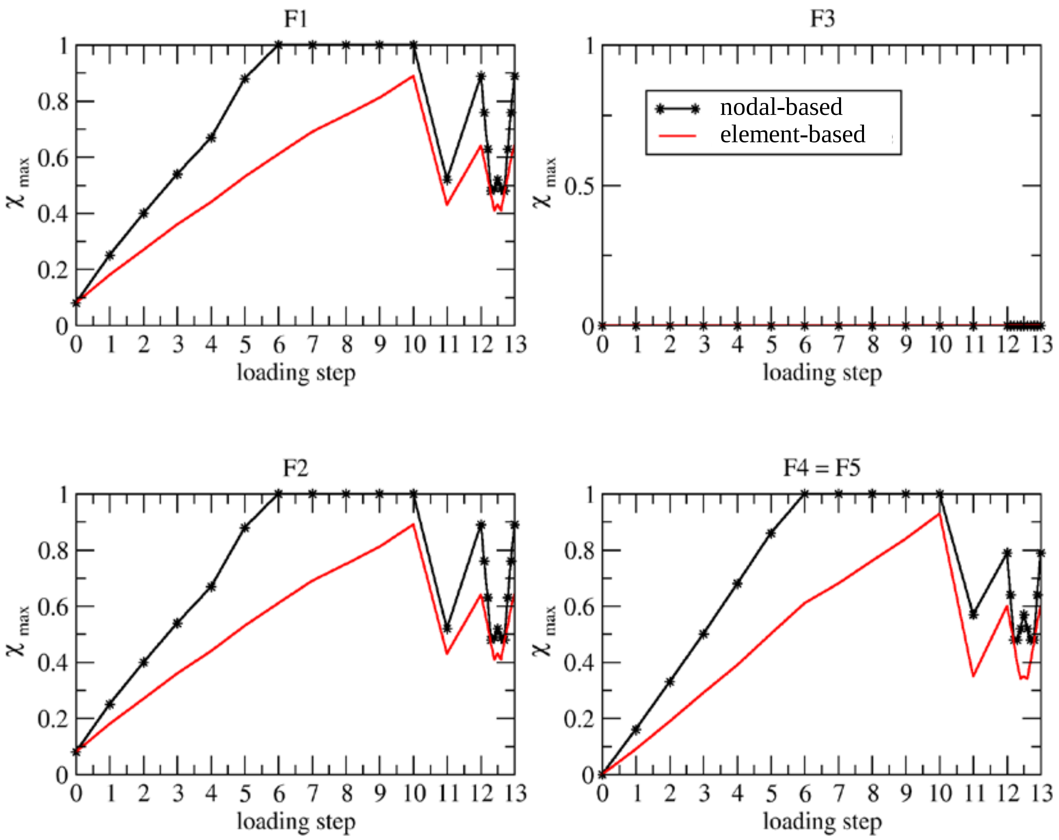

Figure 4 Sub-scenario 1a: comparison between the node-based and the element-based evaluation of χ_{max} at increasing loading steps for each fault. Note that due to symmetry F4 and F5 behave identically.

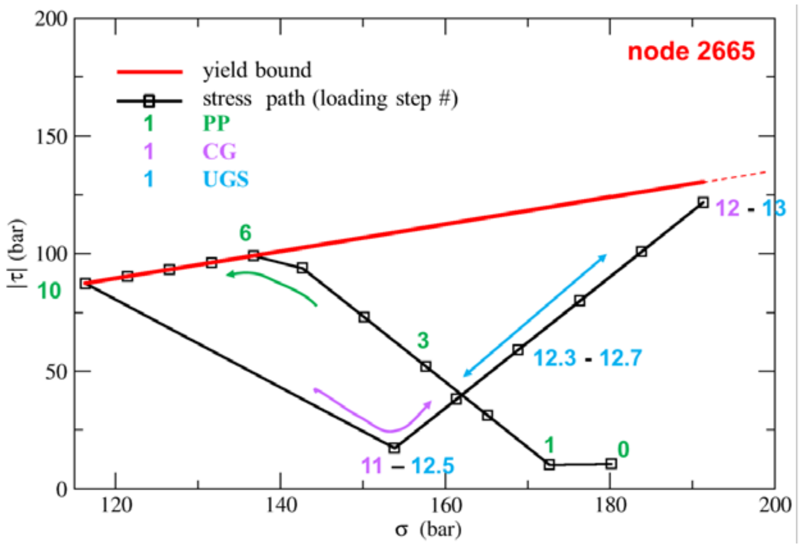

Figure 5 Sub-scenario 1a: stress path |τ| vs σ for the F2 fault node 2665. The red line represents the yield bound and the numbers the various loading steps. Different colours are used for primary production (PP, loading steps #1 – 10), cushion gas (CG, loading steps #11 – 12), and underground gas storage (UGS, loading steps #12.1 – 13).

Sub-scenario 1b

When a fault feels a portion of the pressure change within the reservoir, it results in a less critical condition then the case with ΔPf = 0. Indeed, the pressure decline within a fault acts as a stabilizing force normal to the discontinuity plane, thus contrasting the effect caused by the pressure decline within the reservoir compartments.

The results obtained by the FE-IE model are summarized in Figure 6. Comparison between Figure 4 and Figure 6 reveals that χ_{max} is always lower when ΔPf ≠ 0 (Figure 6). However, the difference between the two cases is relatively small.

Figure 7 shows the stress path for node 2665. The behavior is quite similar to that obtained in scenario 1a (Figure 5), with the main difference represented by a smaller decrease of the normal stress σ (~40 bar instead of ~70 bar) due to the pressure change within the fault.

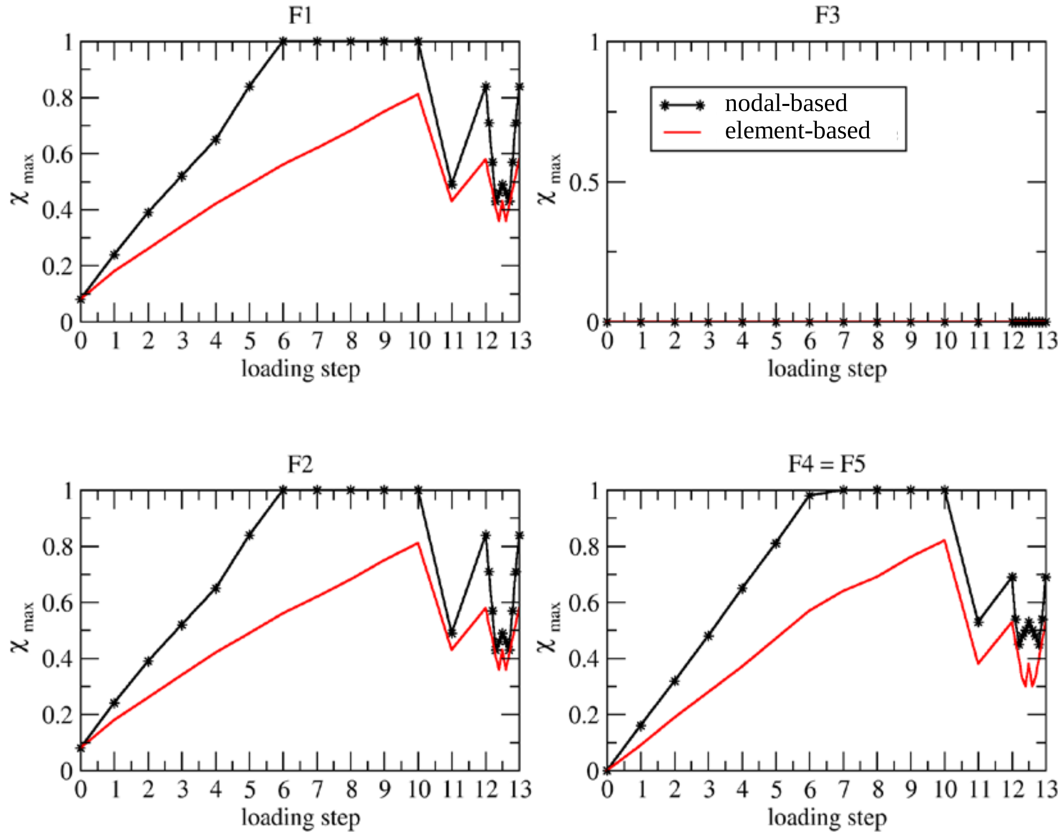

Figure 6 Sub-scenario 1b: comparison between the node-based and the element-based evaluation of χ_{max} at increasing loading steps for each fault. Note that due to symmetry F4 and F5 behave identically.

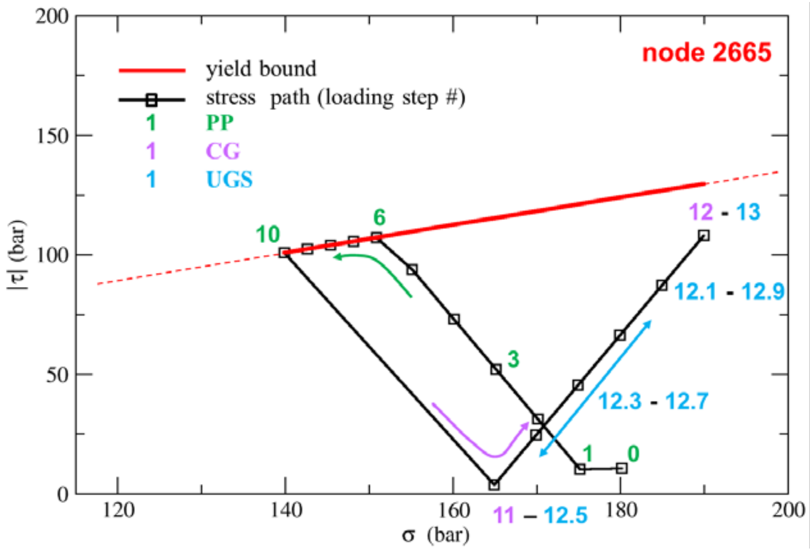

Figure 7 Sub-scenario 1b: stress path $|\tau|$ vs σ for the F2 fault node 2665. The red line represents the yield bound and the numbers the various loading steps. Different colours are used for primary production (PP, loading steps #1 – 10), cushion gas (CG, loading steps #11 – 12), and underground gas storage (UGS, loading steps #12.1 – 13).

Sub-scenario 1c

When a stiffer caprock is introduced, the faults become more stressed. This is clearly highlighted in Figure 8: the limiting value $\chi_{max} = 1$ is reached on faults F1 and F2 at loading step 8. The condition of a reservoir embedded in a sort of stiffer box (overburden, underburden and part of the sideburden are characterized by a Young modulus 2 to 4 times larger than that of the reservoir) causes a stress redistribution with a shear stress concentration along the faults. The faults F1 and F2 are more stressed because, due to the geometrical features of the selected conceptual model (Figure 2 in WP3 Report), they bound rock volumes characterized by different E values. The value χ_{max} peaks to 0.8 during UGS.

Figure 9 provides the stress path for the node 2665. The behavior is similar to that obtained in the previous scenarios during the PP phase with an even more reduced variation of σ (~30 bar) and a faster increase of $|\tau|$ due to the different distribution of the elastic properties. Because of sliding at l.s. #12, the stress path during UGS differs from that during CG (2nd year). Notice also the $|\tau|$ increase/decrease at l.s. #12.3 – 12.4 – 12.5 (and also #12.5 – 12.6 – 12.7) meaning that the shear stress changes the sign just before/after the end of the UGS production phase.

The behaviour versus time of the maximum fault sliding is shown in Figure 10.

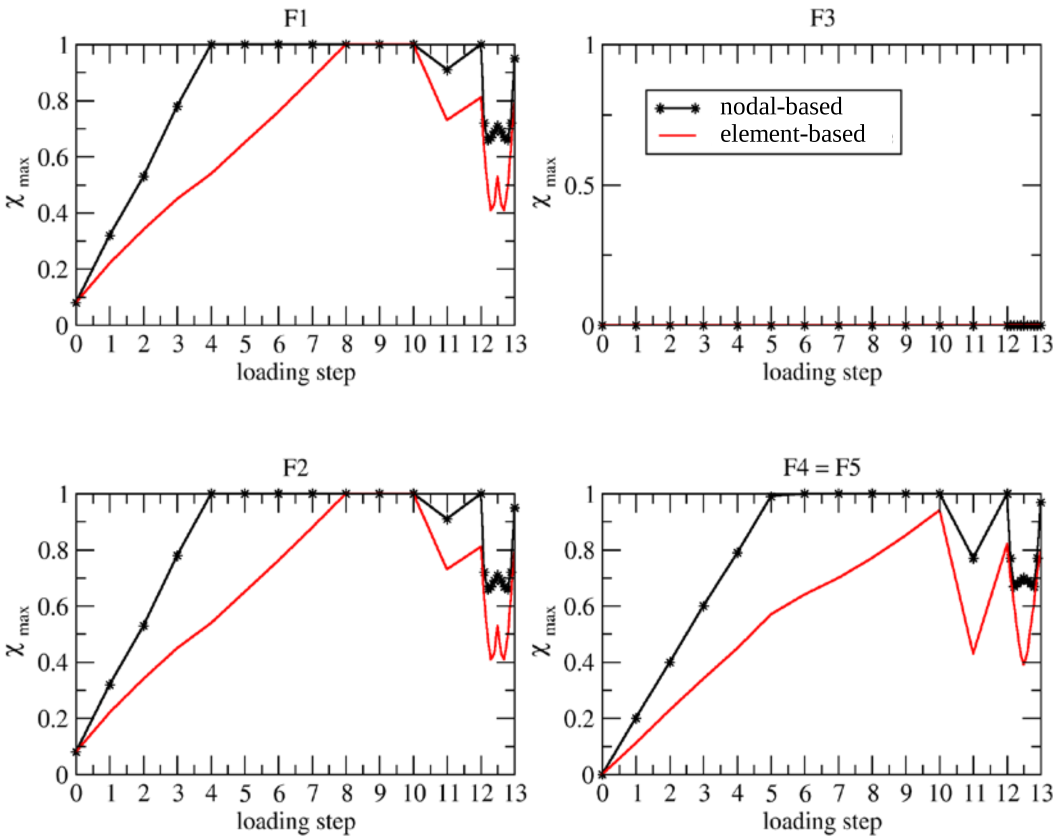

Figure 8 Sub-scenario 1c: comparison between the node-based and the element-based evaluation of χ_{max} at increasing loading steps for each fault. Note that due to symmetry F4 and F5 behave identically.

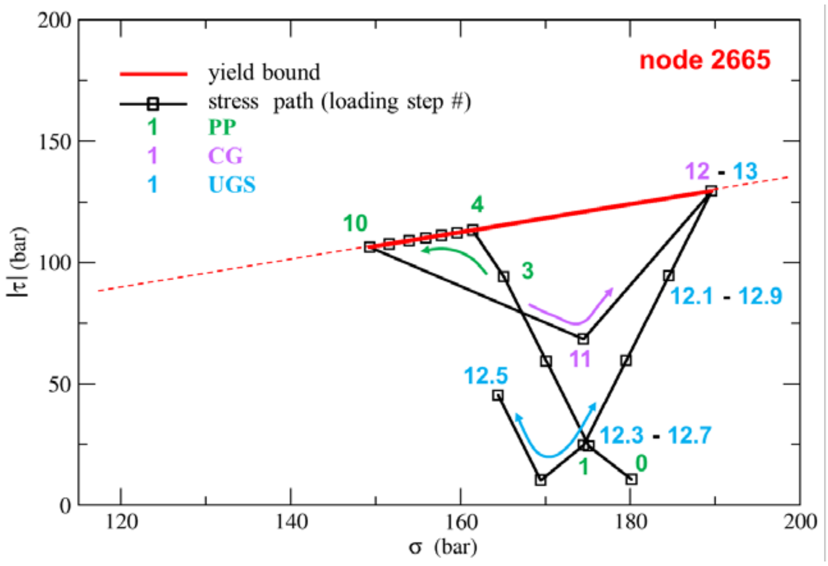

Figure 9 Sub-scenario 1c: stress path $|\tau|$ vs σ for the F2 fault node 2665. The red line represents the yield bound and the numbers the various loading steps. Different colours are used for primary production (PP, loading steps #1 – 10), cushion gas (CG, loading steps #11 – 12), and underground gas storage (UGS, loading steps #12.1 – 13).

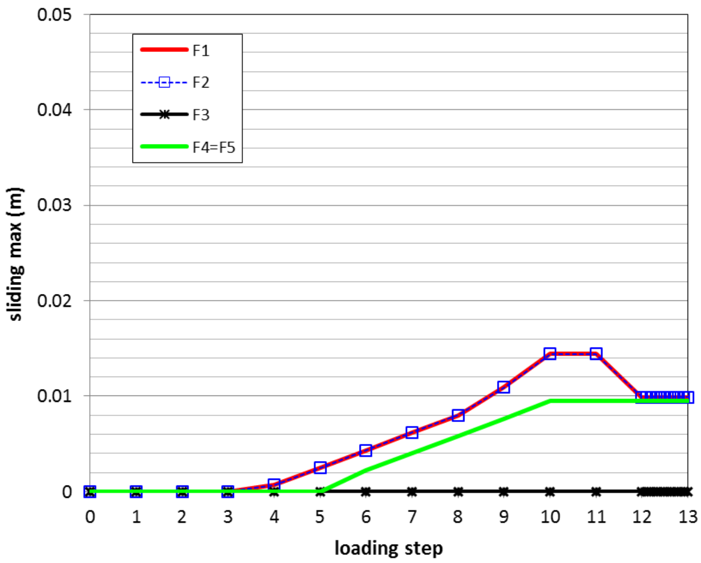

Figure 10 Sub-scenario 1c: maximum sliding δ_{max} versus time.

Sub-scenario 1d

Finally, both ΔPf ≠ 0 and a stiffer Zechstein formation are simultaneously addressed. The results presented above show that these two updates have a contrasting effect on fault reactivation: the former stabilizes the discontinuities by increasing the compressional normal stress acting on the surfaces, the latter leads to a more critical condition increasing the shear stress concentration on the faults.

It can be expected that the superposition of the two changes yields to an intermediate condition. Figure 11 shows the results obtained with this scenario. Indeed, the value χ_{max} = 1 is reached on faults F1 and F2 at loading step 9, with χ_{max} up to 0.8 at the end of CG and UGS injection phases. The behaviour versus time of the maximum fault sliding is shown in Figure 12. A comparison between the behaviour versus depth of the criticality index computed at the node and element level along fault F1 and F4 is shown in Figure 13 and Figure 14, respectively.

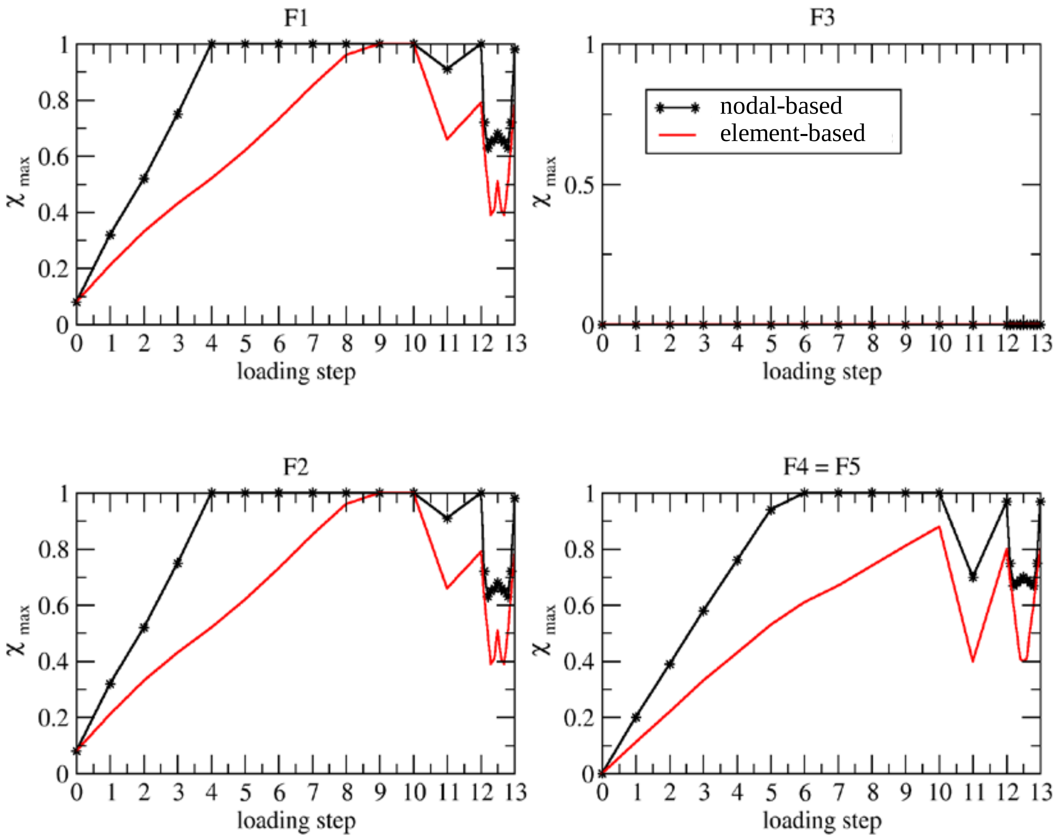

Figure 11 Sub-scenario 1d: comparison between the node-based and the element-based evaluation of χ_{max} at increasing loading steps for each fault. Note that due to symmetry F4 and F5 behave identically.

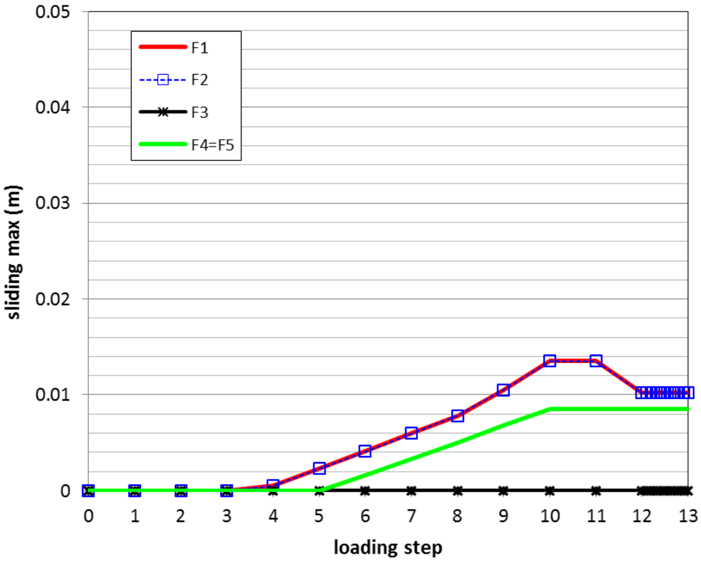

Figure 12 Sub-scenario 1d: maximum sliding δ_{max} versus time.

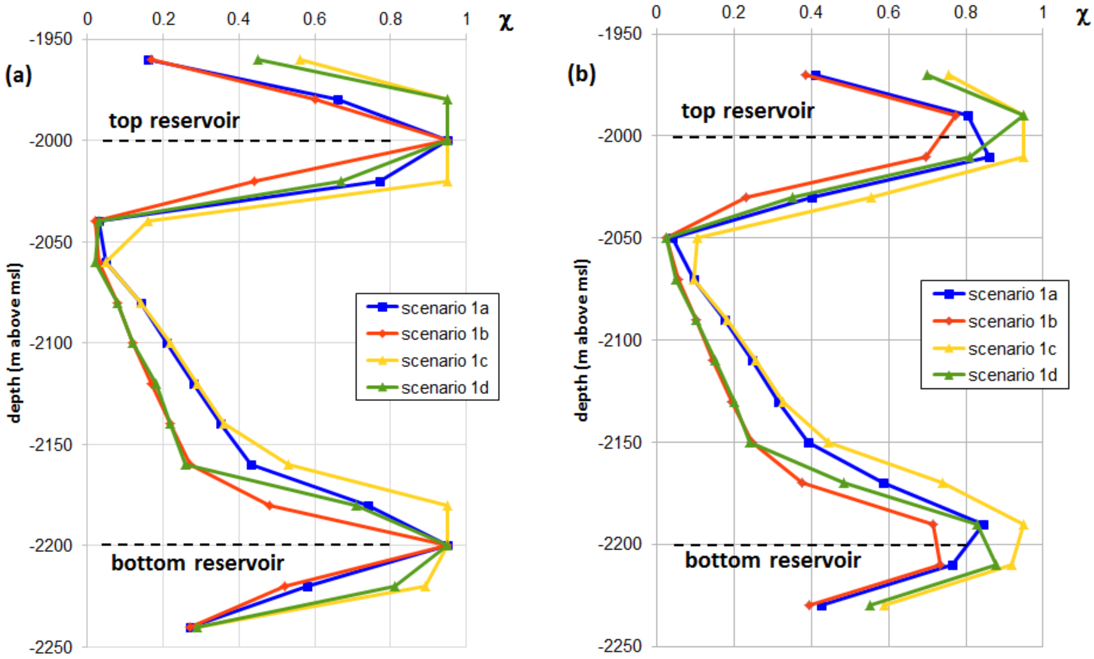

Figure 13 Fault F1, loading step 10: (a) node-based and (b) element-based behavior of the criticality index χ vs depth.

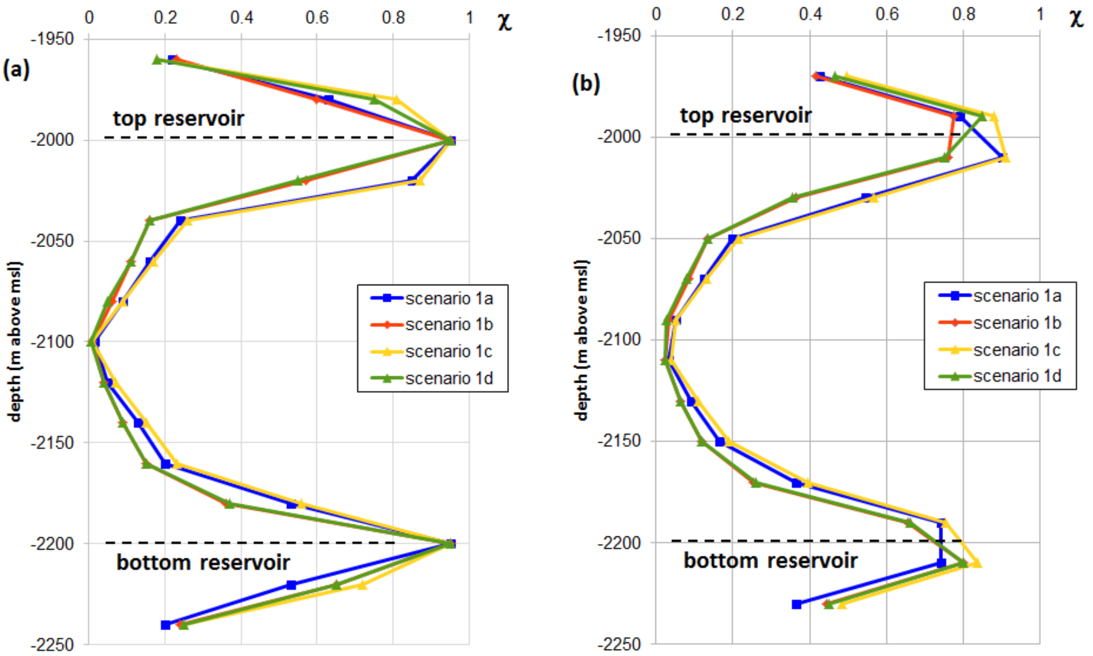

Figure 14 Fault F4, loading step 10: (a) node-based and (b) element-based behavior of the criticality index χ vs depth.

The stress path on node 2665 is shown in Figure 15. The more rigid caprock (side-burden) plus pressure change into the faults reduce even more the excursion of σ. The fact that σ remains almost constant (except when the fault is activated) is caused by the "fortuitous" combination of $E_{Zechstein} = 2E_{reservoir}$ and $\Delta p_{reservoir} = 2\Delta Pf$.

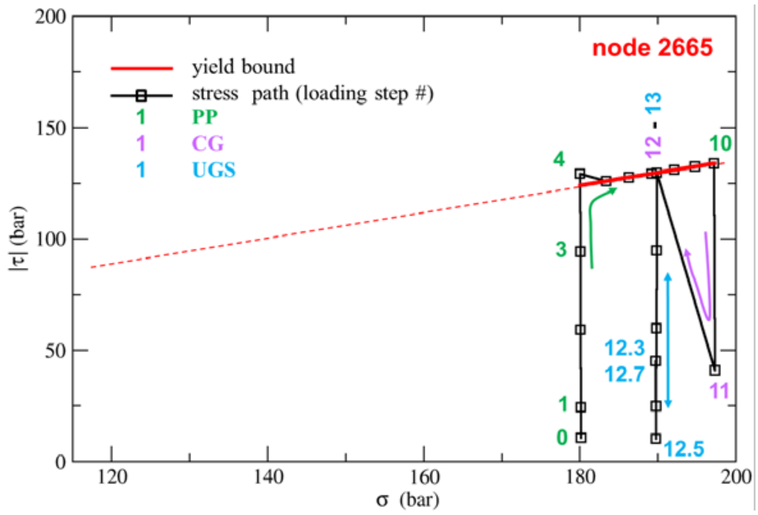

Figure 15 Sub-scenario 1d: stress path $|\tau|$ vs σ for the F2 fault node 2665. The red line represents the yield bound and the numbers the various loading steps. Different colours are used for primary production (PP, loading steps #1 – 10), cushion gas (CG, loading steps #11 – 12), and underground gas storage (UGS, loading steps #12.1 – 13).

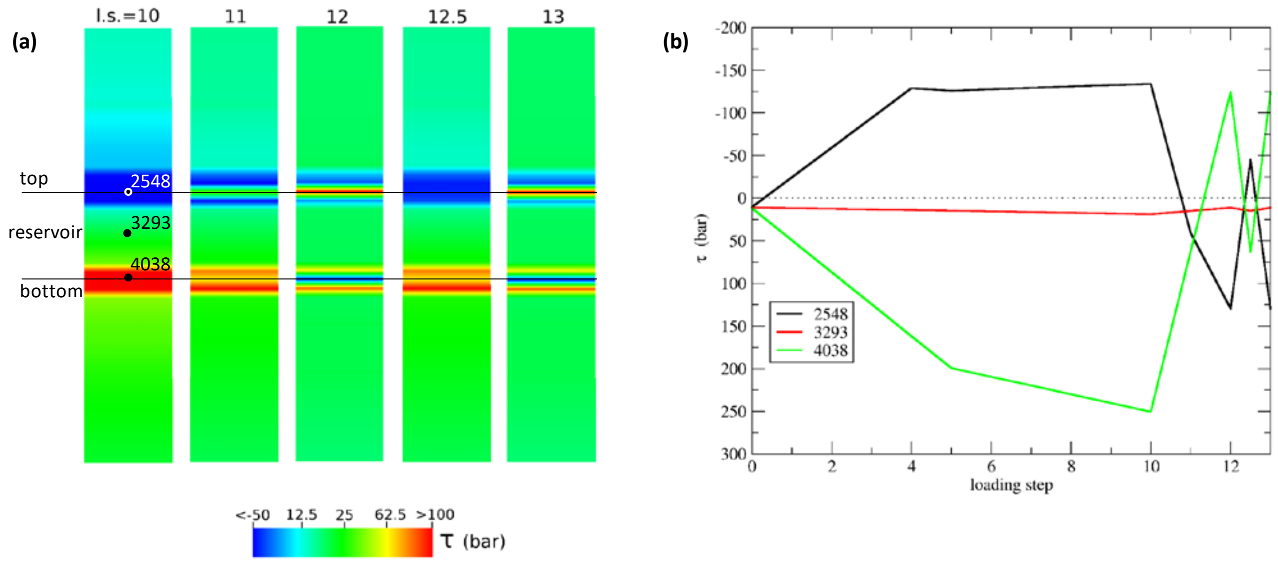

Figure 16 Sub-scenario 1d: (a) distribution of the shear stress τ for the loading steps (l.s.) 10, 11, 12, 12.5, 13 on fault F1 (dip = 80°). (b) Time behavior of τ for the nodes shown in (a) located at the top, bottom, and center of the reservoir. Positive values mean shear stresses with versus consistent with that of the z-axis.

Similar to Figure 14 of WP3 Report, Figure 16a shows the shear stress τ on fault F1 at l.s. #10, 11, 12, 12.5, and 13. Analogous considerations as those reported in WP3 can be developed here. The initial condition of shear stress slightly differs between top and bottom of the reservoir due to the fault dip, with the higher value of τ are observed at the end of PP (l.s. #10). Note that a positive shear stress characterizes the reservoir bottom and negative the reservoir top. The direction of the shear stress is oriented toward the center of the reservoir. Because of the $\Delta Pf \neq 0$, the fault is able to support a larger shear stress than in the case with $\Delta Pf = 0$, as it is confirmed by the largest maximum/minimum τ values in Figure 16 compared to Figure 14 in WP3 Report. At loading step 11, half of the pore pressure change has been recovered. As the reservoir expands due to pressure recovery, τ decreases on the reservoir bottom (the orientation remains the same but the absolute value decreases) and an almost null τ on the previously sliding IEs is obtained at this step at the reservoir top. Differently, τ does not significantly change for the IEs surrounding the activated IEs. The reservoir continues to recover pressure and re-expand until loading step 12. During this second part of cushion gas injection shear stress increases, with a sign opposite to that experienced during primary production (Figure 16b). A specular behavior occurs for the IEs at the reservoir bottom. Therefore, expansion during CG injection increases the criticality condition of the fault (mainly at the reservoir top and bottom) due the stress re-distribution after sliding.

Figure 11 shows that the faults approach a criticality state ($\chi_{max} \cong 0.8$) when the pressure recover the initial value at the end of CG and UGS injection phase, i.e. in a pressure state which is not generally associated to fault reactivation. However, conversely to UGS, the CG phase has been simulated with a rough time stepping. To understand the effect of this choice, a new simulation has been run to investigate more accurately the system behaviour during CG using a 2-month time step. The results are provided in Figure 17 in term of χ_{max} for fault F1 and maximum sliding δ_{max}. Comparison of Figure 17 with Figure 11 and Figure 12 reveals a certain difference with the development of a critical condition over the last three 2-month time steps instead of during the entire second year of CG injection. However, the comparison reveals that the important features of the χ_{max} and δ_{max} profiles remain practically unaltered. This supports the validity of using a 1-year time step during the CG phase in the scenarios that follow.

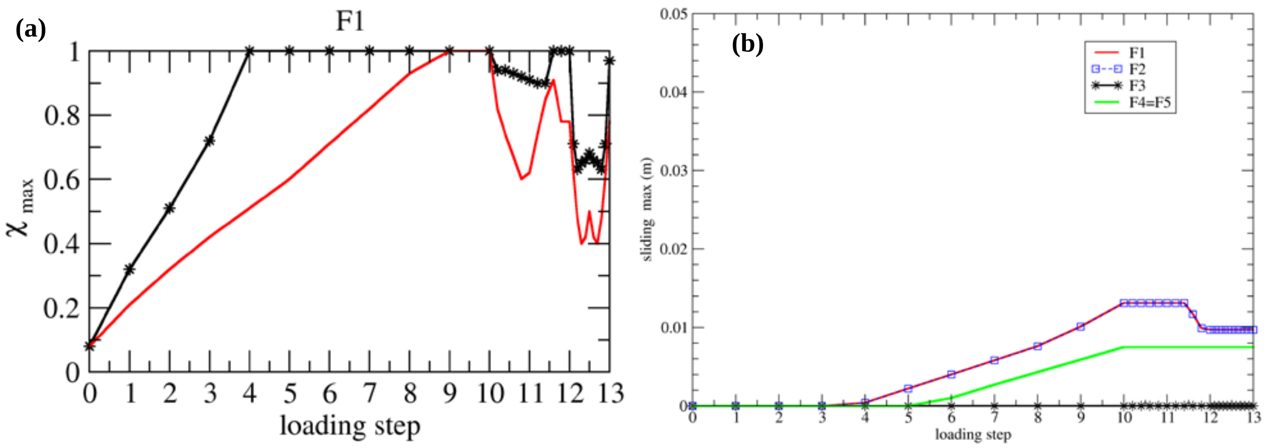

Figure 17 Sub-scenario 1d: (a) node-based and the element-based behavior of χ_{max} at increasing loading steps for fault F1 and (b) maximum sliding δ_{max} versus time obtained by implementing a 2-month time step during the CG phase.

In the following, scenario 1d will be termed the "reference" scenario. Table 1 summarizes the value of the major parameters used in the new reference scenario.

Table 1 Model parametrization for the “reference” test case of Phase 2.

PARAMETER	VALUE
F3 dip	90°
Offset	0 m
θ	0°
M_1	0.74
M_2	0.83
Cohesion	20 bar
Static friction angle	30°
$E_{reservoir}$	11 GPa
$E_{Zechstein\ (below\ 1800\ m)}$	20 GPa
$E_{Zechstein\ (from\ 1800\ m\ to\ 1500\ m)}$	35 GPa
$E_{overburden}$	10 GPa
$E_{underburden}$	30 GPa
Zechstein	linear elastic
α	0.86
$\nu_{reservoir}$	0.15
$\nu_{Zechstein}$	0.30
$\nu_{overburden}$	0.25
$\nu_{underburden}$	0.20
ΔPf	average between ΔP at the two sides of the fault

3. Sensitivity analysis

In this section, the sensitivity analysis carried out in WP3 to clarify the influence of (i) the Biot coefficient, (ii) the model geometry, (iii) the initial stress regime, (iv) the fault and reservoir geomechanical parameters, and (v) the differential pressure in the compartments during UGS is re-run using the updated model set-up described in the previous section. In particular, the following scenarios have been investigated:

2) sensitivity to Biot’s coefficient (1.0 instead of the actual value);
3) sensitivity to reservoir and fault geometry (F3 dip angles +65° and -65°, offset equal to 100 m and 200 m);
4) sensitivity to initial stress regime (θ=90°; M_1= 0.40 and M_2 = 0.47);
5) sensitivity to fault Mohr-Coulomb parameters (c=0 bar; φ_s=20°; φ_d=10° and d_c=2 mm; φ_d=20° and d_c=20 mm);
6) sensitivity to reservoir stiffness (*E*=8 bar; *E*=20 bar);
7) sensitivity to the differential pore pressure in the reservoir compartments (ΔP_1= -100 bar and ΔP_2 = 0 bar; ΔP_1= -100 bar and ΔP_2 = -200 bar).

3.1 Sensitivity to Biot's coefficient (Scenario 2)

In this section, the influence of the Biot coefficient α on the model response is analysed. In particular, the reference simulation is compared to the case where the grain compressibility is equal to zero, hence α = 1.0.

The results of the geomechanical model are provided in Figure 18 and Figure 19. Figure 18 shows the χ_{max} behaviour over time and Figure 19 the maximum sliding. The system criticality in term of fault activation is larger when α=1.0. However, consistently with WP3, the effect of Biot's coefficient on possible fault reactivation is limited.

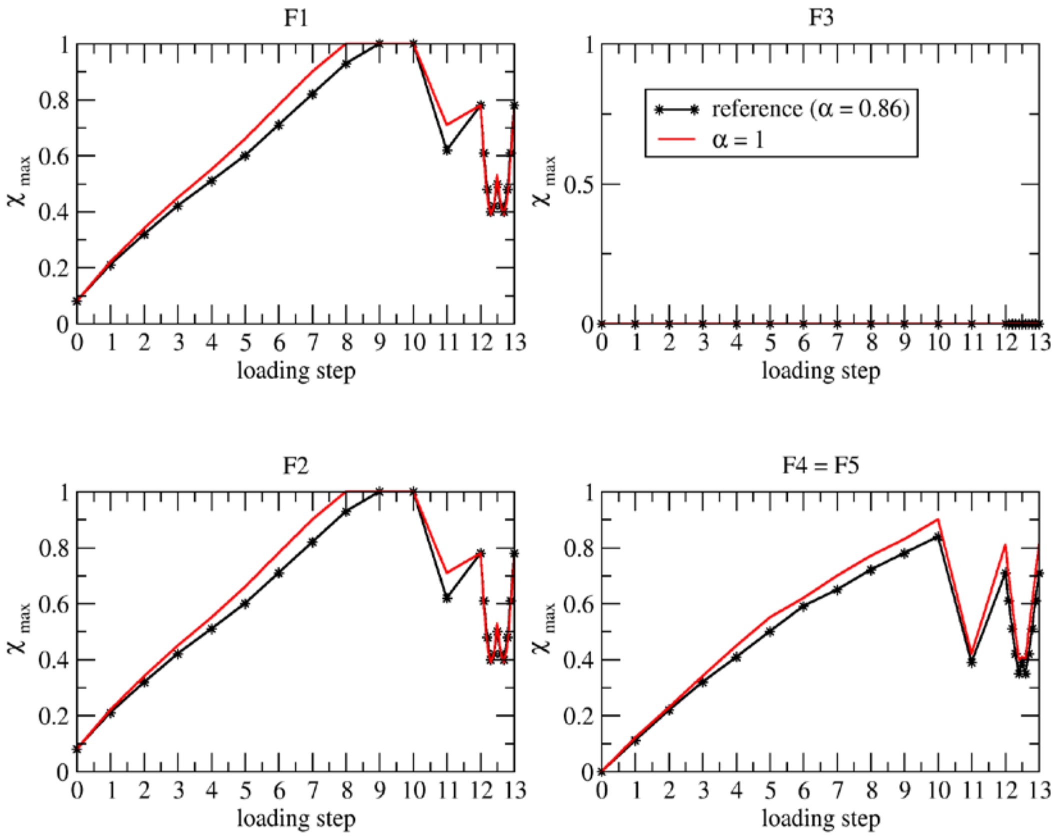

Figure 18 Scenario 2: effect of the Biot coefficient on the χ_{max} behavior at increasing loading steps for each fault. Note that due to symmetry F4 and F5 behave identically.

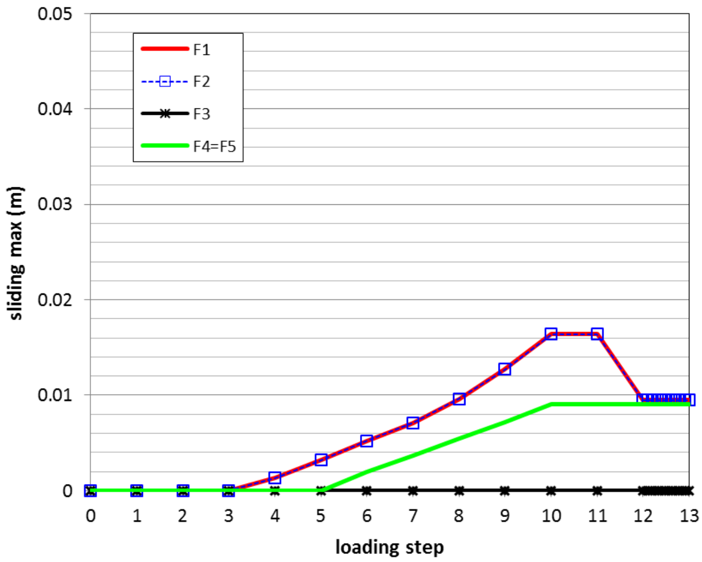

Figure 19 Scenario 2: maximum sliding δ_{max} versus time.

3.2 Sensitivity to reservoir and fault geometry (Scenario 3)

In this section, the reservoir and fault geometry are investigated. In particular, the following sub-scenarios have been analysed:

3a) the fault F3 is characterized by a dip angle equal to +65°;

3b) the fault F3 is characterized by a dip angle equal to -65°;

3c) the vertical offset between the two reservoir compartments along fault F3 is 100 m;

3d) the vertical offset between the two reservoir compartments along fault F3 is 200 m.

The effect on the fault stability is checked using the criticality factor χ_{max} (Figure 20). The results are compared with the reference test case. Similar qualitative considerations to those reported in WP3 Report can be outlined also here. The fault geometry is ineffective on fault F1 because the variations do not change the loading conditions on this fault. A certain increase of instability for faults F4 and F5 is due to compartment offset. Notice that, mainly due to the element-based computation of the criticality index, $\chi_{max} = 1$ on faults F1 and F2 at loading step 9, i.e. later than the outcome obtained in WP3. $\chi_{max} > 0$ also on fault F3, with the criticality that rises as the offset increases. During cushion gas injection and UGS, a maximum value $\chi_{max} = 0.8$ is reached.

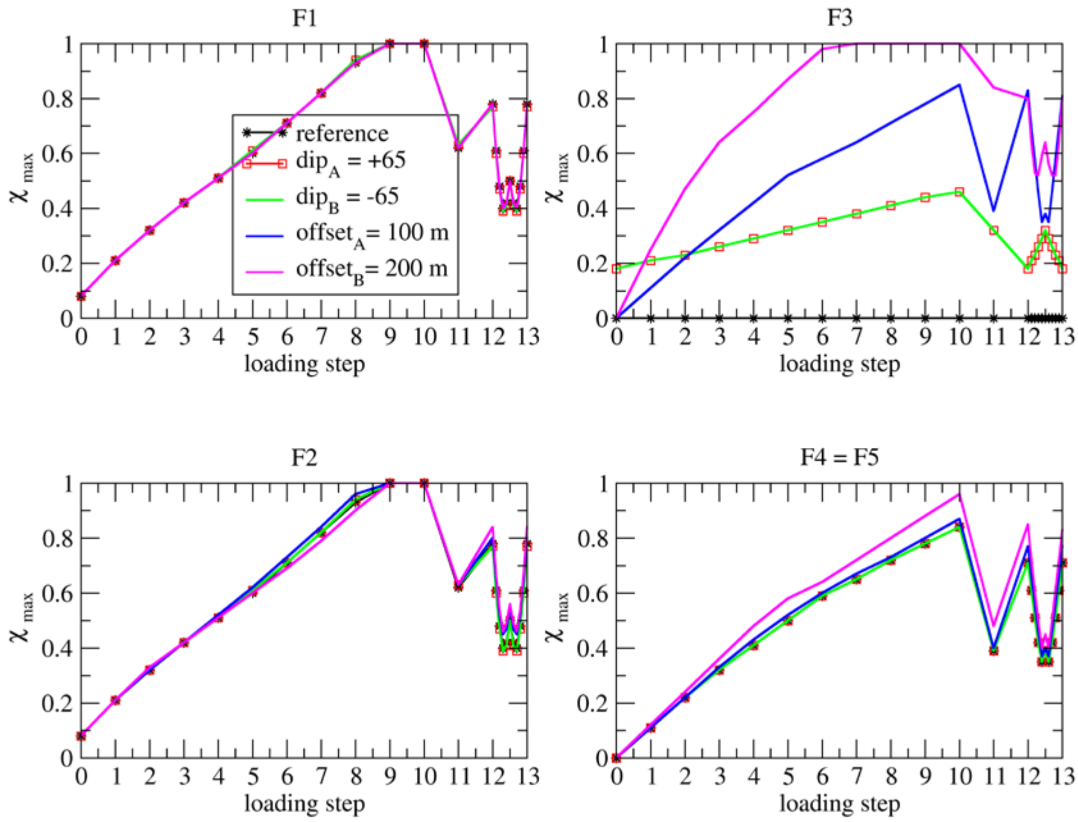

Figure 20 Scenario 3: effect of the reservoir and fault geometry on the χ_{max} behavior at increasing loading steps for each fault. Note that due to symmetry F4 and F5 behave identically. Sub-scenario 3a corresponds to F3 dip angle = +65°, sub-scenario 3b to F3 dip angle = -65°, sub-scenario 3c to a compartment offset = 100 m, and sub-scenario 3d to a compartment offset = 200 m.

Fault F3 behaves more differently from what was observed inWP3. In particular, because of $\Delta Pf \neq 0$, $\chi_{max} = 1$ only in sub-scenario 3d. Scenarios 3a and 3b are characterized by χ values significantly smaller than those obtained with WP3 model set-up.

Figure 21 provides the time behavior of the fault maximum sliding for the various cases addressing reservoir and fault geometry. Notice the value of δ_{max} = 7.4 cm obtained on fault F3 for the 200 m offset; this is the maximum value of the sliding obtained in the study.

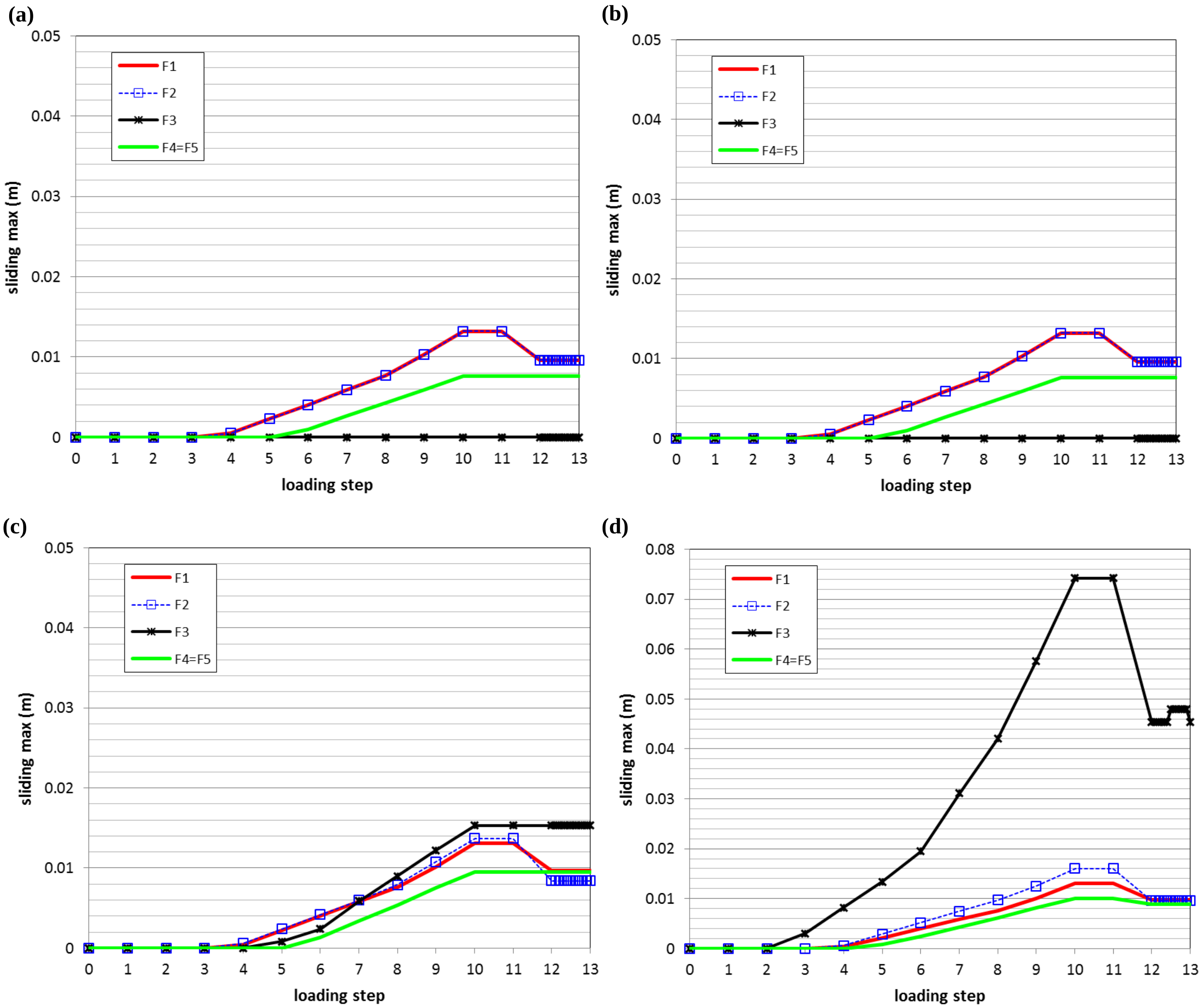

Figure 21 Maximum sliding δ_{max} for the various test cases investigating the effect of the reservoir and fault geometry: (a) sub-scenario 3a, (b) sub-scenario 3b, (c) sub-scenario 3c, and (d) sub-scenario 3d.

3.3 Sensitivity to the initial stress regime (Scenario 4)

In this section, the initial stress regime is investigated. In particular, the following sub-scenarios have been analyzed:

4a) a value of θ=90°, i.e. the principal horizontal stress is aligned parallel to faults F1, F2, and F3;

4b) $M_1 = \sigma_h/\sigma_v = 0.40$ and $M_2 = \sigma_H/\sigma_v = 0.47$.

The effect on the fault stability is checked using the criticality factor χ_{max} (Figure 22). Similarly to the WP3 outcomes, the effect of rotating the maximum horizontal stress by 90° is negligible, although detectable as faults F1 and F2 are a bit more stable and F4 with F5 less stable than in the reference case. Fault F3 is not affect by this variation.

Reducing M_1 and M_2 parameters worsens significantly the fault condition in relation to re-activation. The limit $\chi_{max} = 1$ is reached relatively early during primary production on faults F1 and F2 (loading step 6) but also on F4 and F5 (loading step 8). Faults F1 and F2 are re-activated also at the end of the cushion gas injection and at the end of the UGS injection phase. Differently from the WP3 outcome, because of the pressure change within the discontinuity, fault F3 is not affected by changing the value of the M_1 and M_2. A $\Delta Pf \neq 0$ precludes the normal stress acting on the fault to vanish.

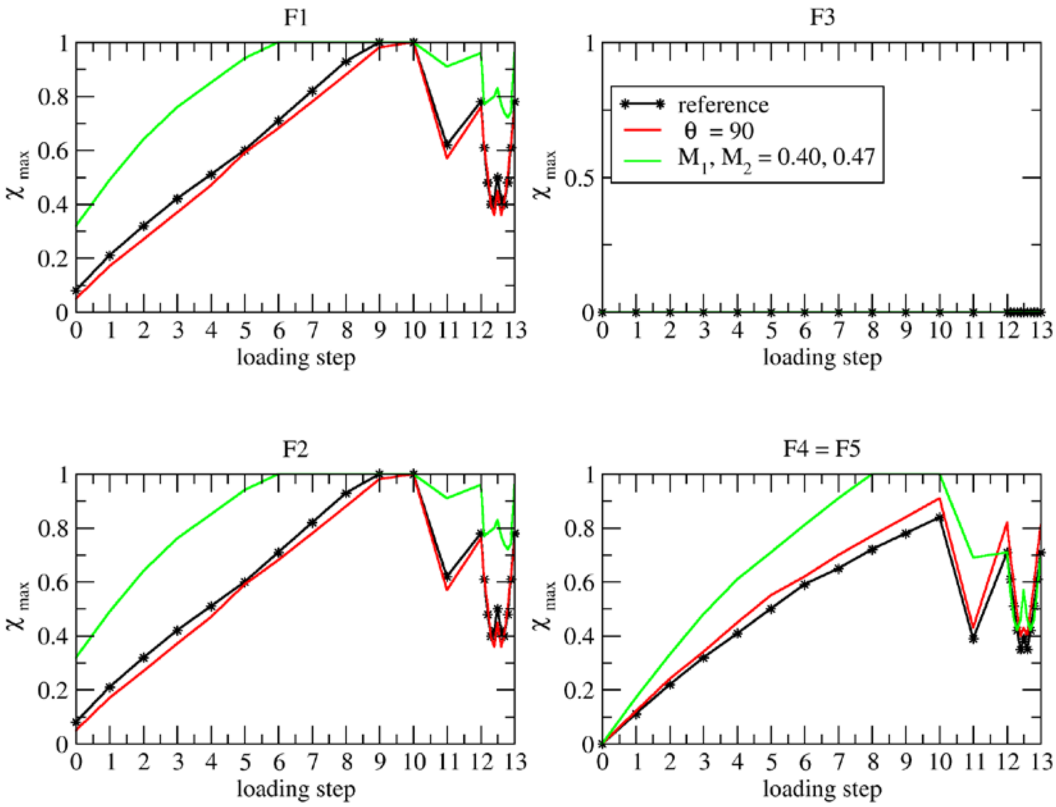

Figure 22 Scenario 4: effect of the initial stress regime on the χ_{max} distribution at increasing loading steps for each fault. Note that due to symmetry F4 and F5 behave identically. Sub-scenario 4a corresponds to a rotation θ=90° of the principal horizontal stresses and sub-scenario 4b to a decrease of the ratio between the principal horizontal stresses and the vertical one (M_1 = 0.49, M_1 = 0.47).

Figure 23 provides the time behavior of the fault maximum sliding for the various cases addressing the initial stress regime.

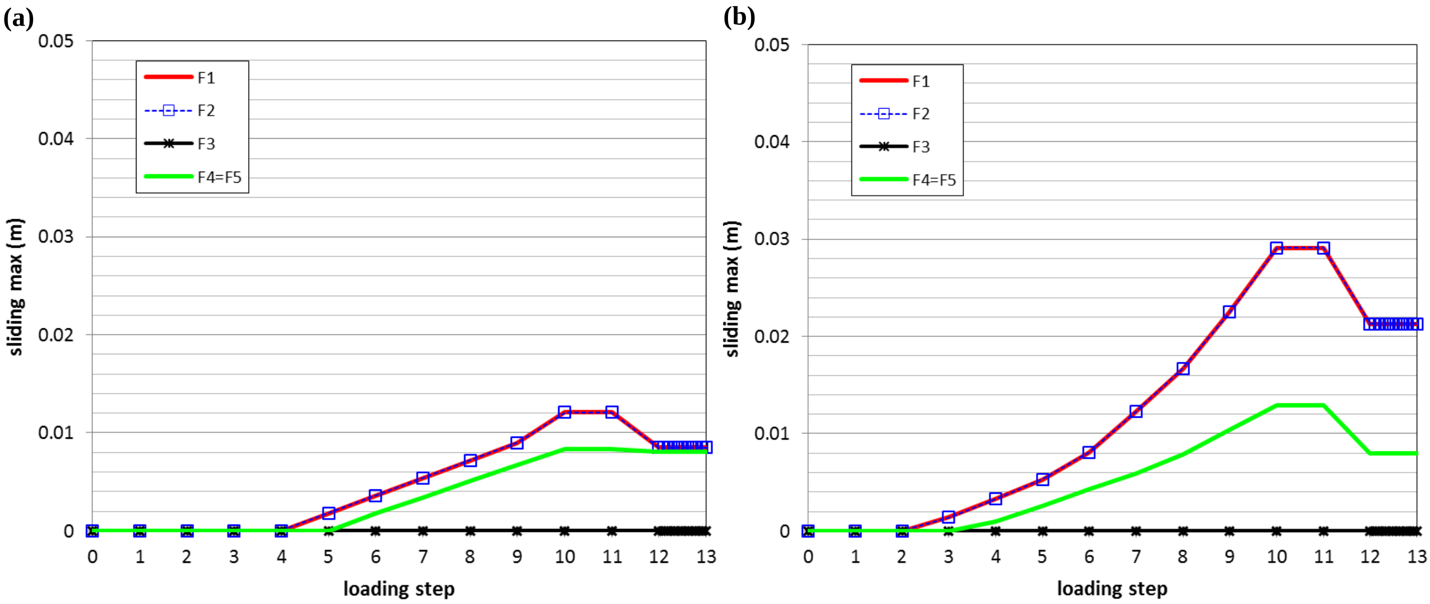

Figure 23 Maximum sliding δ_{max} for the various test cases investigating the effect of the initial stress regime: (a) sub-scenario 4a and (b) sub-scenario 4b.

3.4 Sensitivity to the Mohr-Coulomb fault parameters (Scenario 5)

The Mohr-Coulomb failure criterion is employed and the shear stress limit reads:

$$\tau_L = c - \sigma_n * tan\varphi$$

with c and φ the fault cohesion and friction angle, respectively, and σ_n the normal effective stress acting on the fault (negative in compression). Fault weakening is also accounted for, where the friction angle varies according to the relationship $\varphi = \varphi_s + \frac{\varphi_d - \varphi_s}{d_c} \times \delta$ for $\delta < d_c$ and $\varphi = \varphi_d$ for $\delta \geq d_c$. Therefore, two parameters are necessary to define fault weakening, namely the dynamic friction angle (φ_d) and the slip weakening distance (d_c).

Based on the above notation, the following sub-scenarios are investigated:

5a) c = 0 bar;

5b) $\varphi = \varphi_s = 20°$;

5c) fault weakening: φ reduces from φ_s to φ_d = 10° over a slip distance d_c=2 mm;

5d) fault weakening: φ reduces from φ_s to φ_d = 20° over a slip distance d_c=20 mm.

The results are shown in Figure 24 where the values of the χ_{max} are plotted at increasing loading steps. The results are consistent with those obtained in WP3, with a general reduction of the criticality conditions mainly because of the element-base evaluation of χ as already observed in the scenarios described above. As expected, decreasing the fault cohesion or the static friction angle affects the stability of faults F1, F2, F4 and F5 manly during primary production and cushion gas injection. Conversely, fault F3 remains stable (χ_{max} = 0.0) for the entire simulation because of symmetry conditions.

A certain difference with respect to the WP3 outcome is obtained during UGS. A zoom of the χ_{max} behaviour from loading step 10 to loading step 13 (i.e., during cushion gas injection and UGS phases) is shown in Figure 25. The worst case is obtained for φ_d = 10° and d_c = 2 mm. This causes faults F1, F2, F4 and F5 to slide also at the end of the cushion gas and UGS injection phases but not at loading step 12.5, i.e. at the end of the 6-month UGS production phase, as obtained in WP3.

Figure 26 provides the time behavior of the fault maximum sliding for the various cases addressing the Mohr-Coulomb parameters.

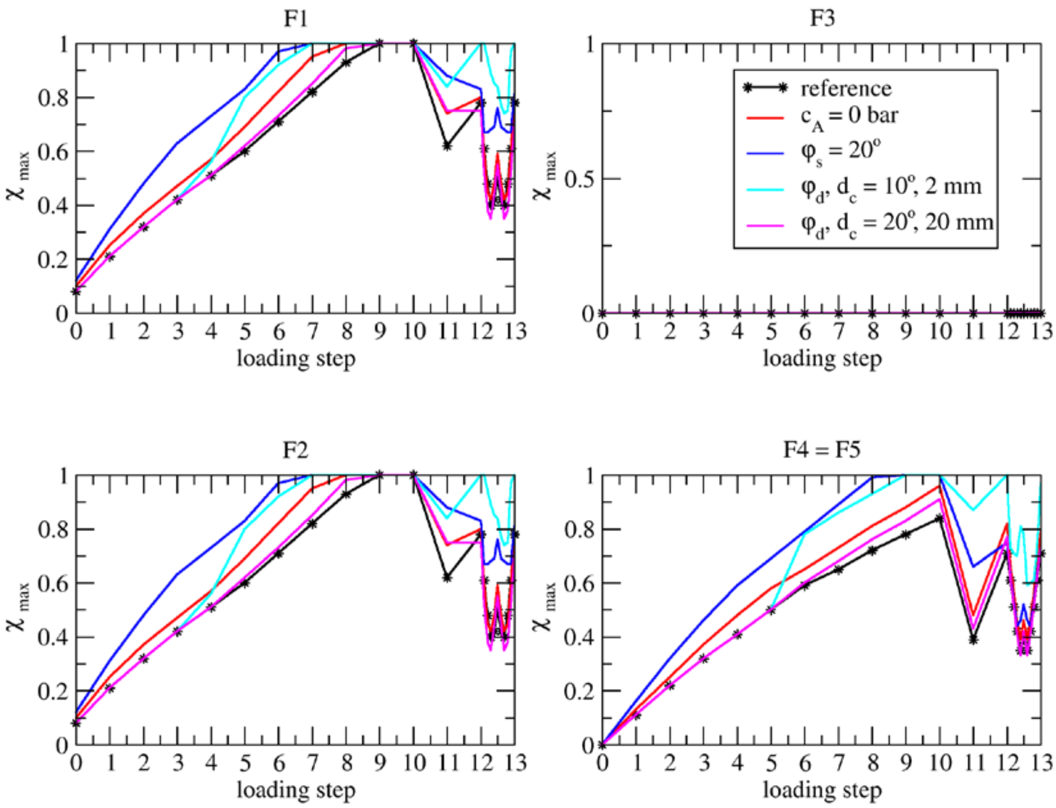

Figure 24 Scenario 5: effect of the Mohr-Coulomb fault parameters on the χ_{max} behavior at increasing loading steps for each fault. Note that due to symmetry F4 and F5 behave identically. Sub-scenario 5a corresponds to c = 0 bar, sub-scenario 5b to $\boldsymbol{\varphi = \varphi_s = 20^{\circ}}$, sub-scenario 5c to φ_d = 10° over a slip distance d_c=2 mm, and sub-scenario 5d to φ_d = 20° over a slip distance d_c=20 mm.

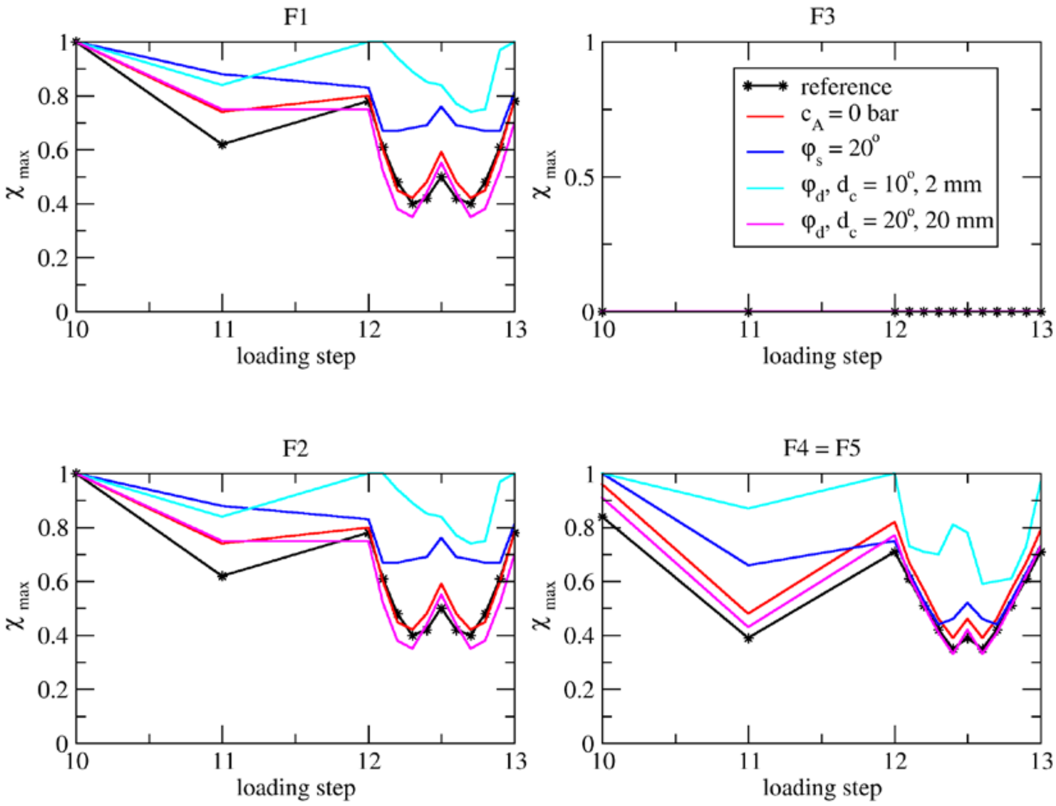

Figure 25 Scenario 5: zoom of Figure 24 over the cushion gas injection and UGS phases. Sub-scenario 5a corresponds to c = 0 bar, sub-scenario 5b to $\varphi = \varphi_s$ = 20°, sub-scenario 5c to φ_d = 10° over a slip distance d_c=2 mm, and sub-scenario 5d to φ_d = 20° over a slip distance d_c=20 mm.

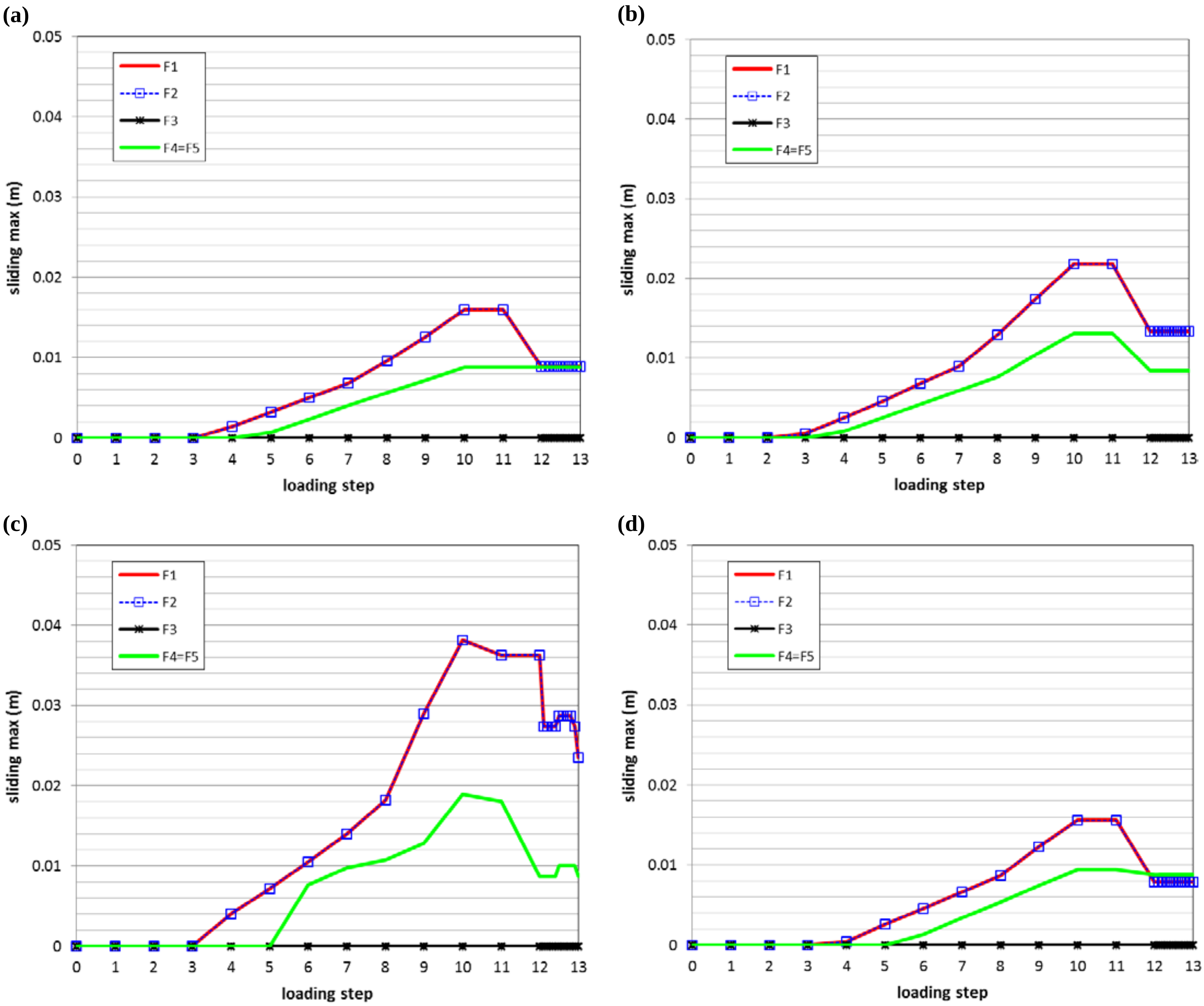

Figure 26 Maximum sliding δ_{max} for the various test cases investigating the effect of the Mohr-Coulomb rupture criterion: (a) scenario 5a, c = 0 bar; (b) scenario 5b, $\varphi_s = 20°$; (c) scenario 5c, $\varphi_d = 10°$ with a slip weakening distance d_c = 2 mm; and (d) scenario 5d, $\varphi_d = 20°$ with a slip weakening distance d_c = 20 mm.

Figure 27 shows the stress path for node 2665 as obtained for scenarios 5b and 5c. Because of the reduced friction angle, the yield surface is reached more easily during PP, at the end of CG, and at the end of UGS production & injection phases. As observed for the scenario 1d, the elastic phases develop with an almost constant normal stress because of the selected ratios between the reservoir and overburden stiffness and between the pressure change in the reservoir and within the fault. The stress path and the yield bound are quite complex in scenario 5c due to weakening (Figure 27b). Due to the very small friction angle ($\varphi_d = 10°$), in scenario 5c also a large part of UGS is characterized by a the stress state that develops on the yield surface.

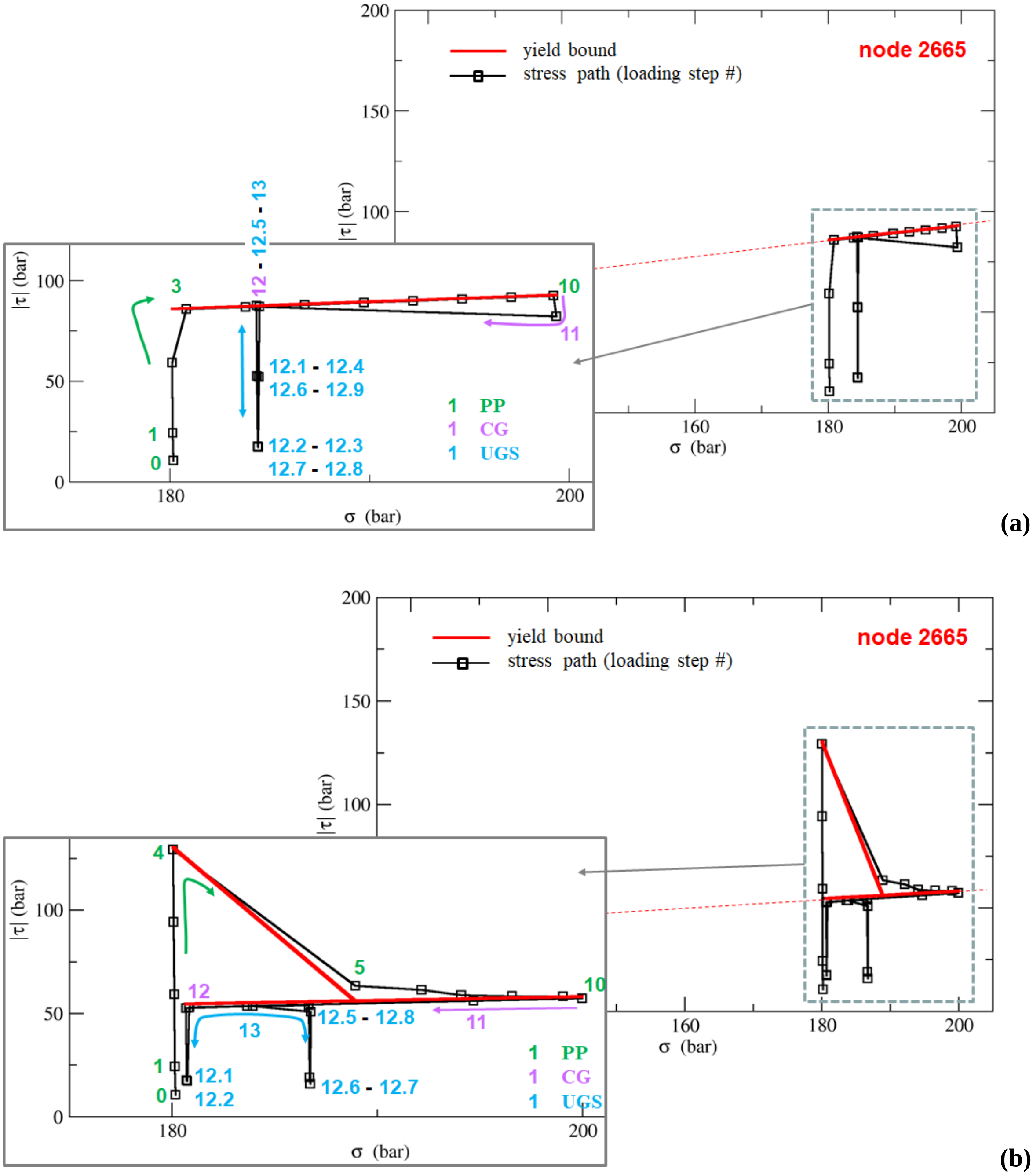

Figure 27 (a) scenario 5b and (b) scenario 5c: stress path $|\tau|$ vs σ for the F2 fault node 2665. The red line represents the yield bound and the numbers the various loading steps. Different colours are used for primary production (PP, loading steps #1 – 10), cushion gas (CG, loading steps #11 – 12), and underground gas storage (UGS, loading steps #12.1 – 13).

3.5 Sensitivity to the reservoir stiffness (Scenario 6)

The reservoir stiffness is investigated by using lower and higher values compared to reference where E = 11 GPa. Two sub-scenarios are investigated:

6a) E = 8 bar;

6b) E = 20 bar.

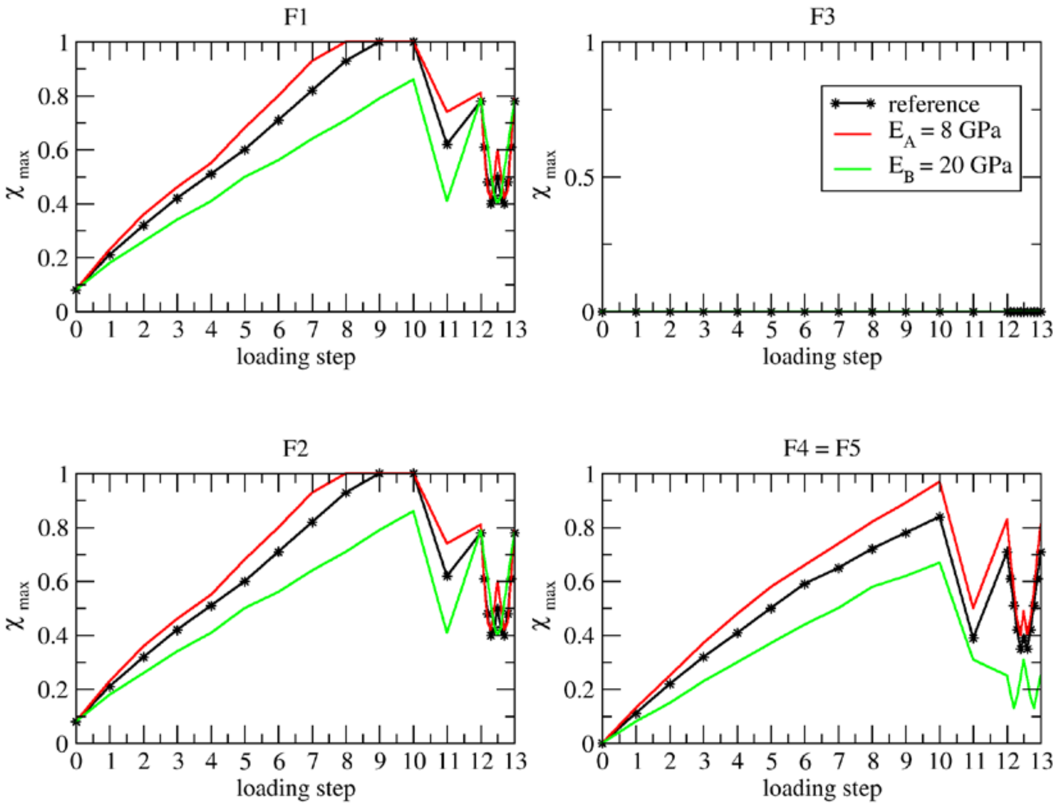

Figure 28 Scenario 6: effect of the reservoir stiffness on the χ_{max} behavior at increasing loading steps for each fault. Note that due to symmetry F4 and F5 behave identically. Sub-scenario 6a corresponds to *E* = 8 GPa and sub-scenario 6b to *E* = 20 GPa.

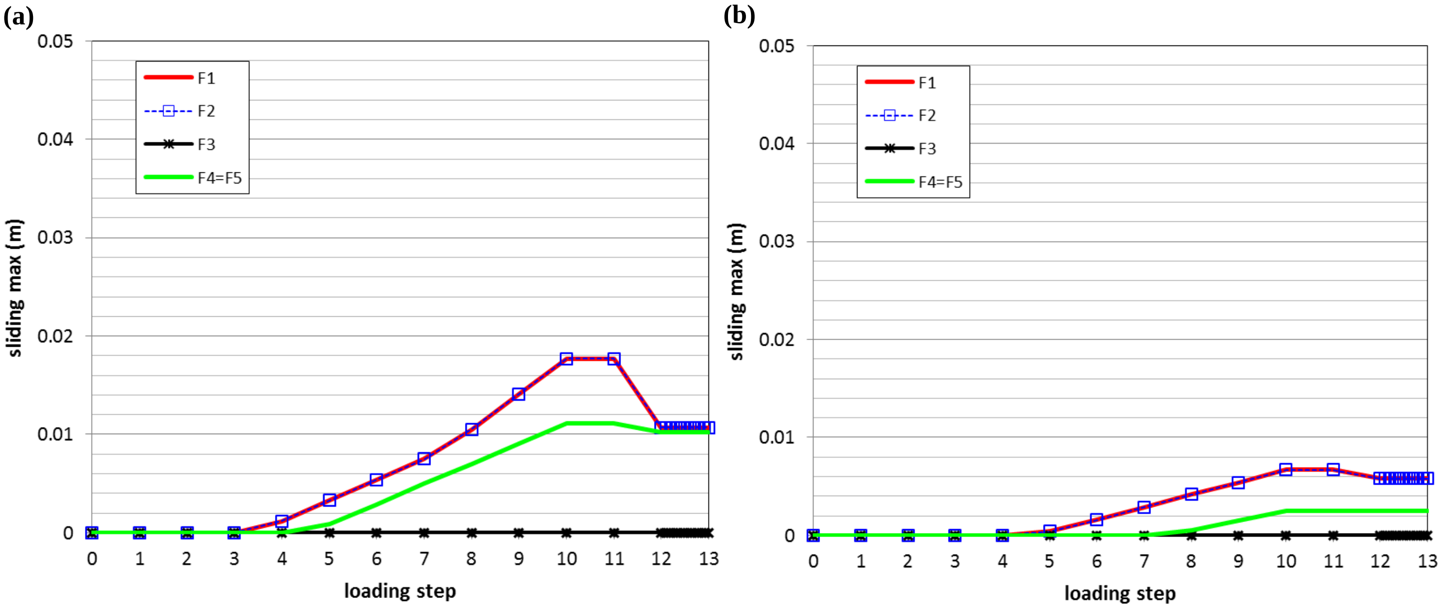

Figure 29 Maximum sliding δ_{max} for the various test cases investigating the effect of the reservoir stiffness: (a) sub-scenario 6a, *E* = 8 GPa and (b) sub-scenario 6b, *E* = 20 GPa.

The results are shown in Figure 28 where the values of the χ_{max} are plotted at increasing loading steps. Decreasing reservoir stiffness enhances fault instability because of a larger compaction and contraction of the depleting formation. Notice that in sub-scenario 6b χ_{max} remains well below 1; as observed in Scenario 1, a more homogeneous distribution of the geomechanical properties in the subsoil reduces the tendency of a fault to be reactivated because of a more uniform redistribution of the stress field. Fault F3 remains stable during the entire simulation due to symmetry. During UGS, $\chi_{max} < 0.8$ irrespective of the *E*. Figure 29 provides the time behavior of the maximum sliding for the various cases addressing the reservoir stiffness.

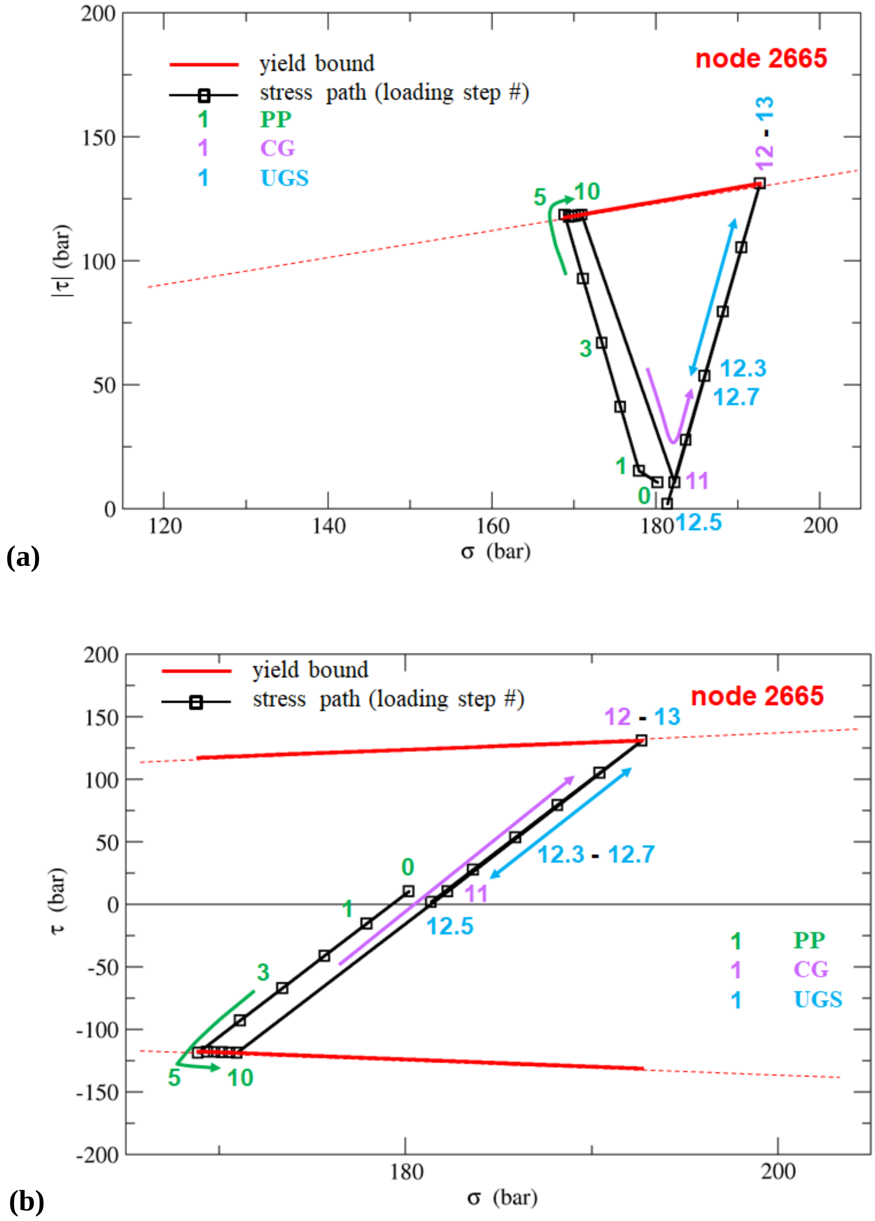

Figure 30 Sub-scenario 6b: (a) stress path $|\tau|$ vs σ and (b) τ vs σ for the F2 fault node 2665. The red line represents the yield bound and the numbers the various loading steps. Different colours are used for primary production (PP, loading steps #1 – 10), cushion gas (CG, loading steps #11 – 12), and underground gas storage (UGS, loading steps #12.1 – 13).

Figure 30 shows the stress path for node 2665. Both $|\tau|$ (Figure 30a) and τ (Figure 30b) are provided. This case confirms that what obtained in scenario 1d, i.e. σ ≅ constant (Figure 15), is a casual occurrence. If the reservoir stiffness is set equal to that of the nearest caprock/sideburden, the normal stress to the fault plane varies over the elastic phases. It is interesting to note that at l.s. #5 (i.e. at Δp = -100 bar) node 2665 starts sliding. Since this l.s. the stress path follows the yield surface until the end of the PP. During CG, at l.s. #11 (i.e. after a pressure recover equal to 100 bar) the node returns almost to the initial stress state and the further 100 bar increase to l.s. #12 loads the fault in the opposite "direction", touching the yield surface when P-Pi. Stress path over UGS superposes to the second part of CG (elastic behavior).

For sub-scenario 6b, whose interpretation is more simple than the previous ones because of the same *E* value in the reservoir and surrounding over- and side-burden, we provide also the stress path for three representative elements of the reservoir. The element locations are sketched in Figure 3. The stress state is represented through the stress invariant p and q that are computed from the model outcomes:

$$p = \frac{1}{3}\mathrm{tr}(\boldsymbol{\sigma}) \quad ; \quad q = \sqrt{3/2}\,\|\boldsymbol{S}\|$$

where $\boldsymbol{\sigma} = \begin{bmatrix} \sigma_x & \tau_{xy} & \tau_{xz} \\ \tau_{yx} & \sigma_y & \tau_{yz} \\ \tau_{zx} & \tau_{zy} & \sigma_z \end{bmatrix}$ and $\boldsymbol{S} = \boldsymbol{\sigma} - p\boldsymbol{I}$. Within the reservoir (element #151788) the change of stress invariants is "simply" proportional to Δp (depending also on Biot and Poisson) with the principal stresses that remain substantially oriented along the reference axes. The stress state evolves in a more complex way at the field bound (elements # 135772 and 152349), with a rotation of principal stresses.

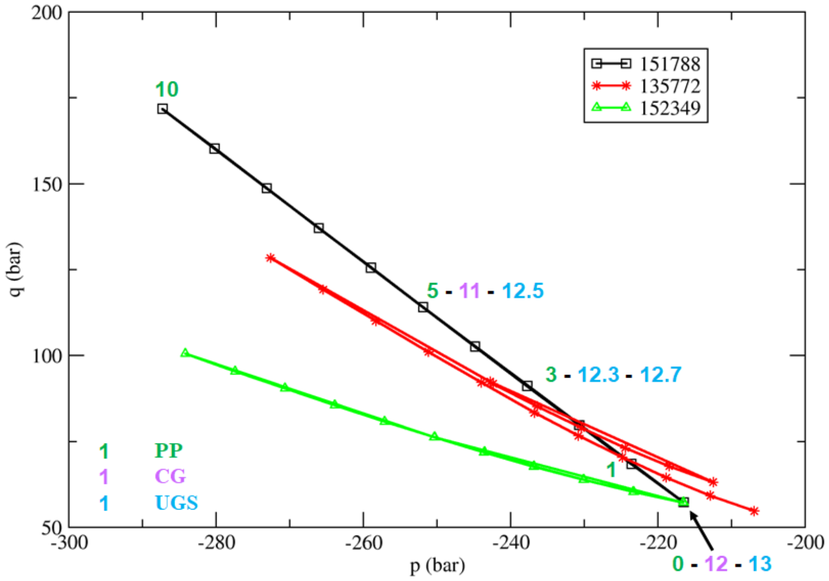

Figure 31 Sub-scenario 6b: stress path $(p\,,\,q)$ for three nodes within the reservoir.

3.6 Sensitivity to the differential pore pressure in the reservoir compartments (Scenario 7)

In this section, the effect of a different pore pressure change in the two reservoir compartments is investigated. The simulations are identical to the reference until the end of the CG injection phase; then, during UGS, in block 1 the pore pressure change ΔP_1 is kept equal to reference test case, i.e., minimum ΔP_1= -100 bar, whereas in block 2 two different sub-scenarios are analyzed:

7a) ΔP_2 = 0 bar for the entire UGS;

7b) ΔP_2 = -200 bar at the end of the production phase.

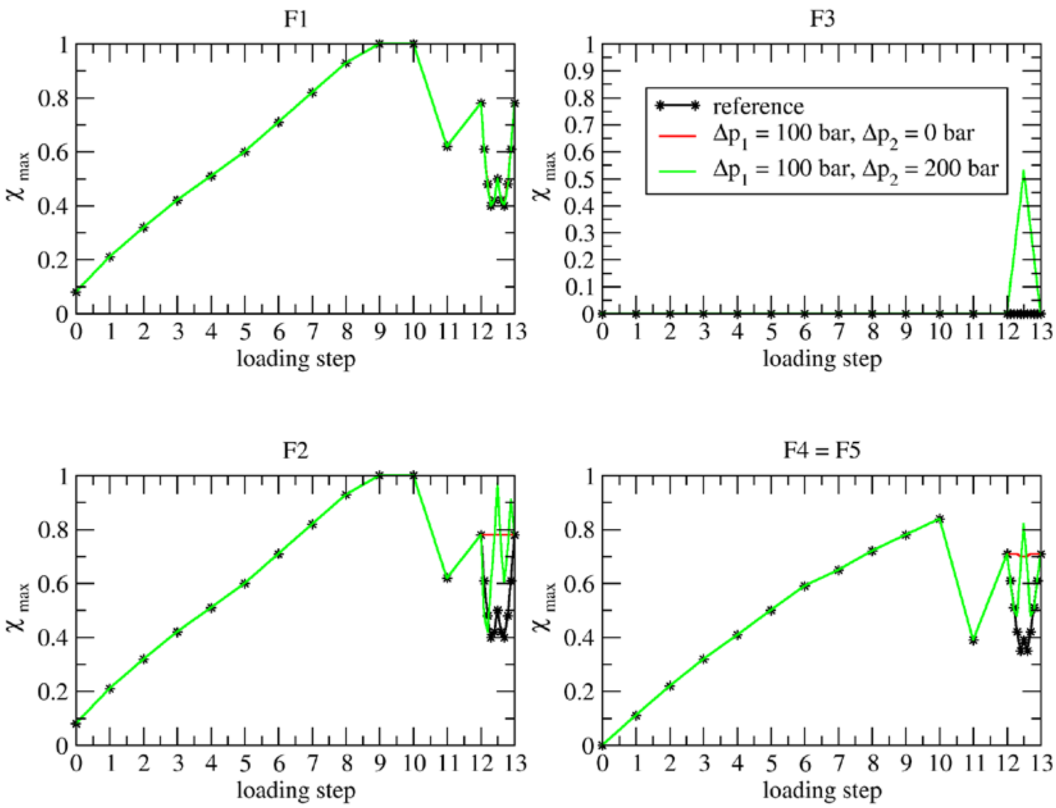

Figure 32 Scenario 7: effect of the differential pressure on the χ_{max} behavior at increasing loading steps for each fault. Note that due to symmetry F4 and F5 behave identically. Sub-scenario 7a corresponds to ΔP_2 = 0 bar and sub-scenario 7b to ΔP_2 = -200 bar.

Fault F1 is not affected by a different pore pressure compared to the reference and consequently the χ_{max} behaviour does not change relative to the reference outcome. Conversely, Figure 32 shows that fault F2 and, secondarily, faults F4 and F5, undergo higher instability at loading step = 12.5 when maximum ΔP_2= -200 bar is prescribed within block 2 (χ_{max} = 1 on fault F2). On fault F2, $\chi_{max} \cong 0.9$ at the end of UGS injection phase. It is interesting to notice the behavior of fault F3 that is critically stressed by application of differential pore pressure change on the two compartments only in sub-scenario 7b but not in sub-scenario 7a for the stabilization effect exerted by ΔPf.

In relation to sub-scenario 7b, Figure 33 shows the shear stress and its modulus at increasing loading steps for a node located at the reservoir bottom on fault F2. The shear stress increases until loading step 10 and reaches the limit shear stress τ_L at loading step 5. The fault slides until loading step 10. The comparison between Figure 32 and Figure 33 suggests that in loading steps from 5 to 8 only the nodes in correspondence of the reservoir top/bottom slide. An entire fault element starts sliding from loading step 9. During CG and UGS cycle, $|\tau|$ equates τ_L at the end of the CG injection and at the end of UGS production and injection cycle. Again, comparing Figure 32 and Figure 33 it emerges that only at loading step 12.5 τ_L is reached within (at least) one element. On fault F2 χ_{max} approaches 1 at the end of the UGS injection phase too (Figure 32), but remains well below the criticality value at loading step 12 (i.e., the end of CG phase) although $\tau = \tau_L$ on the nodes located at the reservoir bottom (Figure 33).

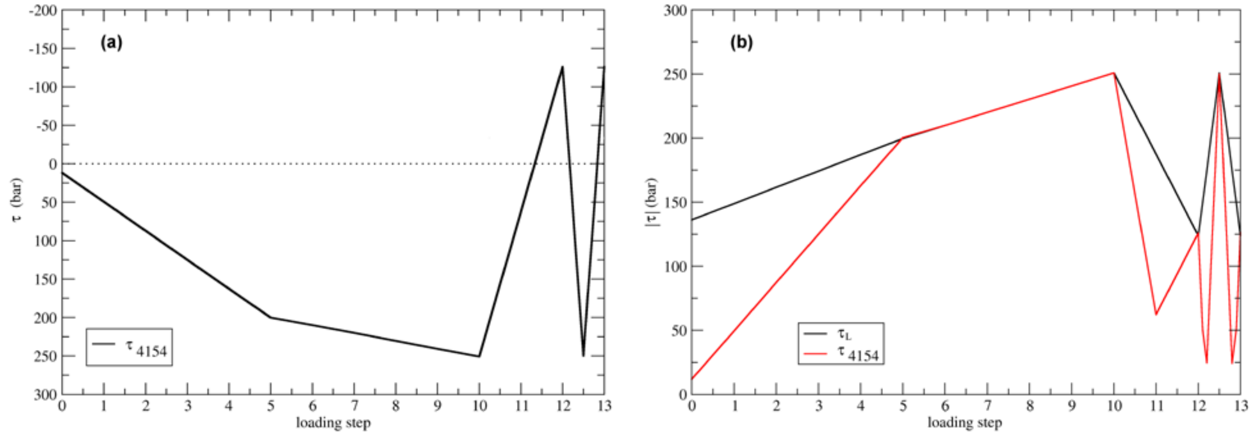

Figure 33 Scenario 7b: (a) time behavior of τ for the node 4154 located at the bottom of the reservoir on fault F2. Positive values mean shear stresses with versus consistent with that of the z-axis. (b) Time behavior of the actual shear stress (in modulus) for the same node versus the limit tangential stress τ_L.

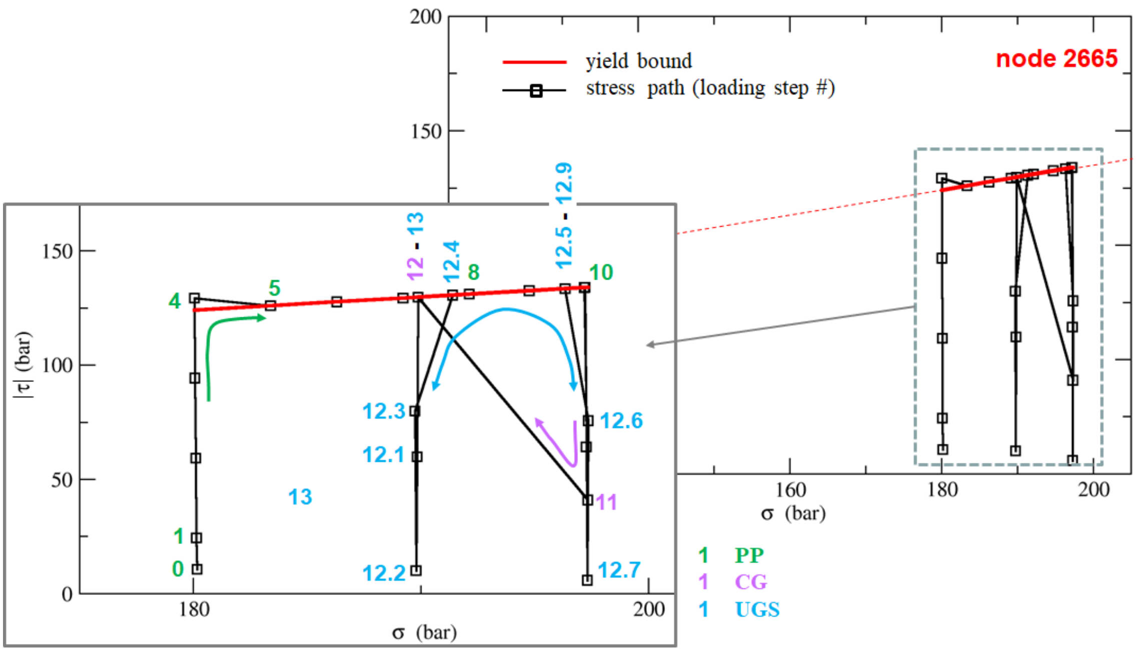

Figure 34 Scenario 5c: stress path $|\tau|$ vs σ for the F2 fault node 2665. The red line represents the yield bound and the numbers the various loading steps. Different colours are used for primary production (PP, loading steps #1 – 10), cushion gas (CG, loading steps #11 – 12), and underground gas storage (UGS, loading steps #12.1 – 13).

The stress path of node 2665 in scenario 7b is provided in Figure 34. The stress behavior during PP and CG is equal to that developed in scenario 1d (Figure 15) but the condition is much more critical then in the reference case around the end of the UGS production (between l.s. #12.4 – 12.5) and injection (between l.s. #12.9 – 13) phases when the stress state develops on the yield bound because of the large (200 bar) pressure changes.

Finally, Figure 35 provides the time behaviour of the maximum sliding for the various cases addressing the reservoir stiffness. Fault F2 slides also during UGS. Fault F3 does not slide despite a χ_{max} larger than in the reference case.

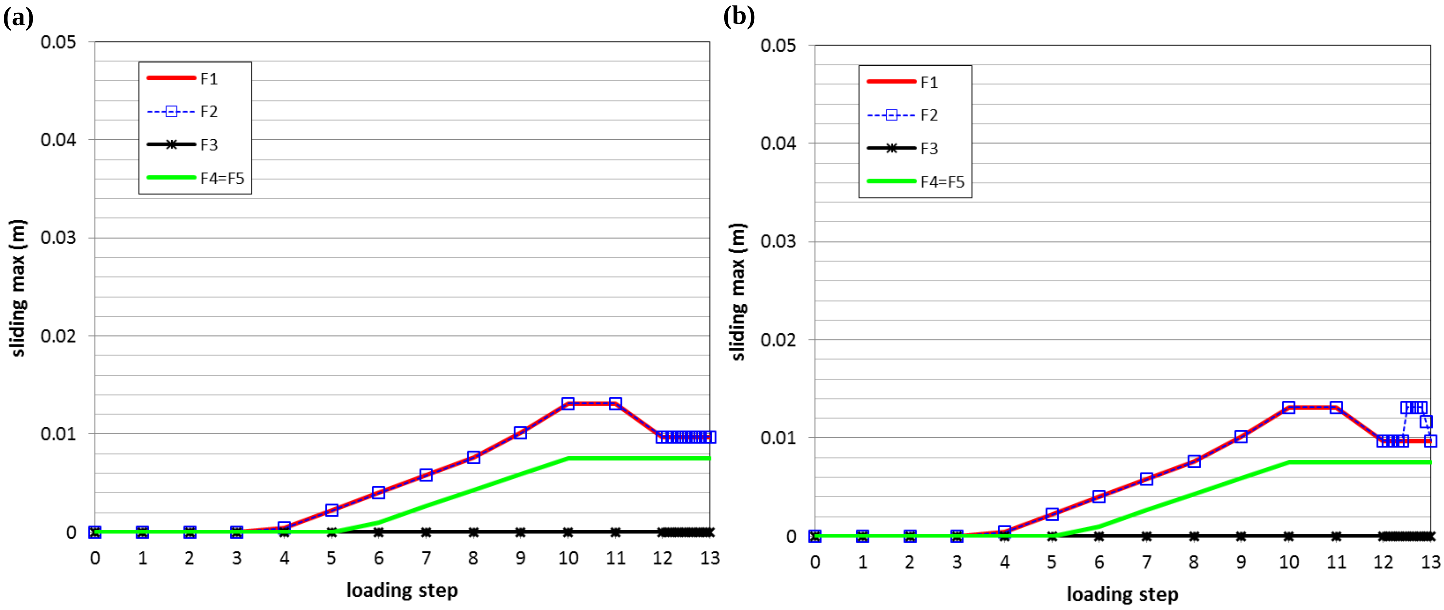

Figure 35 Maximum sliding δ_{max} for the test cases investigating the effect of the differential pore pressure in the reservoir compartments: (a) sub-scenario 7a, ΔP_1 = -100 bar with ΔP_2 = 0 bar; (b) sub-scenario 7b, ΔP_1 = -100 bar with ΔP_2 = -200 bar.

4. Mechanisms and combinations

A number of mechanisms together with combinations of selected mechanisms and parameters have been investigated starting from the updated reference model corresponding to sub-scenario 1d. Specifically, the following scenarios are carried out:

8) mechanism 4 defined in WP3;
9) mechanism 5 defined in WP3;
10) combination 1 defined in WP3 with an offset = 100 m instead of 200 m;
11) combination 2 defined in WP3 with an offset = 100 m instead of 200 m;
12) combination 4: new combination that accounts for a viscous salt layer, c = 0 bar, fault F3 dip = +65, and a compartment offset = 100 m;
13) combination 5: scenario 10 with reservoir stiffness = 20 bar;

14) combination 6: scenario 11 with reservoir stiffness = 20 bar.

The simulation outcomes are presented and discussed in the following sub-sections.

4.1 Mechanism 4: pore pressure variation versus time (Scenario 8)

As defined in WP3, mechanism 4 tests the effect of a larger ΔP per loading step during a UGS cycle. In particular, the pore pressure change during the UGS cycle amounts to -150 bar (Figure 36) instead of -100 bar as in the reference.

The comparison with the reference test case is reported in Figure 37. The distribution of χ_{max} at increasing loading steps for each fault is identical to the reference until the end of the cushion gas phase (the pore pressure change is the same). During UGS, the larger ΔP change per loading step affects the faults behaviour. As expected, the major influence of the investigated mechanism is observed at loading step 12.5, with a ~35% increase of the criticality factor compared to the reference case. The results are similar to the WP3 outcomes.

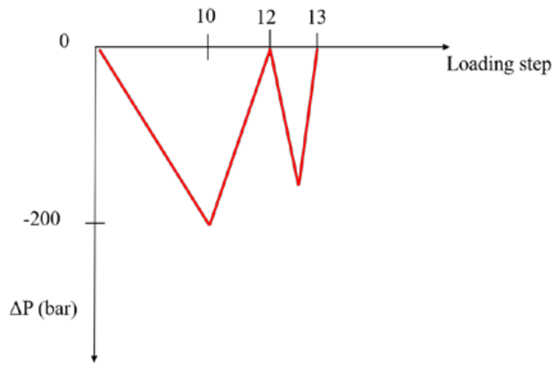

Figure 36 Scenario 8: pore pressure change in the reservoir compartments 1 and 2 used in mechanism 4.

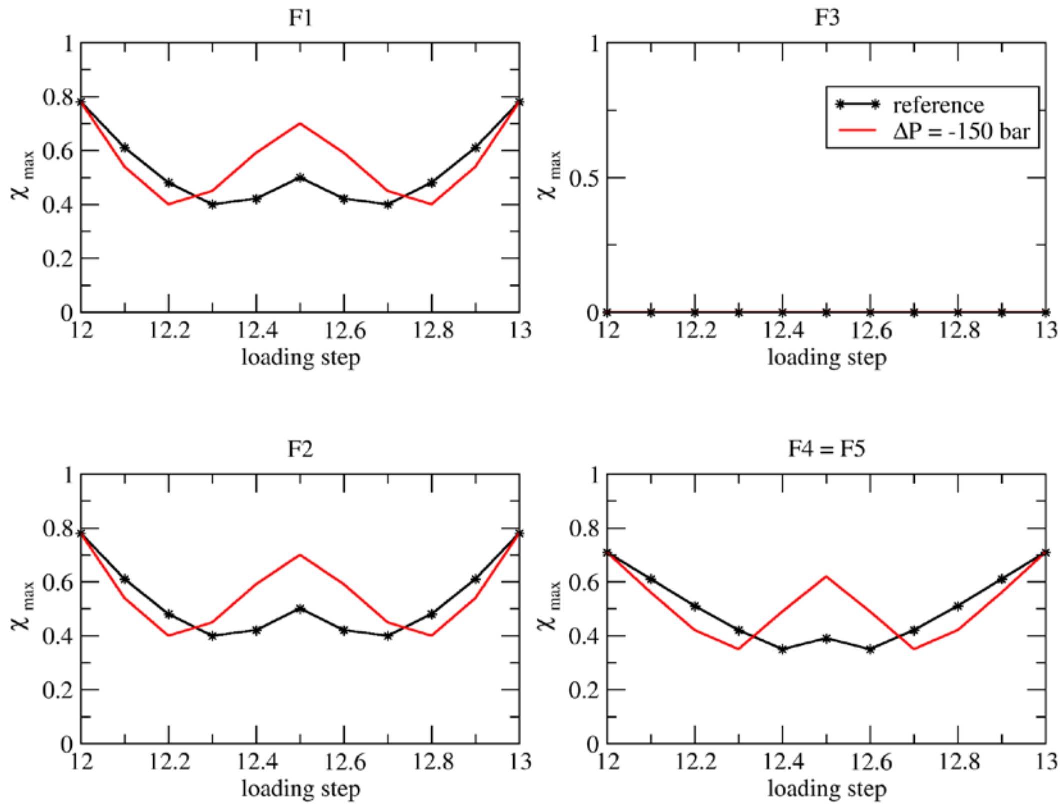

Figure 37 Scenario 8 (mechanism 4): χ_{max} distribution at increasing loading steps for each fault. Note that due to symmetry F4 and F5 behave identically.

4.2 Mechanism 5: viscous salt caprock (Scenario 9)

The reference test is based on a linear elastic model for the caprock. Here, the viscous behaviour of the Zechstein formation is introduced to investigate the effect of this mechanism on the model response. The same Maxwell model used in WP3 is applied also here. The Zechstein caprock is characterized by a viscosity $\mu = 10^{17}$ Pa·s.

Figure 38 compares the vertical displacement d_z versus the loading steps as obtained with the elastic (reference) and the viscous caprock. Note that the plot refers to the surficial node at location (x, y, z) = (0.0, 0.0, 0.0) m, i.e., above the center of the reservoir. The difference between the two outcomes is smaller here than in WP3 because in the Phase 1 analysis $E_{Zechstein}$ was increased from the reference value (10 GPa) to 40 GPa when viscosity is accounted for. Now the elastic properties are kept unchanged (20 GPa and 35 GPa).

Figure 39 compares the distribution of the vertical displacements d_z within a vertical cross-section orthogonal to the y-axis at loading step 10 (10 years). As expected, at the end of primary production the subsidence bowl (negative displacements) is more pronounced when the viscous caprock is accounted for.

The influence of the Zechstein formation on the fault system is investigated in Figure 40. Notice that the simulation with a viscous salt caprock spans 40 years. To appreciate the χ_{max} behaviour during the UGS cycles, a zoom of Figure 40 for loading steps in the range 10-20 years is plotted in

Figure 41. For faults F1 and F2, the criticality index χ_{max} decreases during CG and, during UGS, varies periodically between ~0.4 (in the middle of the production/injection phases, e.g. at l.s. #12.3 and #12.7 within the first cycle) and ~0.75 at the end of the injection phase, with a secondary maximum (χ_{max} ~ 0.5) at the end of the UGS production phase. Notice that the largest χ_{max} value gently increases with the cycle number, growing from 0.70 at l.s. #13 to 0.84 at l.s. #40. Inspection of the t_{80} behavior points out that the fault thickness prone to be activated does not increase with the UGS cycle, remaining substantially equal to the value (17.27 m, i.e. one interface element) provided in Annex II for l.s. #13. Differently, the largest χ_{max} value gently decreases with the cycle number on faults F4 and F5, with t_{80} that from 19.34 m (i.e. one interface element) l.s. #13 (see Annex II) becomes null during the UGS cycles that follow. It must be recalled that these faults are not bounded the Zechstein formation in correspondence of the reservoir depth. Also notice in Figure 40 that maximum χ_{max} values do not differ significantly from the reference case.

It is worth noting that, differently from the WP3 outcome, χ_{max} is now significantly < 1 during UGS. This fact is mainly due to the element-based computation of χ_{max}. In fact, Figure 42 shows that, also with the WP6 model set-up, χ_{max} approaches 1 at the end of each UGS injection phase if a node-based analysis is used.

Finally, the behaviour of the maximum sliding δ_{max} is shown in Figure 43.

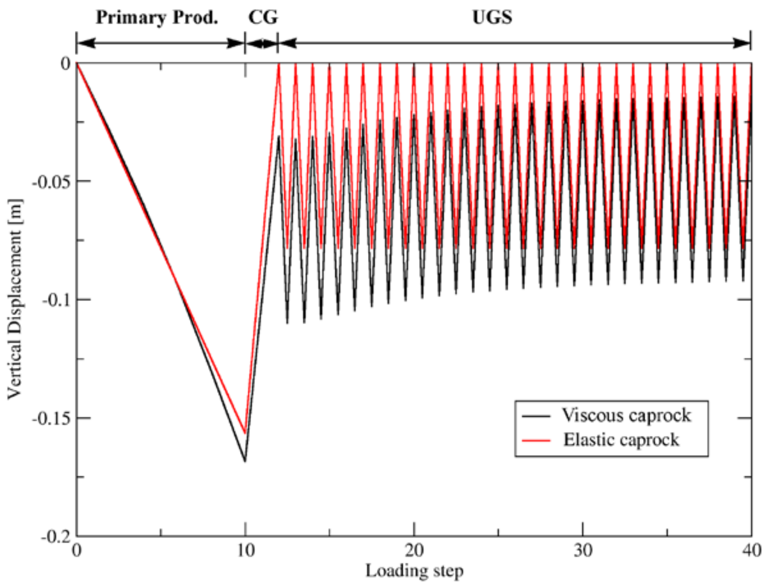

Figure 38 Scenario 9 (mechanism 5): vertical displacements over a time window of 40 loading steps (40 years) in case of elastic and viscous caprock. The plot references to the location (x, y, z) = (0.0, 0.0, 0.0) m, i.e., above the center of the reservoir.

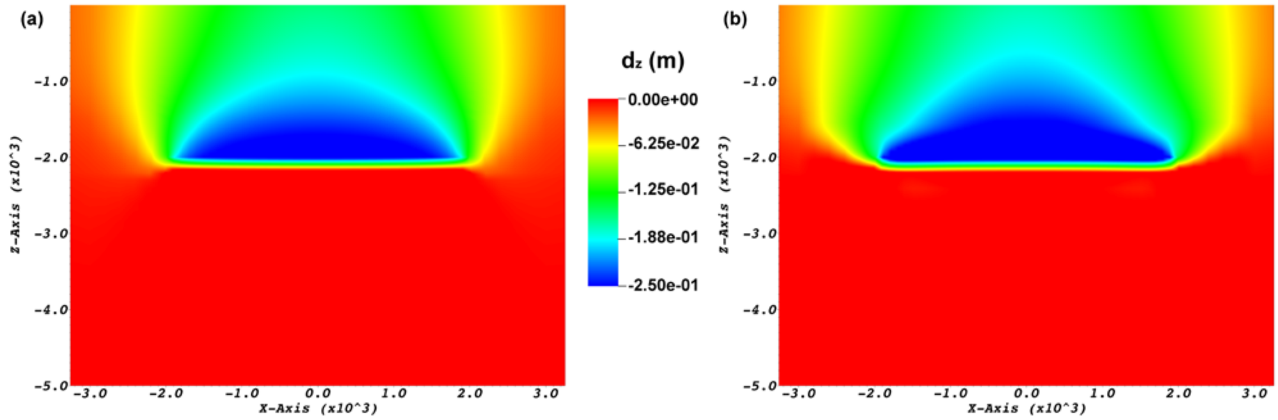

Figure 39 Scenario 9 (mechanism 5): distribution of the vertical displacements (d_z) on a vertical cross-section normal to the y-axis at loading step 10 (10 years) for (a) elastic and (b) viscous caprock. Negative displacements mean subsidence.

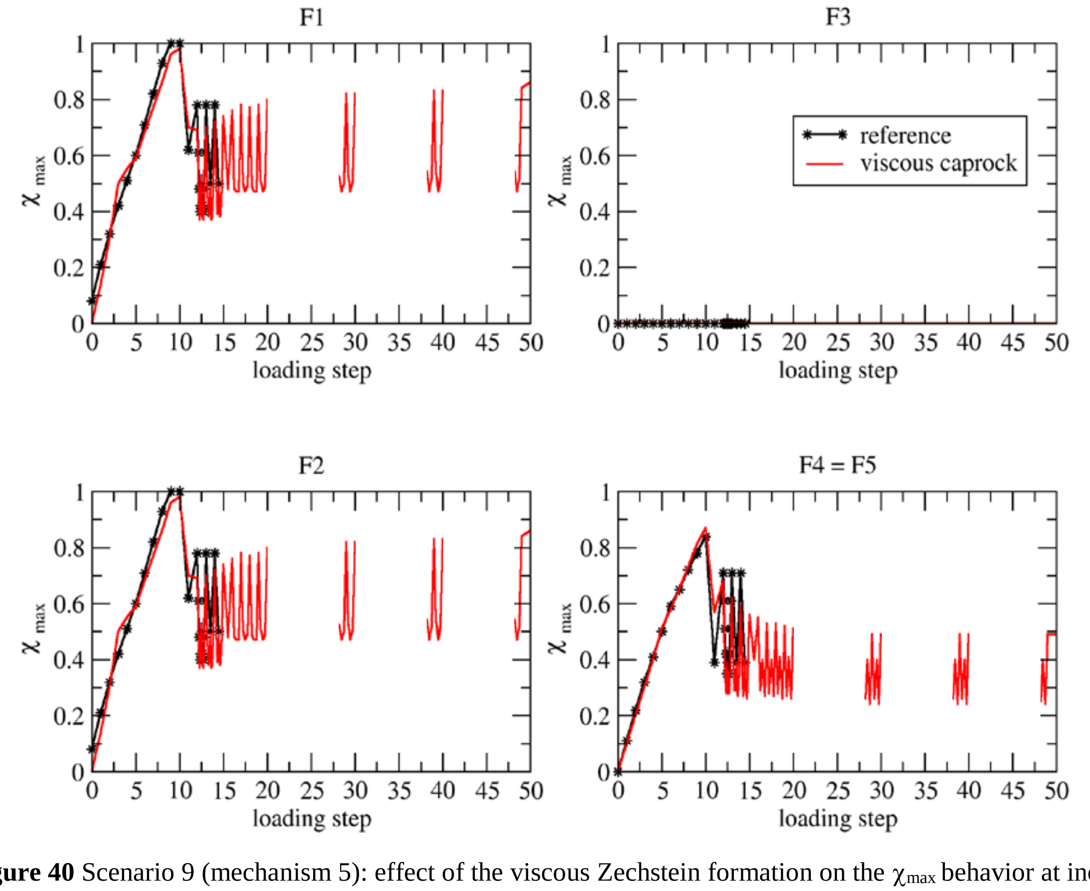

Figure 40 Scenario 9 (mechanism 5): effect of the viscous Zechstein formation on the χ_{max} behavior at increasing loading steps for each fault. Notice that due to symmetry F4 and F5 behave identically. Moreover, at the loading step = 0 (initial conditions) χ_{max} = 0 for F1 and F2 although inclined because $M_1 = M_2 = 1$ (isotropic initial stress regime) for the viscous salt material.

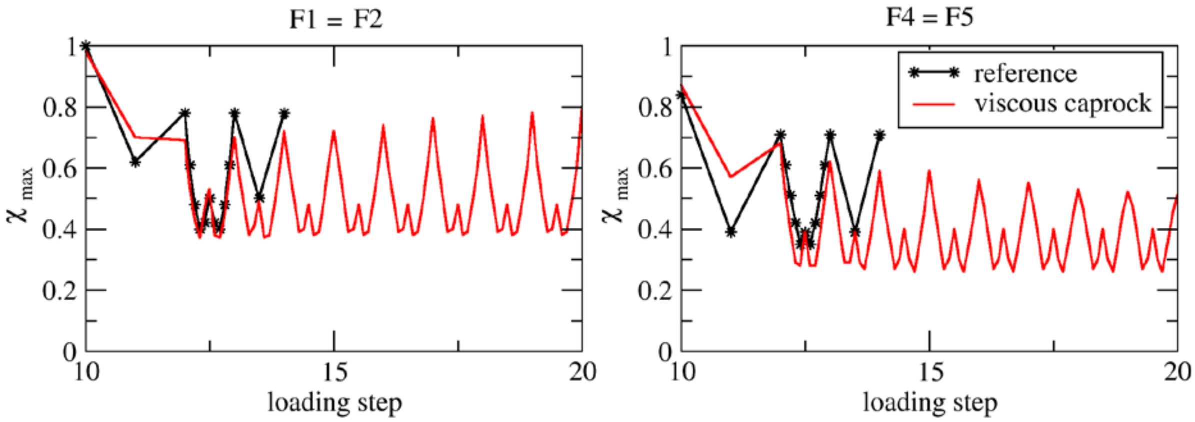

Figure 41 Scenario 9 (mechanism 5): zoom of the χ_{max} (element-based) behaviour for the loading steps between 10 and 20. Notice that the second UGS cycle is simulated with a 6-month time step in the reference (elastic caprock) case.

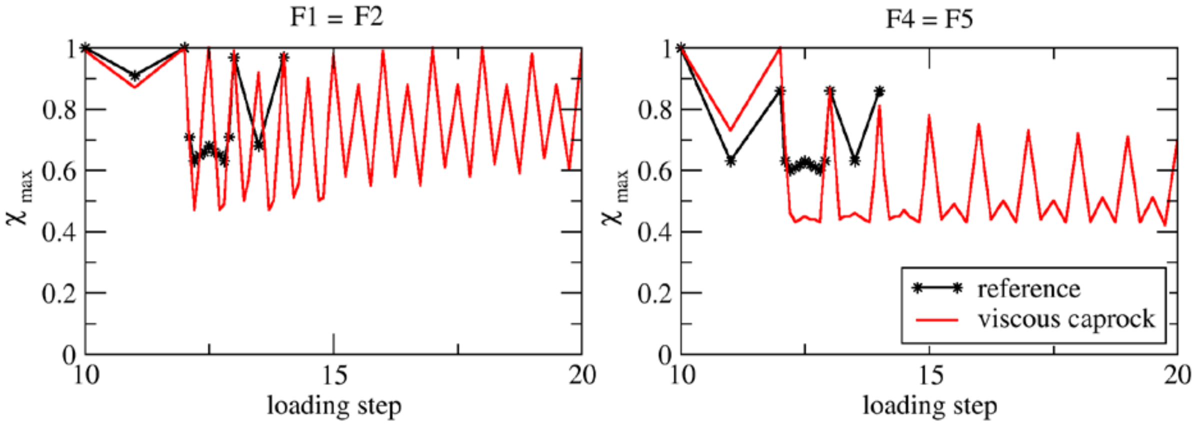

Figure 42 Scenario 9 (mechanism 5): zoom of the χ_{max} (node-based) behaviour for the loading steps between 10 and 20. Notice that the second UGS cycle is simulated with a 6-month time step in the reference (elastic caprock) case.

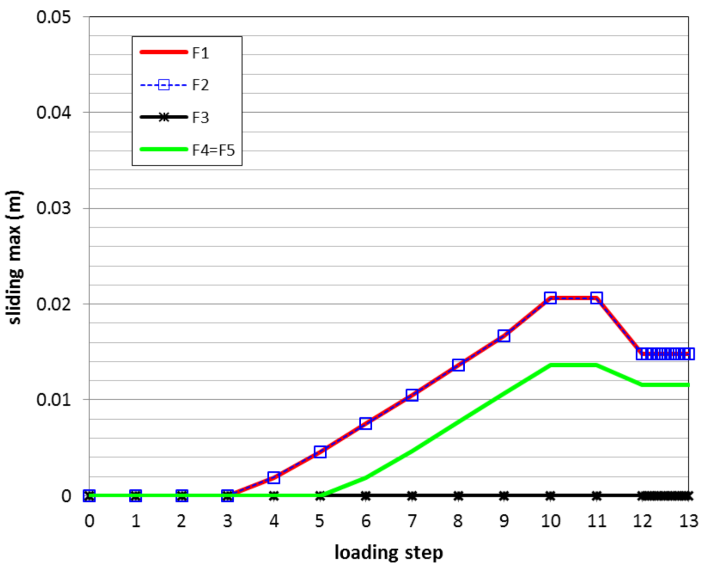

Figure 43 Scenario 9 (mechanism 5): maximum sliding δ_{max} for the case investigating the effect of the viscous behavior of the Zechstein formation. The values remain almost constant until the end of the simulated time interval (40 years).

4.3 Combination 1 (Scenario 10)

Scenario 10 is based on the following hypotheses:

- *c* = 0 bar;
- F3 fault dip = +65°;
- compartment offset = 100 m (instead of 200 m as simulated in WP3).

The values adopted in reference test case (Table 1) have been used for the other parameters. The simulation outcome in terms of χ_{max} is shown in Figure 44. The results highlight that critical conditions for fault reactivation develop earlier during primary production but, similarly to the reference case, $\chi_{max} \leq 0.8$ during CG and UGS phases. Because of the loss of symmetry, F2 is more stressed than F1 and χ_{max} increases also on fault F3, with values up to 0.8 at the end of primary production, CG, and UGS injection phase.

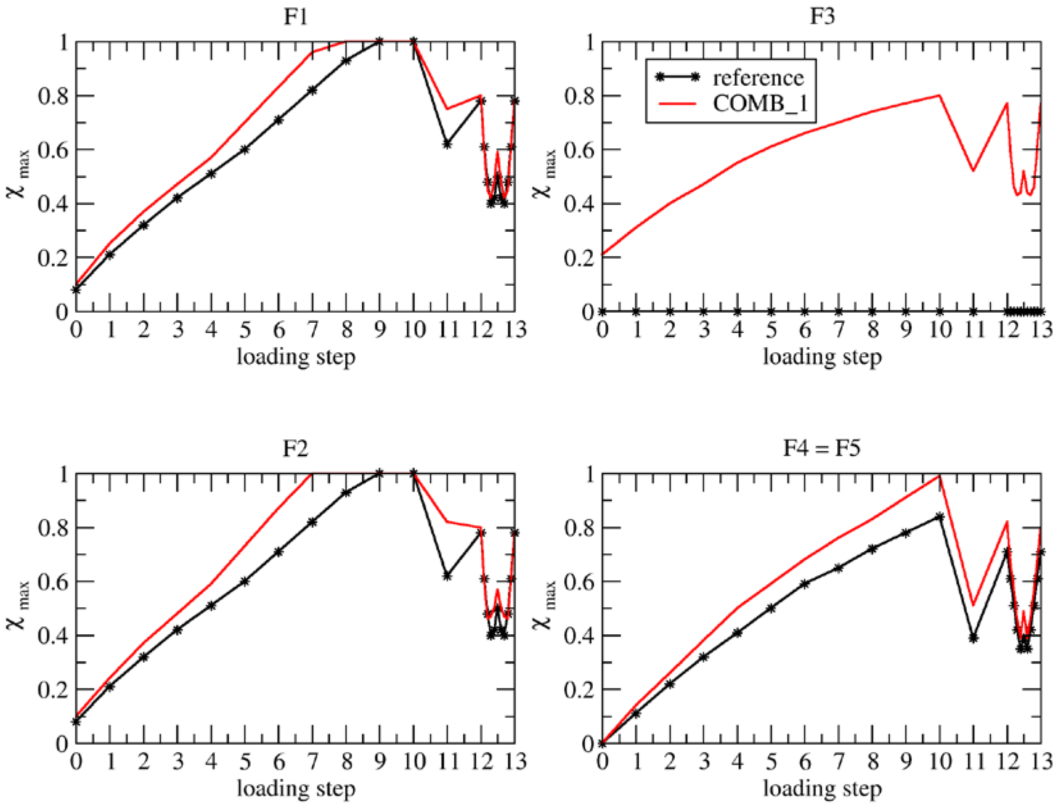

Figure 44 Scenario 10 (updated combination 1): χ_{max} versus loading steps for each fault. Note that due to symmetry F4 and F5 behave identically.

The time behaviour of δ_{max} is shown in Figure 45. Notice that F2 slides more than F1.

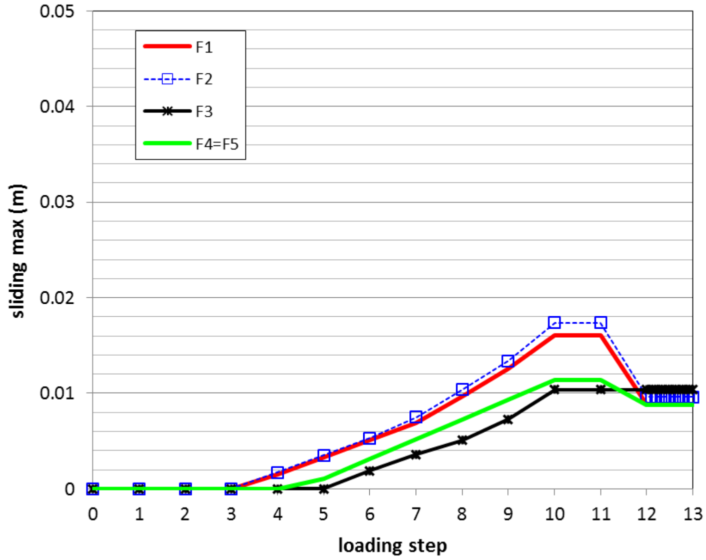

Figure 45 Scenario 10 (updated combination 1): maximum sliding δ_{max} versus time.

4.4 Combination 2 (Scenario 11)

Scenario 11 is based on the following hypotheses:

- static friction angle = 20°;
- F3 dip angle = +65°;
- viscous caprock;
- compartment offset = 100 m (instead of 200 m as simulated in WP3).

The values adopted in reference test case (Table 1) have been used for the other parameters. The simulation outcome in terms of χ_{max} is shown in Figure 46. Comparison between Figure 44 and Figure 46 points out that this combination is more critical than the previous one, mainly during primary production. The behaviour of δ_{max} is provided in Figure 47. All the faults slide during CG too, mainly during the last period between loading step 11 and 12, in the direction opposite than that occurred during primary production. Faults F1, F2, and F3 slightly slide also at the end of the UGS injection phase.

Figure 48 shows the stress path for node 1920. Because of the 100-m offset of block 2, node 2665 is located in the middle of the reservoir thickness, i.e. in an almost symmetric condition, where negligible shear stress develops. Because node 1920 is 100 m higher than 2665, the initial shear condition is characterized by a smaller σ value. During CG The stress state remains on the yield bound over the entire CG phase, with a critical condition that is reached at the end of the UGS production and injection phases. Because of this and the viscous over- and side-burden the stress path during UGS results quite complex with a trend far from elastic.

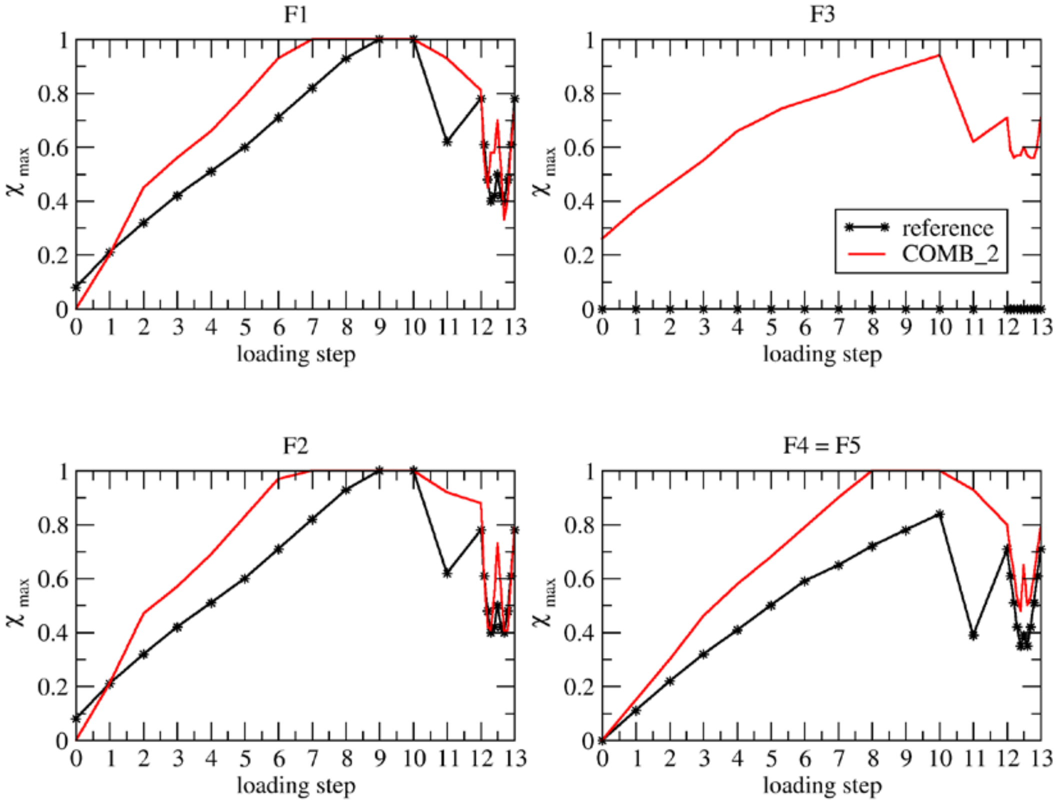

Figure 46 Scenario 11 (updated combination 2): χ_{max} versus loading steps for each fault. Note that due to symmetry F4 and F5 behave identically.

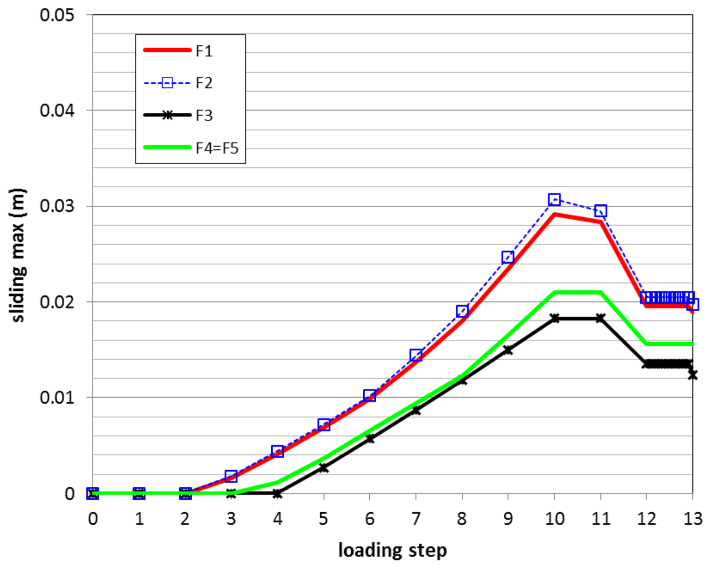

Figure 47 Scenario 11 (updated combination 2): maximum sliding δ_{max} versus time.

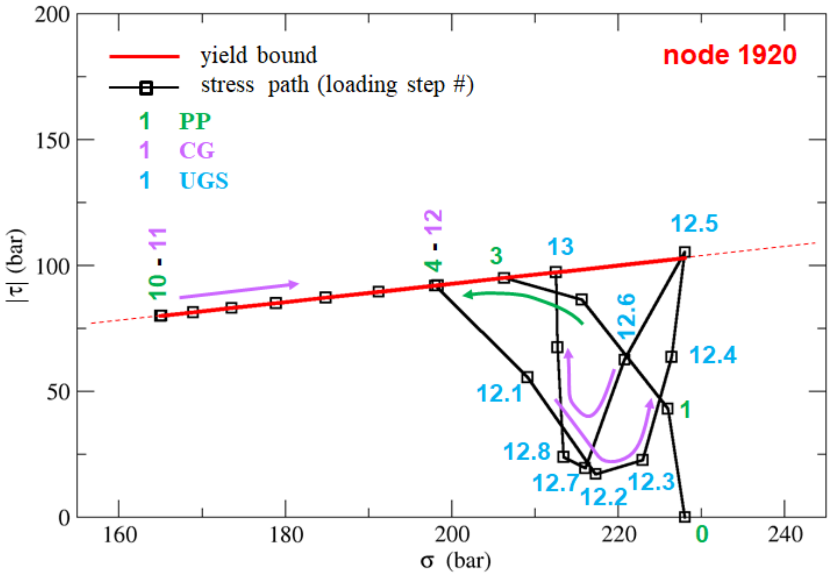

Figure 48 Scenario 11: stress path $|\boldsymbol{\tau}|$ vs $\boldsymbol{\sigma}$ for the F2 fault node 1920. The red line represents the yield bound and the numbers the various loading steps. Different colours are used for primary production (PP, loading steps #1 – 10), cushion gas (CG, loading steps #11 – 12), and underground gas storage (UGS, loading steps #12.1 – 13).

4.5 Combination 4 (Scenario 12)

This is a new parameter combination, not explored in WP3. Scenario 12 is based on the following hypotheses:

- *c* = 0 bar;
- F3 dip angle = +65°;
- viscous caprock;
- compartment offset = 100 m.

With respect to scenario 11, here cohesion is reduced from the reference value (20 bar) to 0 bar and, conversely, the static friction angle is increased from 20° to the reference value 30°. The values adopted in reference test case (Table 1) have been used for the other parameters.

The simulation outcome in terms of (element-based) χ_{max} is shown in Figure 49. Generally, the criticality index χ_{max} is a bit smaller than in Scenario 11, meaning that a 20-bar decrease of cohesion plays a smaller effect than the 10° decrease of the friction angle. This is supported by the results of Scenario 5 (Figure 24). The unusual behaviour of χ_{max} on fault F3 is due to the superposition of two factors: i) at loading step 6 the fault nodes at the reservoir top start sliding, yielding a stress redistribution; ii) a change of the element that experiences the most critical condition at loading steps 7 to 10. In fact, a node-based computation of χ_{max} does not reveal any unexpected fluctuation of the criticality index behaviour (Figure 50). The behaviour of δ_{max} is provided in Figure 51.

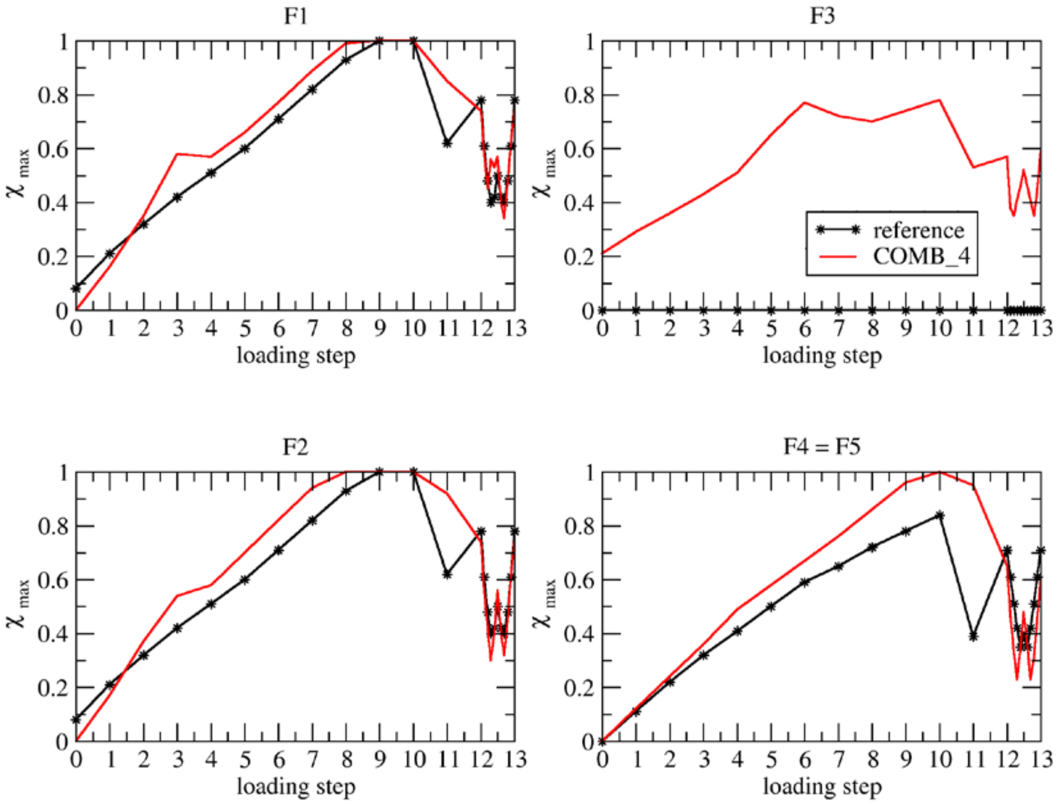

Figure 49 Scenario 12 (combination 4): element-based χ_{max} versus loading steps. Note that due to symmetry F4 and F5 behave identically.

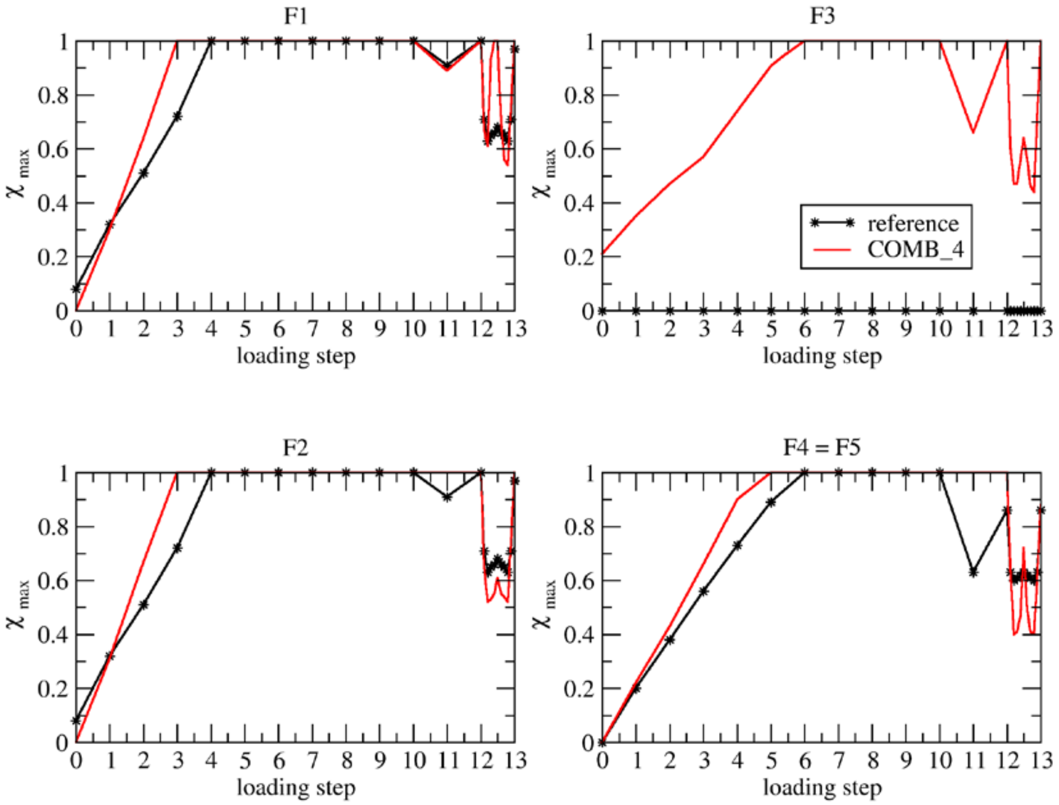

Figure 50 Scenario 12 (combination 4): nodal-based χ_{max} versus loading steps. Note that due to symmetry F4 and F5 behave identically.

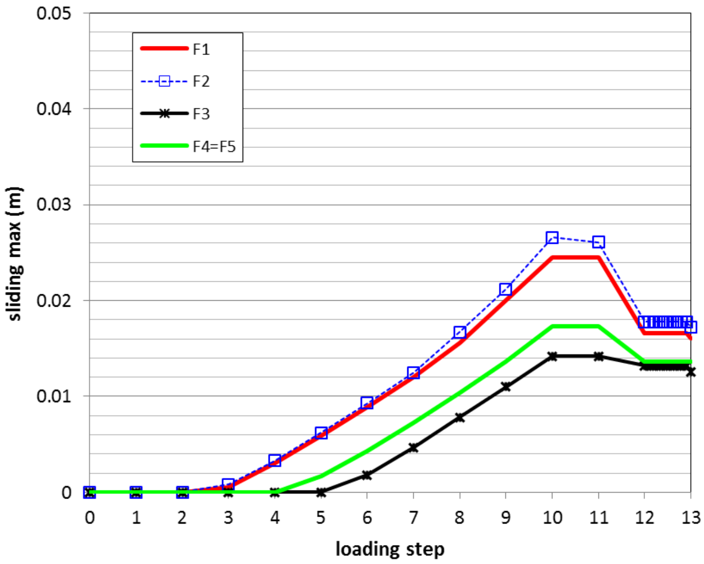

Figure 51 Scenario 12 (combination 4): maximum sliding δ_{max} versus time.

Similar with Scenario 11, the faults slide during CG too, mainly during the last period between loading step 11 and 12, in the direction opposite than that occurred during primary production. Faults F1, F2, and F3 slightly slide also at the end of the UGS injection phase.

4.6 Combination 5 (Scenario 13)

Scenario 13 is based on the following hypotheses:

- c = 0 bar;
- F3 fault dip = +65°;
- compartment offset = 100 m;
- $E_{reservoir}$ = 20 GPa.

The values adopted in reference test case (Table 1) have been used for the other parameters. The simulation outcome in terms of χ_{max} is shown in Figure 52. Comparison between Figure 44 (Scenario 10) and Figure 52 clearly shows the stabilizing effect exerted by the increase of the reservoir stiffness and, simultaneously, by the less heterogeneous distribution of the mechanical properties in the subsurface. The differences during CG and UGS phases are smaller. The behaviour of δ_{max} is provided in Figure 53. Only faults F1 and F2 slide during CG; no fault activation develops during UGS.

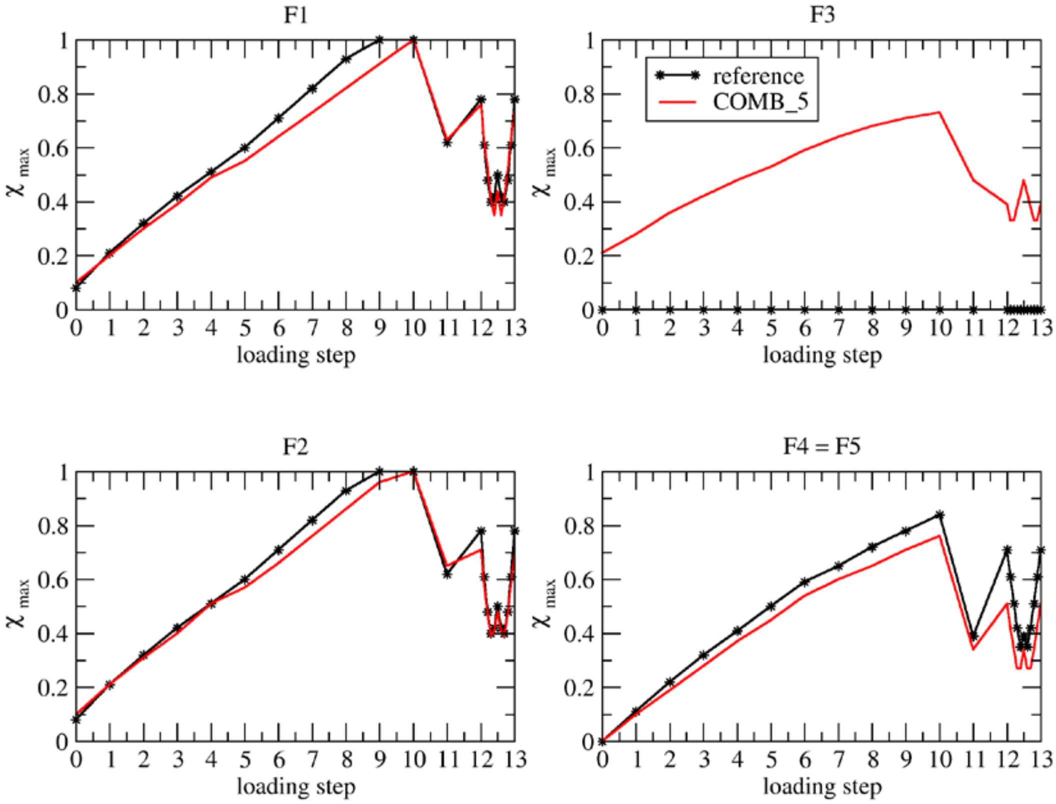

Figure 52 Scenario 13 (combination 5): behaviour of χ_{max} versus loading steps. Note that due to symmetry F4 and F5 behave identically.

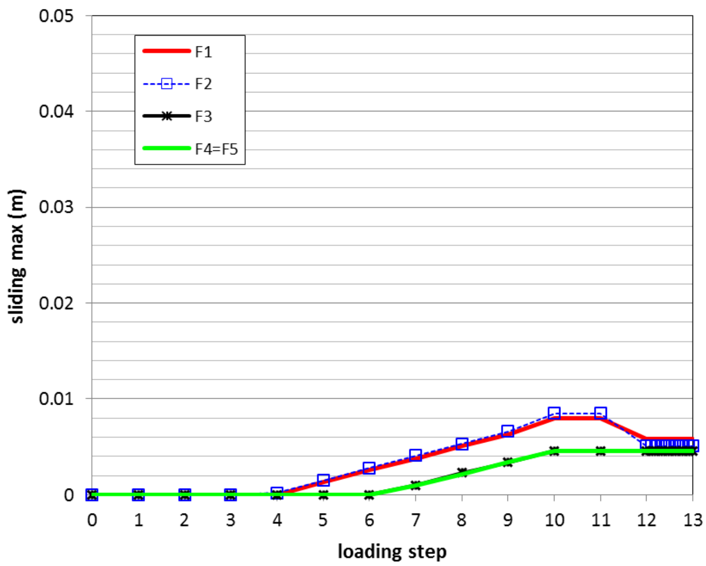

Figure 53 Scenario 13 (combination 5): maximum sliding δ_{max} versus time.

4.7 Combination 6 (Scenario 14)

Scenario 14 is based on the following hypotheses:

- static friction angle = 20°;
- F3 dip angle = +65°;
- viscous caprock;
- compartment offset = 100 m;
- $E_{reservoir}$ = 20 GPa.

The values adopted in reference test case (Table 1) have been used for the other parameters. The simulation outcome in terms of χ_{max} is shown in Figure 54. Comparison between Figure 46 (Scenario 11) and Figure 54 reveals again that a reservoir stiffness larger and more similar to that of the caprock/sideburden reduces the possibility of fault reactivation. The behaviour of δ_{max} is provided in Figure 55.

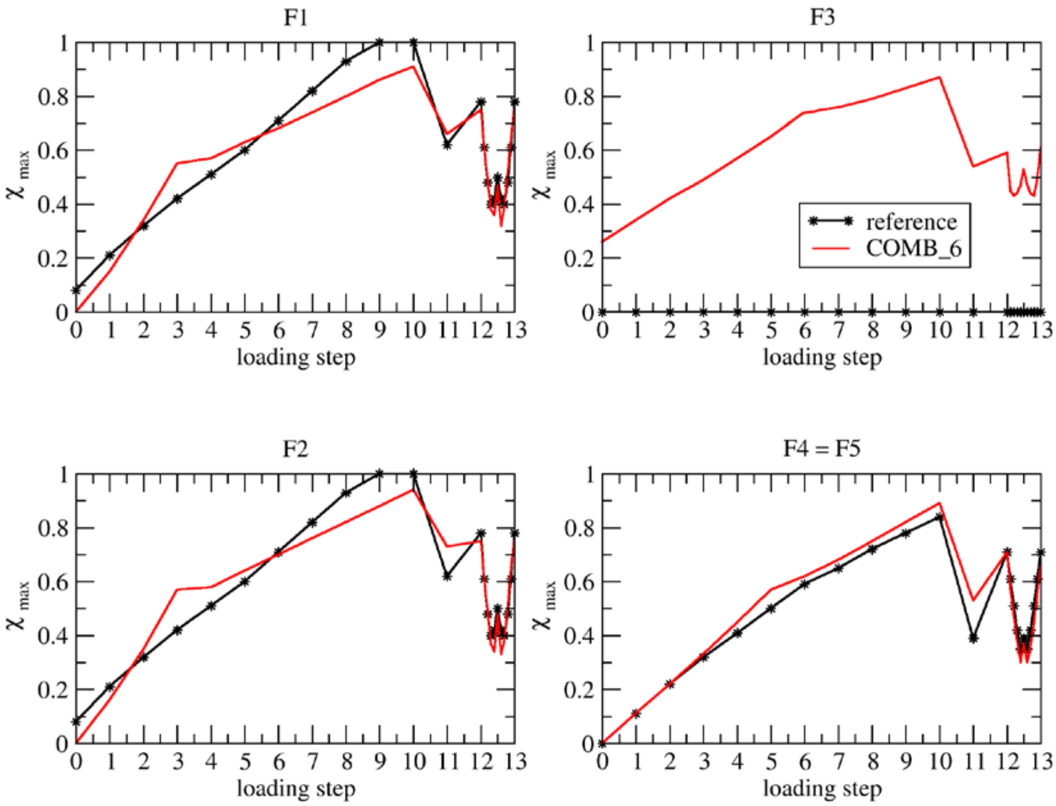

Figure 54 Scenario 14 (combination 6): behavior of χ_{max} versus loading steps. Note that due to symmetry F4 and F5 behave identically.

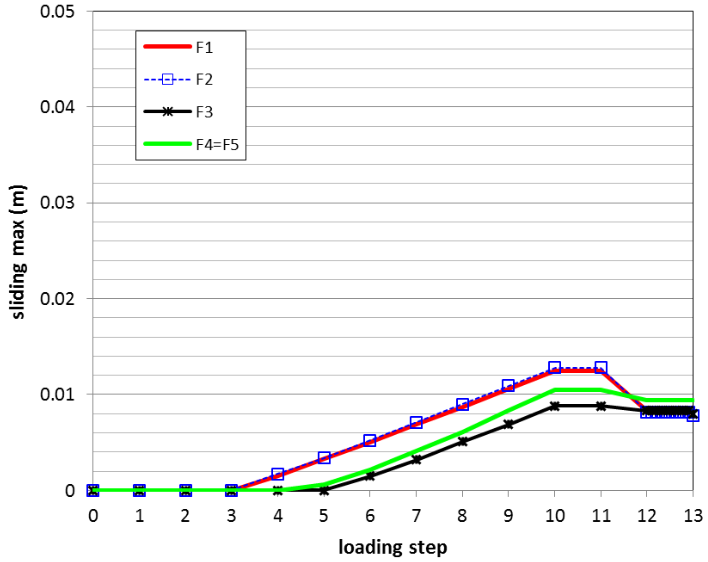

Figure 55 Scenario 14 (combination 6): maximum sliding δ_{max} versus time.

References

Gambolati, G., M. Ferronato, P. Teatini, R. Deidda and G. Lecca (2001), Finite element analysis of land subsidence above depleted reservoirs with pore pressure gradient and total stress formulations. International Journal for Numerical and Analytical Methods in Geomechanics, 25(4), 307-327.

Garipov, T. T., M. Karimi-Fard and H. A. Tchelepi (2016), Discrete fracture model for coupled flow and geomechanics. Computational Geosciences, 20(1), 149-160.

Annex I - |τ| and (node-based) χ at the end of primary production (l.s. = 10)

Scenario 1a

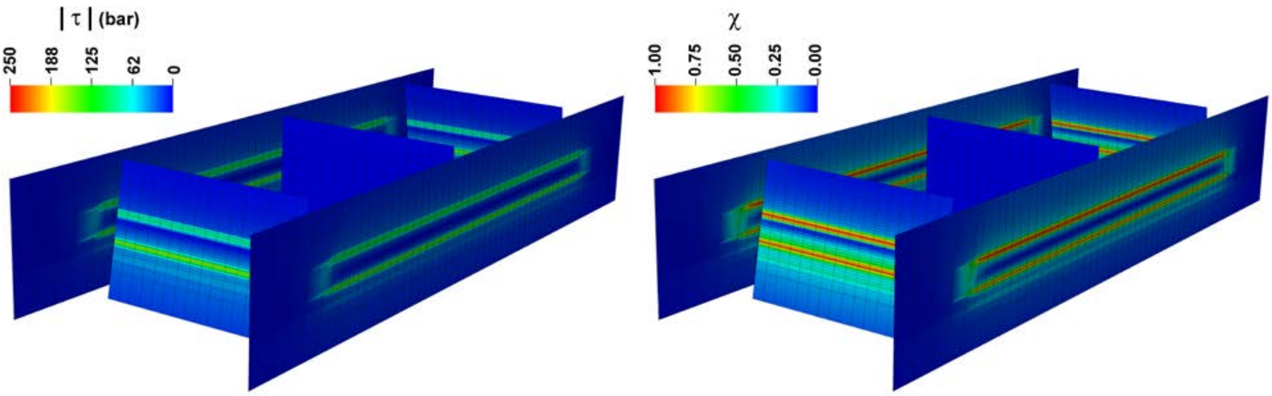

Scenario 1b

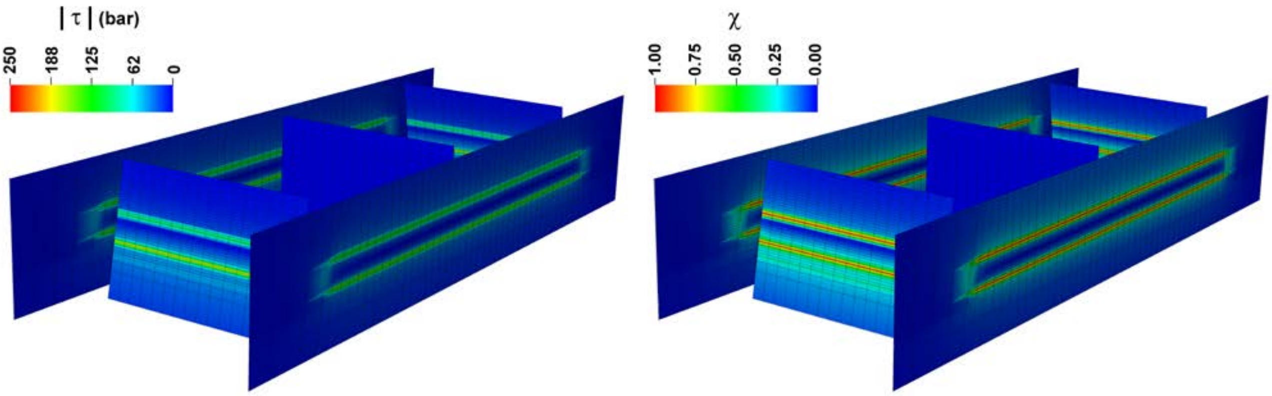

Scenario 1c

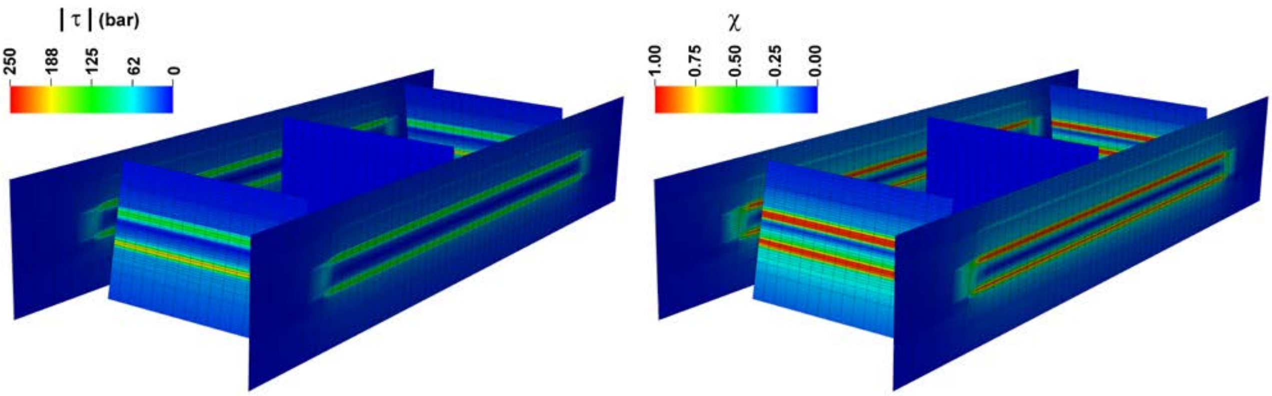

Scenario 1d

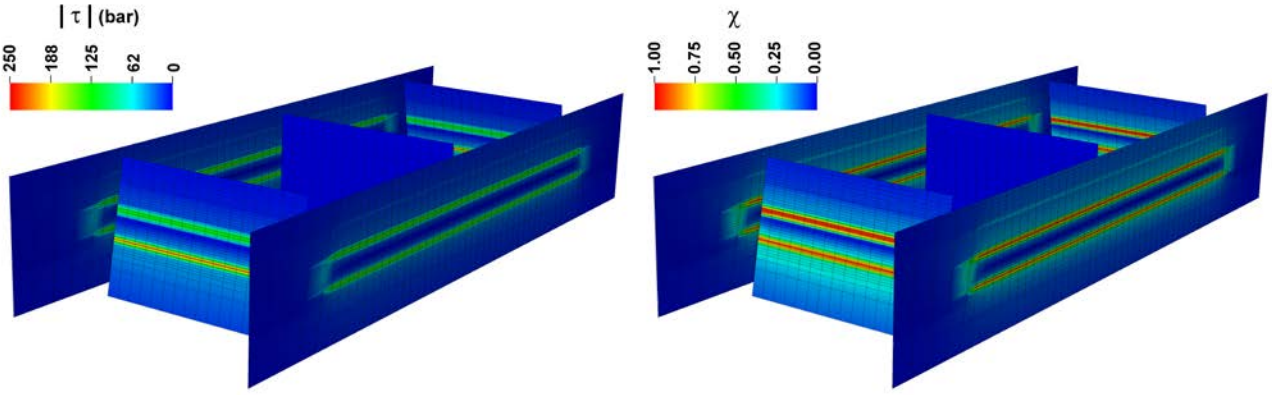

Scenario 2

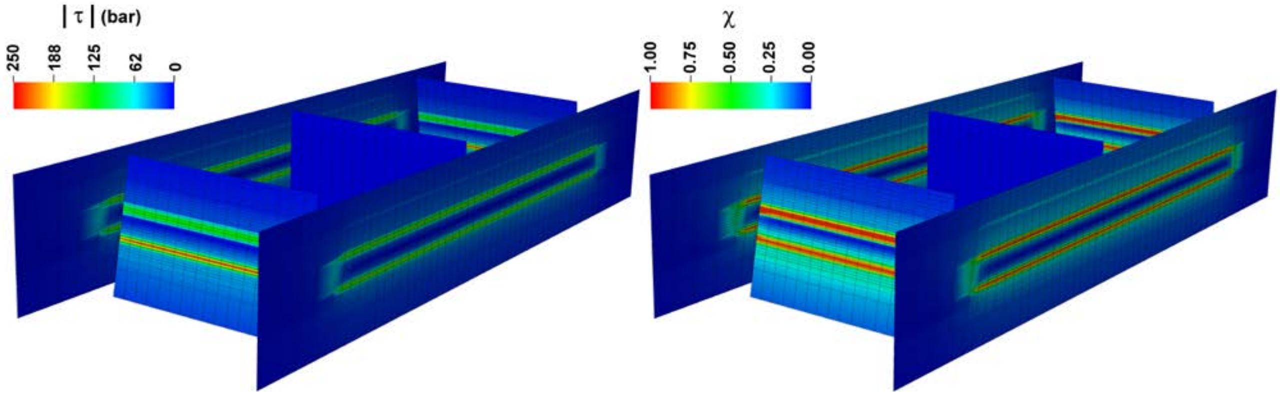

Scenario 3a

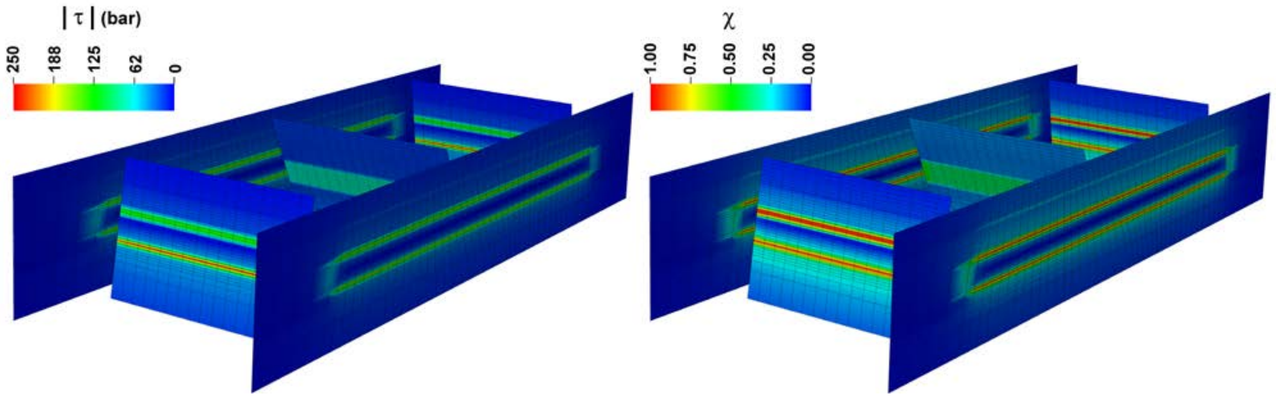

Scenario 3b

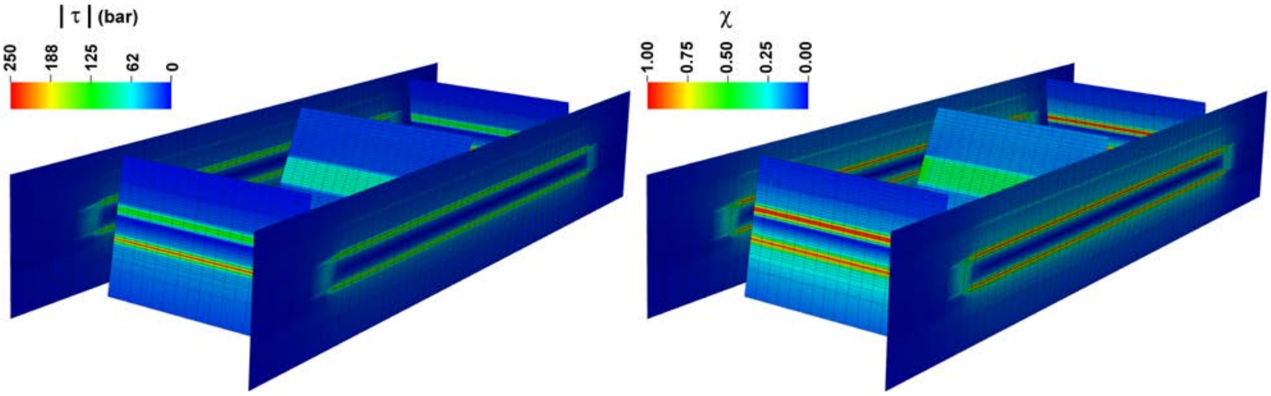

Scenario 3c

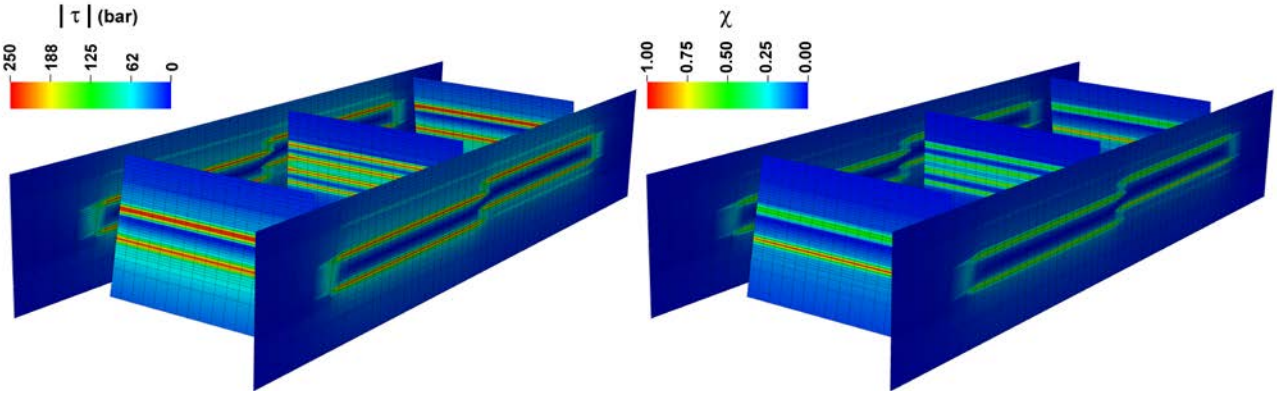

Scenario 3d

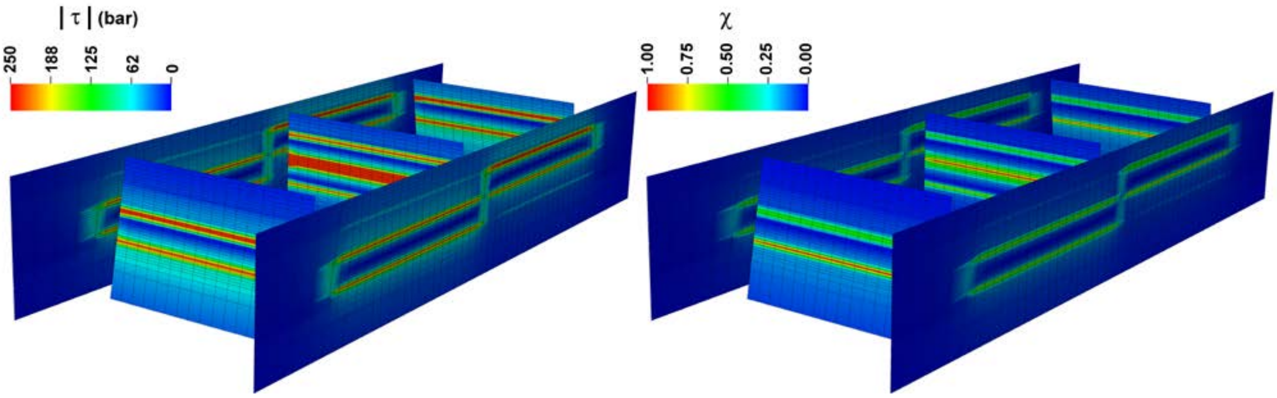

Scenario 4a

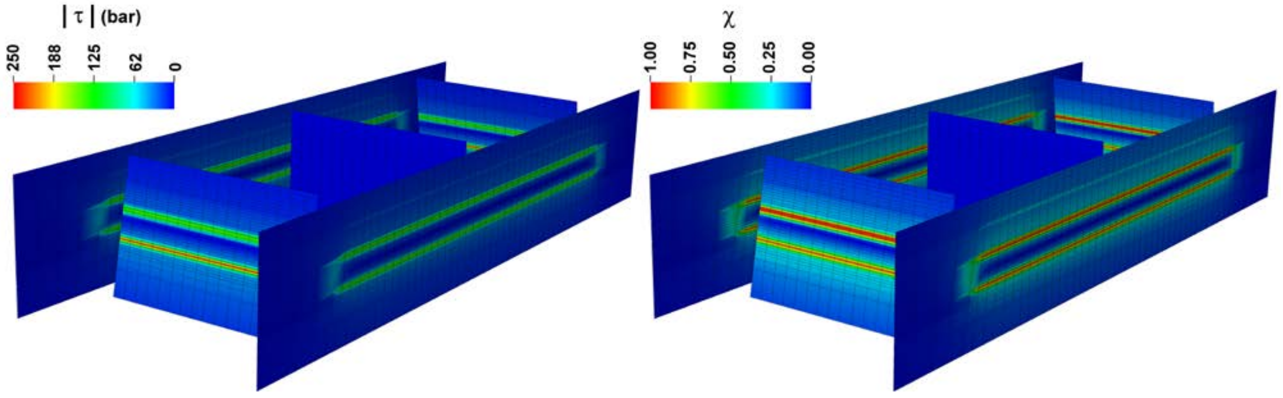

Scenario 4b

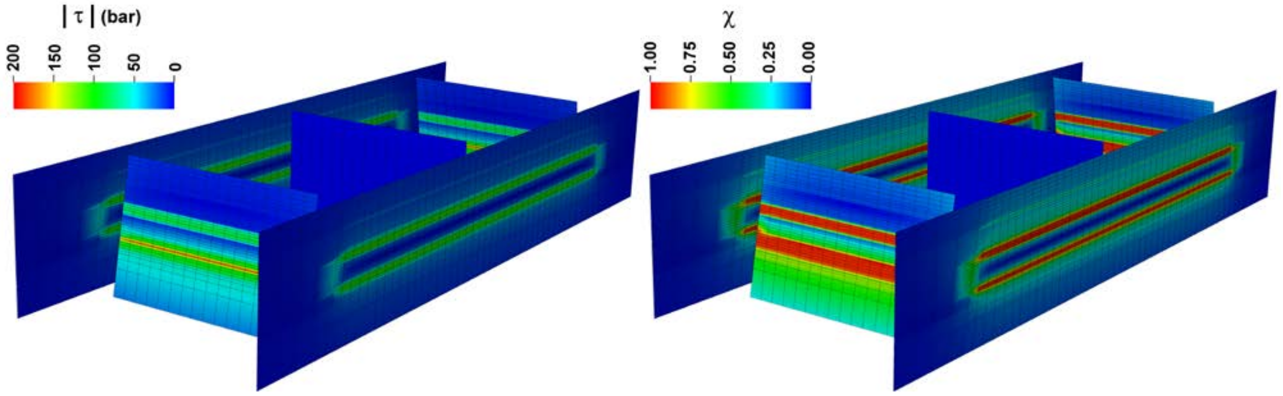

Scenario 5a

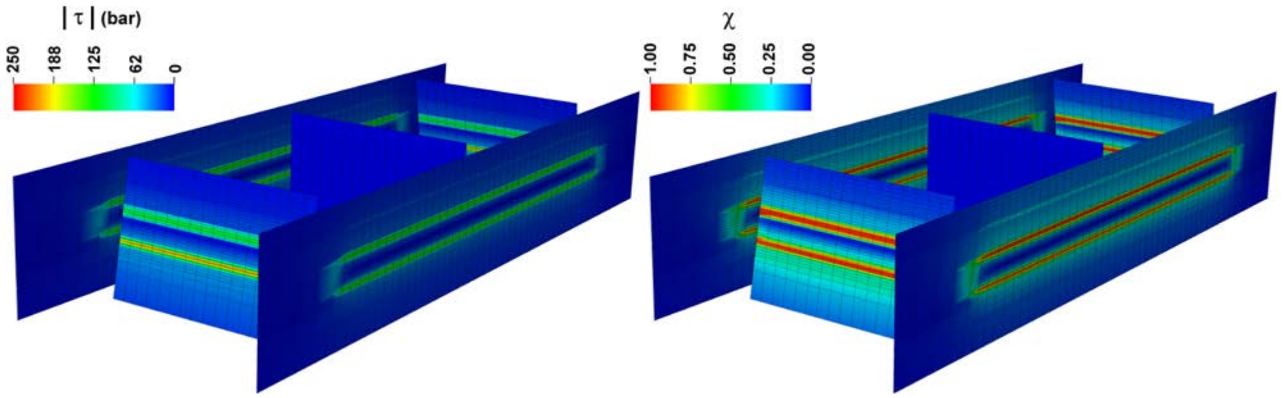

Scenario 5b

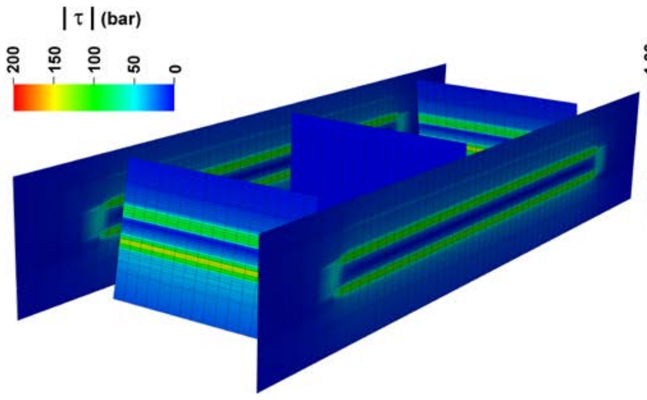

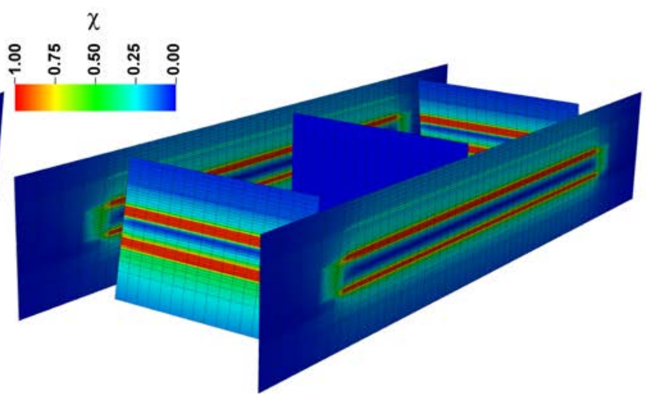

Scenario 5c

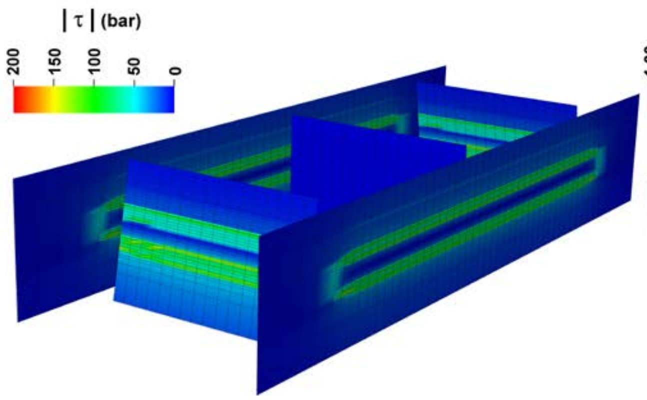

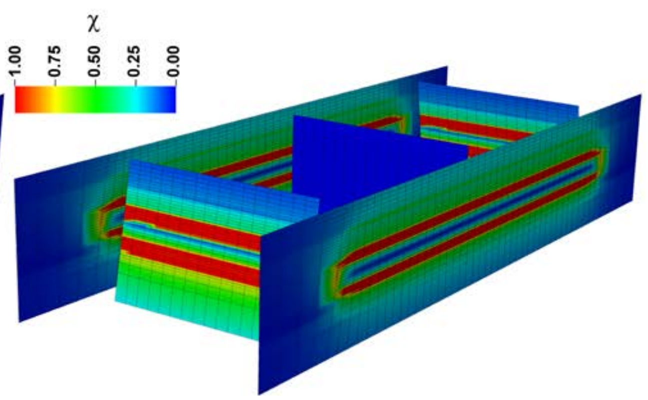

Scenario 5d

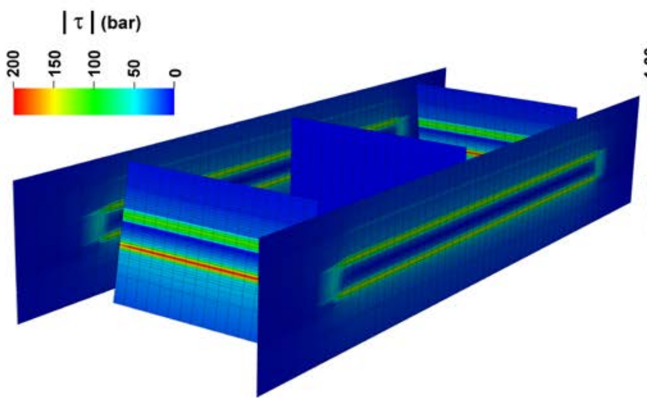

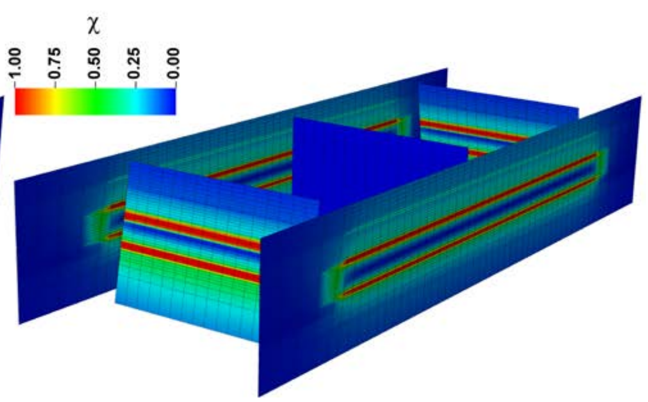

Scenario 6a

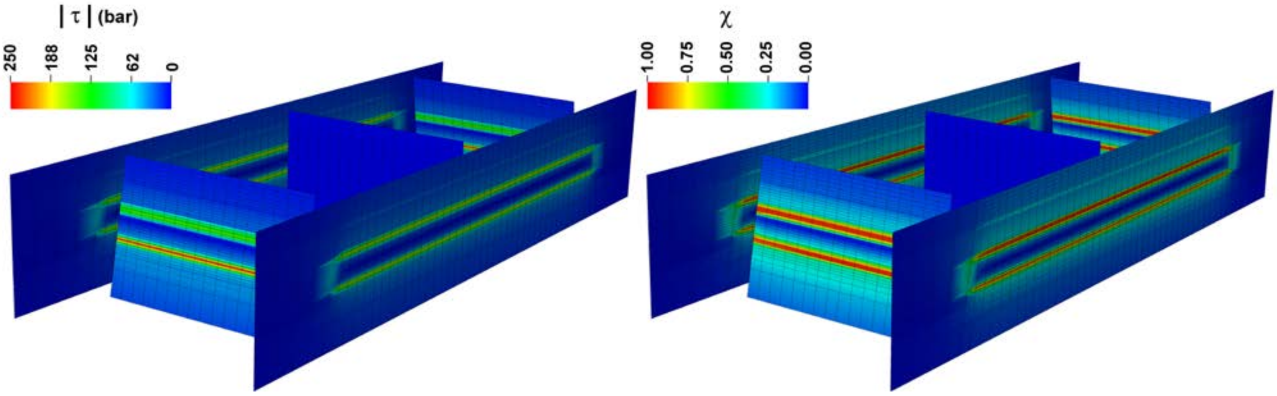

Scenario 6b

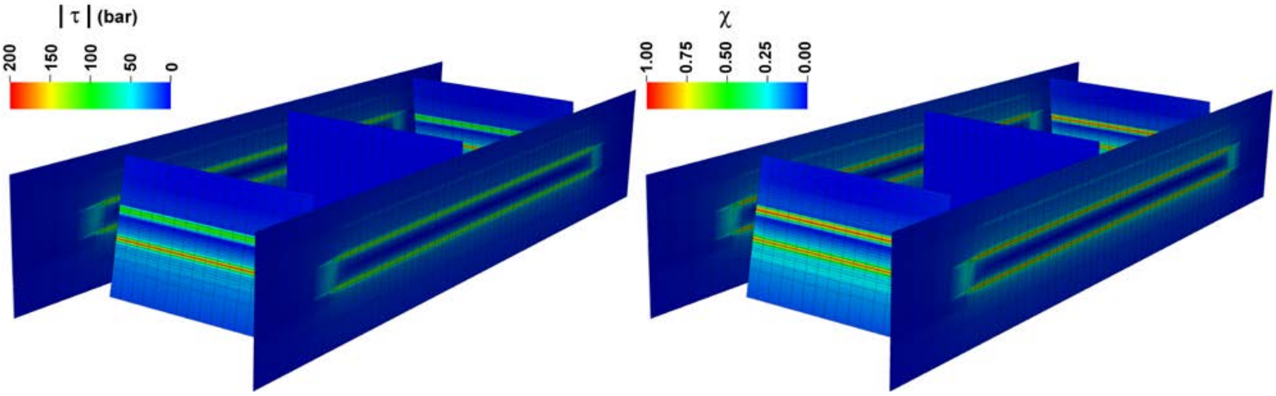

Scenarios 7a - 7b - 8

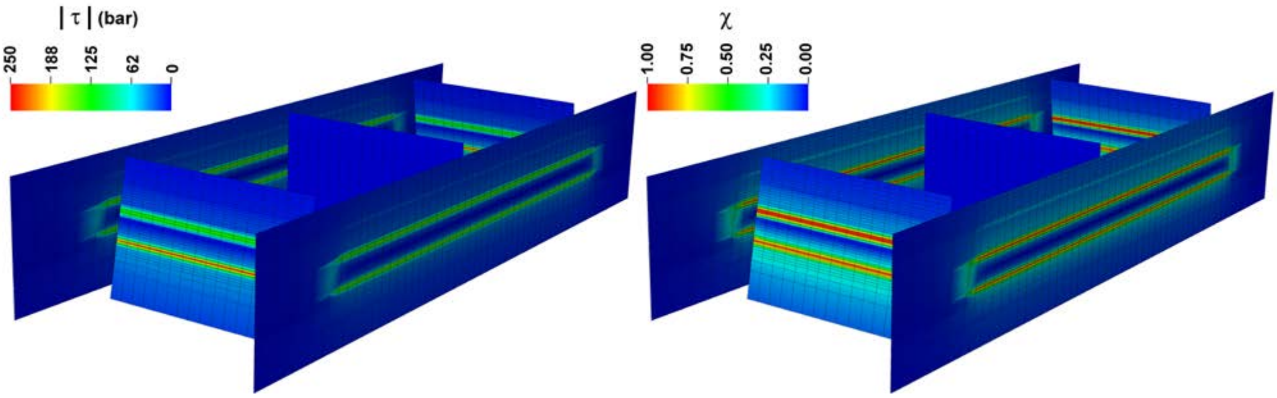

Scenario 9

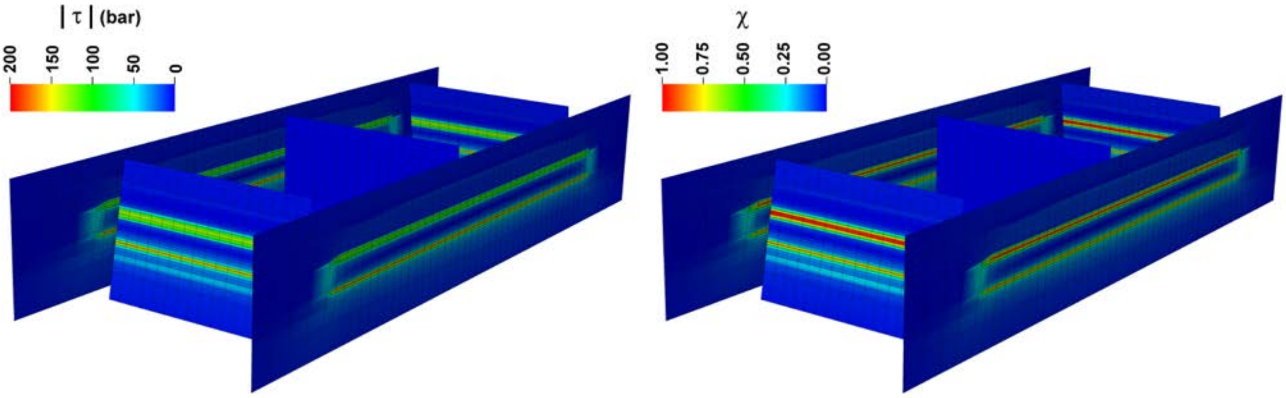

Scenario 10

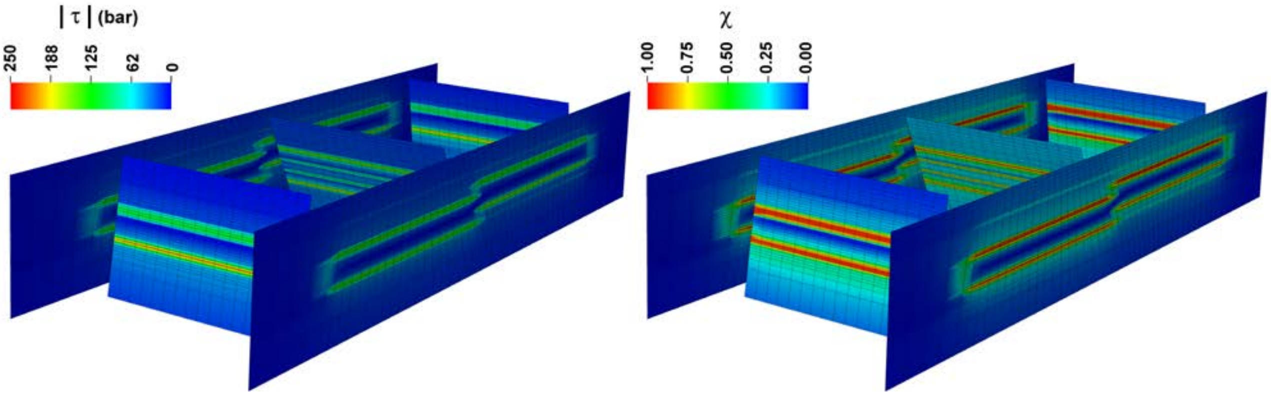

Scenario 11

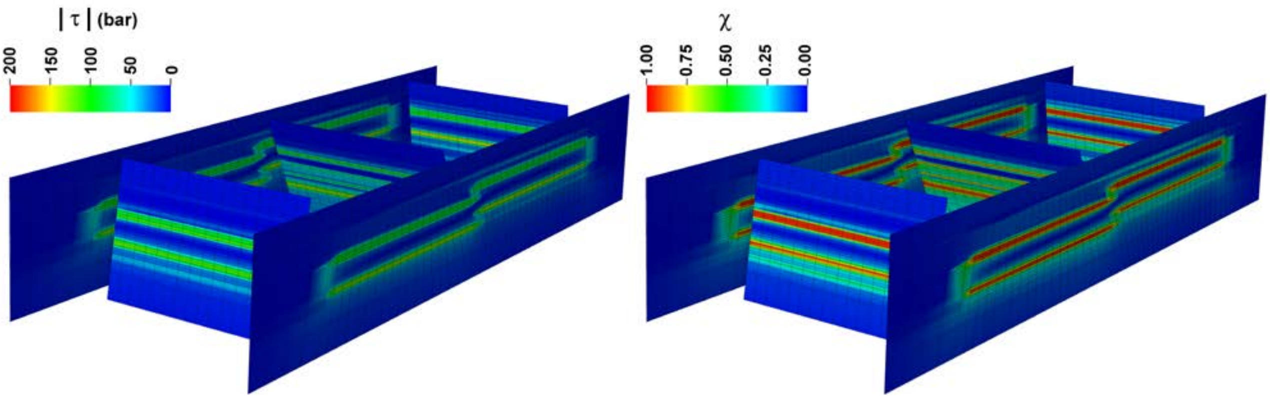

Scenario 12

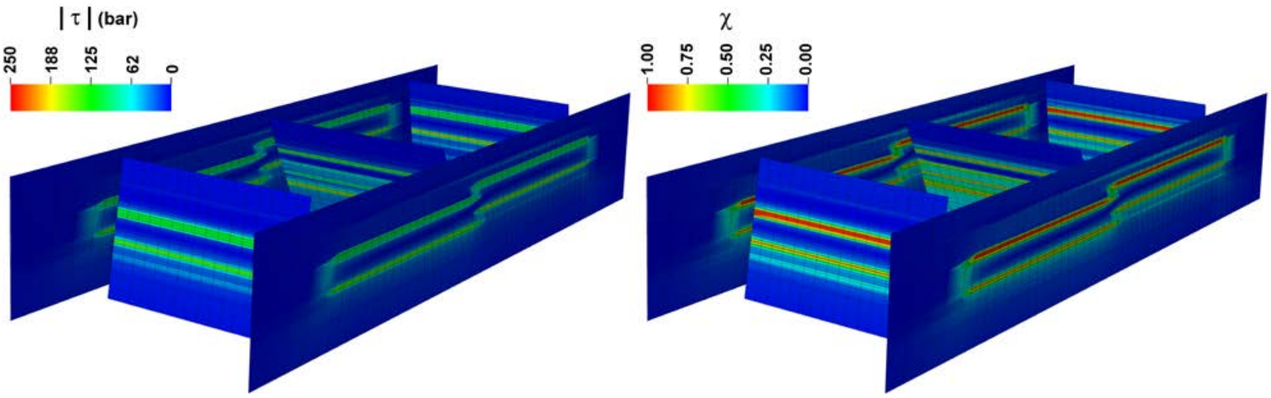

Scenario 13

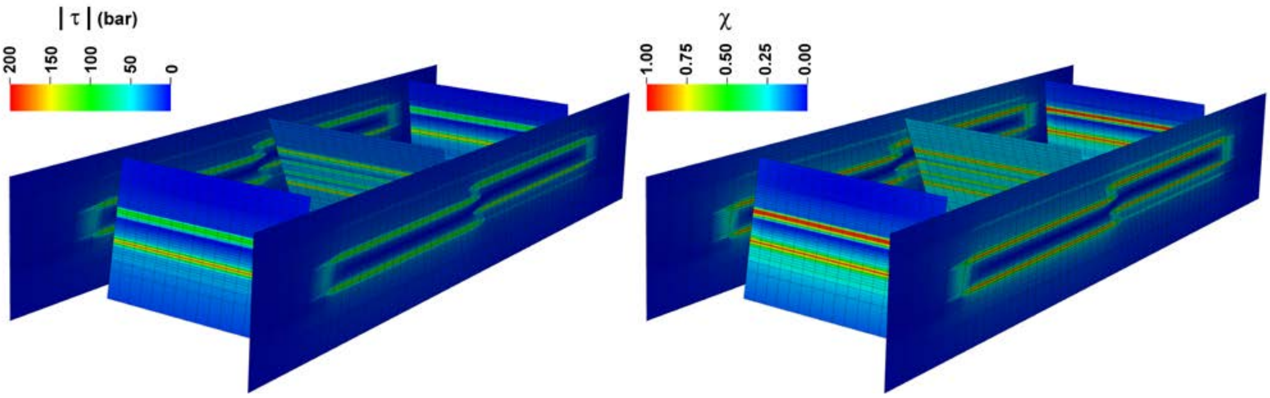

Scenario 14

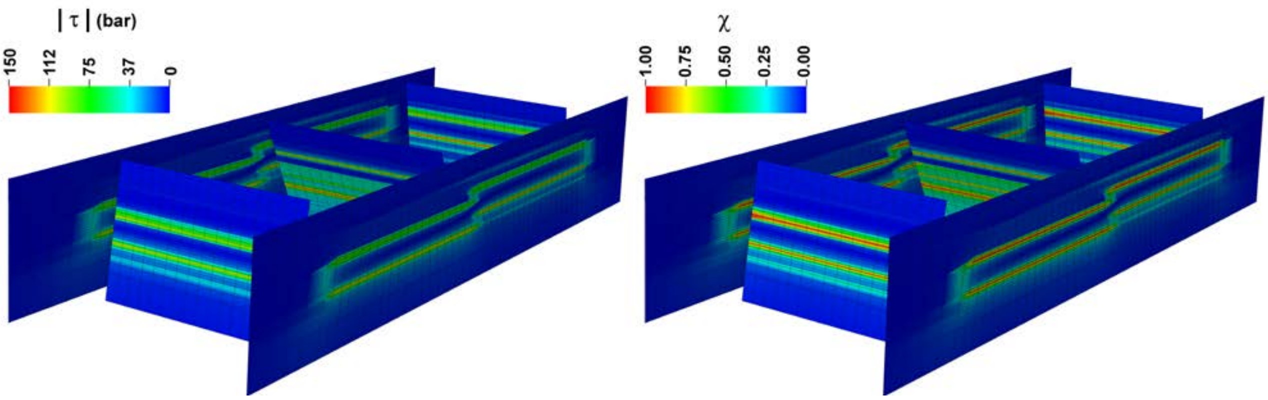

Annex II - t_a, t_{80}, and t_{50}

The critically stressed fault area is normalized over the fault length, thus in the following tables the active thickness t_a, the fault thickness with $\chi > 0.8$ (t_{80}) and $\chi > 0.5$ (t_{50}) are reported for each model simulation, fault and loading step. Note that the values derive directly form the simulator node-based computation. The IE element in the reservoir is 100m-wide by 20m-thick. Therefore, when a new row of nodes is activated, a 20m-thickness is added to the cumulative active thickness t_a. Due to fault boundary and fixed normalization factor, the computed thickness at activation of a new row might be slightly lower than 20 m. Notice that the activation of a row of elements requires that two adjacent nodes (along the same vertical) become active. In the t_a tables that follow, the condition of element activation is marked by yellow cells.

Scenario 1d - t_a

Scenario 1d				
Step	**F1**	**F2**	**F3**	**F4 = F5**
0.00	0.00	0.00	0.00	0.00
1.00	0.00	0.00	0.00	0.00
2.00	0.00	0.00	0.00	0.00
3.00	0.00	0.00	0.00	0.00
4.00	17.27	17.27	0.00	0.00
5.00	0.00	0.00	0.00	0.00
6.00	17.27	17.27	0.00	19.34
7.00	0.00	0.00	0.00	18.62
8.00	0.00	0.00	0.00	1.04
9.00	17.27	17.27	0.00	0.00
10.00	0.00	0.00	0.00	0.00
11.00	0.00	0.00	0.00	0.00
12.00	30.47	30.47	0.00	0.00
12.10	0.00	0.00	0.00	0.00
12.20	0.00	0.00	0.00	0.00
12.30	0.00	0.00	0.00	0.00
12.40	0.00	0.00	0.00	0.00
12.50	0.00	0.00	0.00	0.00
12.60	0.00	0.00	0.00	0.00
12.70	0.00	0.00	0.00	0.00
12.80	0.00	0.00	0.00	0.00
12.90	0.00	0.00	0.00	0.00
13.00	0.00	0.00	0.00	0.00

Scenario 1d - t_{80}

Scenario 1d				
Step	**F1**	**F2**	**F3**	**F4 = F5**
0.00	0.00	0.00	0.00	0.00
1.00	0.00	0.00	0.00	0.00
2.00	0.00	0.00	0.00	0.00
3.00	0.00	0.00	0.00	0.00
4.00	34.53	34.53	0.00	0.00
5.00	34.53	34.53	0.00	19.34
6.00	34.53	34.53	0.00	39.00
7.00	34.53	34.53	0.00	39.00
8.00	51.80	51.80	0.00	39.00
9.00	51.80	51.80	0.00	39.00
10.00	62.97	62.97	0.00	39.00
11.00	17.27	17.27	0.00	0.00
12.00	34.53	34.53	0.00	18.38
12.10	0.00	0.00	0.00	0.00
12.20	0.00	0.00	0.00	0.00
12.30	0.00	0.00	0.00	0.00
12.40	0.00	0.00	0.00	0.00
12.50	0.00	0.00	0.00	0.00
12.60	0.00	0.00	0.00	0.00
12.70	0.00	0.00	0.00	0.00
12.80	0.00	0.00	0.00	0.00
12.90	0.00	0.00	0.00	0.00
13.00	34.53	34.53	0.00	18.38

Scenario 1d - t_{50}

Scenario 1d				
Step	**F1**	**F2**	**F3**	**F4 = F5**
0.00	0.00	0.00	0.00	0.00
1.00	0.00	0.00	0.00	0.00
2.00	15.23	15.23	0.00	0.00
3.00	34.53	34.53	0.00	19.34
4.00	34.53	34.53	0.00	39.00
5.00	34.53	34.53	0.00	39.00
6.00	34.53	34.53	0.00	39.00
7.00	51.80	51.80	0.00	39.00
8.00	84.29	84.29	0.00	39.00
9.00	103.58	103.58	0.00	76.96
10.00	103.58	103.58	0.00	97.92
11.00	69.05	69.05	0.00	37.96
12.00	51.80	51.80	0.00	57.27
12.10	51.80	51.80	0.00	38.65
12.20	19.30	19.30	0.00	35.76
12.30	34.52	34.52	0.00	19.31
12.40	34.52	34.52	0.00	36.92
12.50	34.52	34.52	0.00	37.96
12.60	34.52	34.52	0.00	36.92
12.70	34.52	34.52	0.00	19.31
12.80	19.30	19.30	0.00	35.76
12.90	51.80	51.80	0.00	38.65
13.00	51.80	51.80	0.00	57.27

Scenario 2 - t_a

Scenario 2 (Biot)				
Step	**F1**	**F2**	**F3**	**F4 = F5**
0.00	0.00	0.00	0.00	0.00
1.00	0.00	0.00	0.00	0.00
2.00	0.00	0.00	0.00	0.00
3.00	0.00	0.00	0.00	0.00
4.00	17.27	17.27	0.00	0.00
5.00	15.23	15.23	0.00	0.00
6.00	2.03	2.03	0.00	19.34
7.00	0.00	0.00	0.00	19.66
8.00	17.27	17.27	0.00	0.00
9.00	0.00	0.00	0.00	0.00
10.00	2.03	2.03	0.00	0.00
11.00	0.00	0.00	0.00	0.00
12.00	34.53	34.53	0.00	16.45
12.10	0.00	0.00	0.00	0.00
12.20	0.00	0.00	0.00	0.00
12.30	0.00	0.00	0.00	0.00
12.40	0.00	0.00	0.00	0.00
12.50	0.00	0.00	0.00	0.00
12.60	0.00	0.00	0.00	0.00
12.70	0.00	0.00	0.00	0.00
12.80	0.00	0.00	0.00	0.00
12.90	0.00	0.00	0.00	0.00
13.00	0.00	0.00	0.00	0.00

Scenario 2 - t_{80}

Scenario 2 (Biot)				
Step	**F1**	**F2**	**F3**	**F4 = F5**
0.00	0.00	0.00	0.00	0.00
1.00	0.00	0.00	0.00	0.00
2.00	0.00	0.00	0.00	0.00
3.00	17.27	17.27	0.00	0.00
4.00	34.53	34.53	0.00	0.00
5.00	34.53	34.53	0.00	37.96
6.00	34.53	34.53	0.00	39.00
7.00	41.64	41.64	0.00	39.00
8.00	51.80	51.80	0.00	39.00
9.00	53.83	53.83	0.00	39.00
10.00	73.12	73.12	0.00	51.50
11.00	17.27	17.27	0.00	0.00
12.00	34.53	34.53	0.00	19.34
12.10	0.00	0.00	0.00	0.00
12.20	0.00	0.00	0.00	0.00
12.30	0.00	0.00	0.00	0.00
12.40	0.00	0.00	0.00	0.00
12.50	0.00	0.00	0.00	0.00
12.60	0.00	0.00	0.00	0.00
12.70	0.00	0.00	0.00	0.00
12.80	0.00	0.00	0.00	0.00
12.90	0.00	0.00	0.00	0.00
13.00	34.53	34.53	0.00	19.34

Scenario 2 - t_{50}

Scenario 2 (Biot)				
Step	**F1**	**F2**	**F3**	**F4 = F5**
0.00	0.00	0.00	0.00	0.00
1.00	0.00	0.00	0.00	0.00
2.00	34.53	34.53	0.00	0.00
3.00	34.53	34.53	0.00	19.34
4.00	34.53	34.53	0.00	39.00
5.00	34.53	34.53	0.00	39.00
6.00	51.80	51.80	0.00	39.00
7.00	62.97	62.97	0.00	39.00
8.00	88.35	88.35	0.00	56.39
9.00	103.58	103.58	0.00	88.02
10.00	120.84	120.84	0.00	97.92
11.00	71.08	71.08	0.00	39.00
12.00	51.80	51.80	0.00	58.31
12.10	51.80	51.80	0.00	56.26
12.20	34.52	34.52	0.00	40.85
12.30	34.52	34.52	0.00	37.96
12.40	34.52	34.52	0.00	39.00
12.50	34.52	34.52	0.00	39.00
12.60	34.52	34.52	0.00	39.00
12.70	34.52	34.52	0.00	37.96
12.80	34.52	34.52	0.00	40.85
12.90	51.80	51.80	0.00	56.26
13.00	51.80	51.80	0.00	58.31

Scenarios 3a, 3b - t_a

Scenario 3a - F3 dip +65					Scenario 3b - F3 dip -65				
Step	**F1**	**F2**	**F3**	**F4 = F5**	**Step**	**F1**	**F2**	**F3**	**F4 = F5**
0.00	0.00	0.00	0.00	0.00	0.00	0.00	0.00	0.00	0.00
1.00	0.00	0.00	0.00	0.00	1.00	0.00	0.00	0.00	0.00
2.00	0.00	0.00	0.00	0.00	2.00	0.00	0.00	0.00	0.00
3.00	0.00	0.00	0.00	0.00	3.00	0.00	0.00	0.00	0.00
4.00	11.17	11.17	0.00	0.00	4.00	11.17	11.17	0.00	0.00
5.00	6.09	6.09	0.00	0.00	5.00	6.09	6.09	0.00	0.00
6.00	17.27	17.27	0.00	18.35	6.00	17.27	17.27	0.00	18.35
7.00	0.00	0.00	0.00	0.98	7.00	0.00	0.00	0.00	0.98
8.00	0.00	0.00	0.00	19.67	8.00	0.00	0.00	0.00	19.67
9.00	17.27	17.27	0.00	0.00	9.00	17.27	17.27	0.00	0.00
10.00	0.00	0.00	0.00	0.00	10.00	0.00	0.00	0.00	0.00
11.00	0.00	0.00	0.00	0.00	11.00	0.00	0.00	0.00	0.00
12.00	17.27	17.27	0.00	0.00	12.00	17.27	17.27	0.00	0.00
12.10	0.00	0.00	0.00	0.00	12.10	0.00	0.00	0.00	0.00
12.20	0.00	0.00	0.00	0.00	12.20	0.00	0.00	0.00	0.00
12.30	0.00	0.00	0.00	0.00	12.30	0.00	0.00	0.00	0.00
12.40	0.00	0.00	0.00	0.00	12.40	0.00	0.00	0.00	0.00
12.50	0.00	0.00	0.00	0.00	12.50	0.00	0.00	0.00	0.00
12.60	0.00	0.00	0.00	0.00	12.60	0.00	0.00	0.00	0.00
12.70	0.00	0.00	0.00	0.00	12.70	0.00	0.00	0.00	0.00
12.80	0.00	0.00	0.00	0.00	12.80	0.00	0.00	0.00	0.00
12.90	0.00	0.00	0.00	0.00	12.90	0.00	0.00	0.00	0.00
13.00	0.00	0.00	0.00	0.00	13.00	0.00	0.00	0.00	0.00

Scenario 3a, 3b - t_{80}

Scenario 3a - F3 dip +65					Scenario 3b - F3 dip -65				
Step	**F1**	**F2**	**F3**	**F4 = F5**	**Step**	**F1**	**F2**	**F3**	**F4 = F5**
0.00	0.00	0.00	0.00	0.00	0.00	0.00	0.00	0.00	0.00
1.00	0.00	0.00	0.00	0.00	1.00	0.00	0.00	0.00	0.00
2.00	0.00	0.00	0.00	0.00	2.00	0.00	0.00	0.00	0.00
3.00	0.00	0.00	0.00	0.00	3.00	0.00	0.00	0.00	0.00
4.00	32.50	32.50	0.00	0.00	4.00	32.50	32.50	0.00	0.00
5.00	34.53	34.53	0.00	19.33	5.00	34.53	34.53	0.00	19.33
6.00	34.53	34.53	0.00	39.00	6.00	34.53	34.53	0.00	39.00
7.00	34.53	34.53	0.00	39.00	7.00	34.53	34.53	0.00	39.00
8.00	51.80	51.80	0.00	39.00	8.00	51.80	51.80	0.00	39.00
9.00	51.80	51.80	0.00	39.00	9.00	51.80	51.80	0.00	39.00
10.00	51.80	51.80	0.00	39.00	10.00	51.80	51.80	0.00	39.00
11.00	17.27	17.27	0.00	0.00	11.00	17.27	17.27	0.00	0.00
12.00	34.53	34.53	0.00	16.39	12.00	34.53	34.53	0.00	16.39
12.10	0.00	0.00	0.00	0.00	12.10	0.00	0.00	0.00	0.00
12.20	0.00	0.00	0.00	0.00	12.20	0.00	0.00	0.00	0.00
12.30	0.00	0.00	0.00	0.00	12.30	0.00	0.00	0.00	0.00
12.40	0.00	0.00	0.00	0.00	12.40	0.00	0.00	0.00	0.00
12.50	0.00	0.00	0.00	0.00	12.50	0.00	0.00	0.00	0.00
12.60	0.00	0.00	0.00	0.00	12.60	0.00	0.00	0.00	0.00
12.70	0.00	0.00	0.00	0.00	12.70	0.00	0.00	0.00	0.00
12.80	0.00	0.00	0.00	0.00	12.80	0.00	0.00	0.00	0.00
12.90	0.00	0.00	0.00	0.00	12.90	0.00	0.00	0.00	0.00
13.00	34.53	34.53	0.00	16.39	13.00	34.53	34.53	0.00	16.39

Scenario 3a, 3b - t_{50}

Scenario 3a - F3 dip +65					Scenario 3b - F3 dip -65				
Step	**F1**	**F2**	**F3**	**F4 = F5**	**Step**	**F1**	**F2**	**F3**	**F4 = F5**
0.00	0.00	0.00	0.00	0.00	0.00	0.00	0.00	0.00	0.00
1.00	0.00	0.00	0.00	0.00	1.00	0.00	0.00	0.00	0.00
2.00	13.20	13.20	0.00	0.00	2.00	13.20	13.20	0.00	0.00
3.00	34.53	34.53	0.00	19.33	3.00	34.53	34.53	0.00	19.33
4.00	34.53	34.53	0.00	39.00	4.00	34.53	34.53	0.00	39.00
5.00	34.53	34.53	0.00	39.00	5.00	34.53	34.53	0.00	39.00
6.00	34.53	34.53	0.00	39.00	6.00	34.53	34.53	0.00	39.00
7.00	51.80	51.80	0.00	39.00	7.00	51.80	51.80	0.00	39.00
8.00	69.06	69.06	0.00	39.00	8.00	69.06	69.06	0.00	39.00
9.00	86.32	86.32	4.41	57.32	9.00	86.32	86.32	4.41	57.32
10.00	103.58	103.58	19.86	78.49	10.00	103.58	103.58	19.86	78.49
11.00	51.79	51.79	0.00	19.30	11.00	51.79	51.79	0.00	19.30
12.00	51.80	51.80	0.00	37.65	12.00	51.80	51.80	0.00	37.65
12.10	51.80	51.80	0.00	36.67	12.10	51.80	51.80	0.00	36.67
12.20	17.27	17.27	0.00	18.32	12.20	17.27	17.27	0.00	18.32
12.30	17.27	17.27	0.00	18.32	12.30	17.27	17.27	0.00	18.32
12.40	28.43	28.43	0.00	18.32	12.40	28.43	28.43	0.00	18.32
12.50	32.49	32.49	0.00	19.30	12.50	32.49	32.49	0.00	19.30
12.60	28.43	28.43	0.00	18.32	12.60	28.43	28.43	0.00	18.32
12.70	17.27	17.27	0.00	18.32	12.70	17.27	17.27	0.00	18.32
12.80	17.27	17.27	0.00	18.32	12.80	17.27	17.27	0.00	18.32
12.90	51.80	51.80	0.00	36.67	12.90	51.80	51.80	0.00	36.67
13.00	51.80	51.80	0.00	37.65	13.00	51.80	51.80	0.00	37.65

Scenario 3c, 3d - t_a

Scenario 3c - Disloc 100 m					Scenario 3d - Disloc 200 m				
Step	**F1**	**F2**	**F3**	**F4 = F5**	**Step**	**F1**	**F2**	**F3**	**F4 = F5**
0.00	0.00	0.00	0.00	0.00	0.00	0.00	0.00	0.00	0.00
1.00	0.00	0.00	0.00	0.00	1.00	0.00	0.00	0.00	0.00
2.00	0.00	0.00	0.00	0.00	2.00	0.00	0.00	0.00	0.00
3.00	0.00	0.00	0.00	0.00	3.00	0.00	0.00	17.00	0.00
4.00	2.03	17.27	0.00	0.00	4.00	2.03	2.03	0.00	0.00
5.00	15.23	0.00	2.00	0.00	5.00	15.23	15.23	17.00	5.97
6.00	17.27	17.26	19.00	17.81	6.00	17.27	17.27	2.00	11.73
7.00	0.00	0.00	26.00	0.95	7.00	0.00	0.00	47.00	0.98
8.00	0.00	0.00	21.00	18.08	8.00	0.00	0.00	2.00	18.52
9.00	17.27	17.26	0.00	1.00	9.00	17.27	11.17	11.00	0.48
10.00	0.00	0.00	0.00	0.00	10.00	0.00	6.09	21.00	0.00
11.00	0.00	0.00	0.00	0.00	11.00	0.00	0.00	0.00	0.00
12.00	17.27	17.27	17.00	0.00	12.00	17.27	19.29	34.00	9.26
12.10	0.00	0.00	0.00	0.00	12.10	0.00	0.00	0.00	0.00
12.20	0.00	0.00	0.00	0.00	12.20	0.00	0.00	0.00	0.00
12.30	0.00	0.00	0.00	0.00	12.30	0.00	0.00	0.00	0.00
12.40	0.00	0.00	0.00	0.00	12.40	0.00	0.00	0.00	0.00
12.50	0.00	0.00	0.00	0.00	12.50	0.00	0.00	17.00	0.00
12.60	0.00	0.00	0.00	0.00	12.60	0.00	0.00	0.00	0.00
12.70	0.00	0.00	0.00	0.00	12.70	0.00	0.00	0.00	0.00
12.80	0.00	0.00	0.00	0.00	12.80	0.00	0.00	0.00	0.00
12.90	0.00	0.00	0.00	0.00	12.90	0.00	0.00	0.00	0.00
13.00	0.00	0.00	0.00	0.00	13.00	0.00	0.00	17.00	0.00

Scenario 3c, 3d - t_{80}

Scenario 3c - Disloc 100 m					Scenario 3d - Disloc 200 m				
Step	**F1**	**F2**	**F3**	**F4 = F5**	**Step**	**F1**	**F2**	**F3**	**F4 = F5**
0.00	0.00	0.00	0.00	0.00	0.00	0.00	0.00	0.00	0.00
1.00	0.00	0.00	0.00	0.00	1.00	0.00	0.00	0.00	0.00
2.00	0.00	0.00	0.00	0.00	2.00	0.00	0.00	15.00	0.00
3.00	0.00	0.00	0.00	0.00	3.00	0.00	0.00	17.00	0.00
4.00	34.53	34.52	15.00	0.00	4.00	34.53	34.52	34.00	8.81
5.00	34.53	34.52	26.00	18.76	5.00	34.53	34.52	34.00	18.68
6.00	34.53	34.52	68.00	36.84	6.00	34.53	34.52	85.00	37.20
7.00	34.53	34.52	68.00	37.84	7.00	34.53	34.52	85.00	37.68
8.00	51.80	51.78	68.00	37.84	8.00	51.80	36.56	89.00	37.68
9.00	51.80	51.78	68.00	38.34	9.00	51.80	51.79	115.00	37.68
10.00	51.80	69.05	70.00	38.34	10.00	51.80	71.08	123.00	46.49
11.00	17.27	17.26	0.00	0.00	11.00	17.27	26.40	30.00	8.80
12.00	34.53	34.52	19.00	16.85	12.00	34.53	34.52	34.00	16.74
12.10	0.00	0.00	0.00	0.00	12.10	0.00	0.00	0.00	0.00
12.20	0.00	0.00	0.00	0.00	12.20	0.00	0.00	0.00	0.00
12.30	0.00	0.00	0.00	0.00	12.30	0.00	0.00	0.00	0.00
12.40	0.00	0.00	0.00	0.00	12.40	0.00	0.00	1.00	0.00
12.50	0.00	0.00	0.00	0.00	12.50	0.00	7.11	32.00	0.00
12.60	0.00	0.00	0.00	0.00	12.60	0.00	0.00	0.00	0.00
12.70	0.00	0.00	0.00	0.00	12.70	0.00	0.00	0.00	0.00
12.80	0.00	0.00	0.00	0.00	12.80	0.00	0.00	0.00	0.00
12.90	0.00	0.00	0.00	0.00	12.90	0.00	0.00	0.00	0.00
13.00	34.53	34.52	19.00	16.85	13.00	34.53	34.52	34.00	16.74

Scenario 3c, 3d - t_{50}

Scenario 3c - Disloc 100 m					Scenario 3d - Disloc 200 m				
Step	F1	F2	F3	F4 = F5	Step	F1	F2	F3	F4 = F5
0.00	0.00	0.00	0.00	0.00	0.00	0.00	0.00	0.00	0.00
1.00	0.00	0.00	0.00	0.00	1.00	0.00	0.00	0.00	0.00
2.00	13.20	9.14	0.00	0.00	2.00	13.20	17.27	17.00	0.00
3.00	34.53	34.52	32.00	18.76	3.00	34.53	34.52	34.00	18.68
4.00	34.53	34.52	68.00	37.84	4.00	34.53	34.52	62.00	37.68
5.00	34.53	34.52	68.00	38.34	5.00	34.53	34.52	85.00	37.68
6.00	34.53	34.52	68.00	39.34	6.00	34.53	34.52	85.00	37.68
7.00	51.80	51.78	68.00	39.84	7.00	51.80	62.96	98.00	38.18
8.00	71.09	69.05	72.00	39.84	8.00	71.09	71.08	121.00	47.49
9.00	88.35	73.11	93.00	57.63	9.00	88.35	88.35	140.00	56.35
10.00	103.58	103.58	119.00	68.65	10.00	103.58	103.58	189.00	82.23
11.00	51.79	51.79	23.00	18.73	11.00	51.79	51.79	93.00	18.65
12.00	51.80	51.79	68.00	36.55	12.00	51.80	51.78	115.00	36.35
12.10	51.80	51.79	40.00	36.53	12.10	51.80	51.78	77.00	35.87
12.20	17.27	17.27	23.00	18.25	12.20	17.27	17.26	55.00	19.12
12.30	19.30	17.27	21.00	18.25	12.30	19.30	17.26	53.00	18.17
12.40	30.46	17.27	21.00	18.25	12.40	30.46	17.26	74.00	18.17
12.50	32.49	17.27	23.00	18.73	12.50	32.49	17.26	72.00	18.65
12.60	30.46	17.27	21.00	18.25	12.60	30.46	17.26	72.00	18.17
12.70	19.30	17.27	21.00	18.25	12.70	19.30	17.26	53.00	18.17
12.80	17.27	17.27	23.00	18.25	12.80	17.27	17.26	53.00	19.12
12.90	51.80	51.79	40.00	36.53	12.90	51.80	51.78	83.00	35.87
13.00	51.80	51.79	68.00	36.55	13.00	51.80	51.78	115.00	36.35

Scenario 4a, 4b - t_a

Scenario 4a - Theta					Scenario 4b - M				
Step	F1	F2	F3	F4 = F5	Step	F1	F2	F3	F4 = F5
0.00	0.00	0.00	0.00	0.00	0.00	0.00	0.00	0.00	0.00
1.00	0.00	0.00	0.00	0.00	1.00	0.00	0.00	0.00	0.00
2.00	0.00	0.00	0.00	0.00	2.00	0.00	0.00	0.00	0.00
3.00	0.00	0.00	0.00	0.00	3.00	17.27	17.27	0.00	0.00
4.00	0.00	0.00	0.00	0.00	4.00	17.27	17.27	0.00	19.34
5.00	17.27	17.27	0.00	0.00	5.00	0.00	0.00	0.00	19.66
6.00	0.00	0.00	0.00	19.34	6.00	17.26	17.26	0.00	0.00
7.00	17.27	17.27	0.00	19.66	7.00	32.49	32.49	0.00	0.00
8.00	0.00	0.00	0.00	0.00	8.00	4.06	4.06	0.00	15.48
9.00	0.00	0.00	0.00	0.00	9.00	19.29	19.29	0.00	22.48
10.00	17.27	17.27	0.00	0.00	10.00	22.34	22.34	0.00	1.04
11.00	0.00	0.00	0.00	0.00	11.00	0.00	0.00	0.00	0.00
12.00	17.27	17.27	0.00	15.48	12.00	32.50	32.50	0.00	39.00
12.10	0.00	0.00	0.00	0.00	12.10	0.00	0.00	0.00	0.00
12.20	0.00	0.00	0.00	0.00	12.20	0.00	0.00	0.00	0.00
12.30	0.00	0.00	0.00	0.00	12.30	0.00	0.00	0.00	0.00
12.40	0.00	0.00	0.00	0.00	12.40	0.00	0.00	0.00	0.00
12.50	0.00	0.00	0.00	0.00	12.50	17.27	17.27	0.00	0.00
12.60	0.00	0.00	0.00	0.00	12.60	0.00	0.00	0.00	0.00
12.70	0.00	0.00	0.00	0.00	12.70	0.00	0.00	0.00	0.00
12.80	0.00	0.00	0.00	0.00	12.80	0.00	0.00	0.00	0.00
12.90	0.00	0.00	0.00	0.00	12.90	0.00	0.00	0.00	0.00
13.00	0.00	0.00	0.00	0.00	13.00	17.27	17.27	0.00	0.00

Scenario 4a, 4b - t_{80}

Scenario 4a - Theta					Scenario 4b - M				
Step	**F1**	**F2**	**F3**	**F4 = F5**	**Step**	**F1**	**F2**	**F3**	**F4 = F5**
0.00	0.00	0.00	0.00	0.00	0.00	0.00	0.00	0.00	0.00
1.00	0.00	0.00	0.00	0.00	1.00	0.00	0.00	0.00	0.00
2.00	0.00	0.00	0.00	0.00	2.00	17.27	17.27	0.00	0.00
3.00	0.00	0.00	0.00	0.00	3.00	34.53	34.53	0.00	18.38
4.00	17.27	17.27	0.00	0.00	4.00	34.53	34.53	0.00	39.00
5.00	34.53	34.53	0.00	19.34	5.00	53.83	53.83	0.00	39.00
6.00	34.53	34.53	0.00	39.00	6.00	71.09	71.09	0.00	39.00
7.00	34.53	34.53	0.00	39.00	7.00	88.35	88.35	0.00	55.44
8.00	34.53	34.53	0.00	39.00	8.00	105.61	105.61	0.00	76.96
9.00	51.80	51.80	0.00	39.00	9.00	122.87	122.87	0.00	94.46
10.00	51.80	51.80	0.00	52.50	10.00	174.64	174.64	0.00	96.40
11.00	17.27	17.27	0.00	0.00	11.00	108.65	108.65	0.00	38.75
12.00	17.27	17.27	0.00	19.34	12.00	59.92	59.92	0.00	39.00
12.10	0.00	0.00	0.00	0.00	12.10	30.46	30.46	0.00	0.00
12.20	0.00	0.00	0.00	0.00	12.20	30.46	30.46	0.00	0.00
12.30	0.00	0.00	0.00	0.00	12.30	28.43	28.43	0.00	0.00
12.40	0.00	0.00	0.00	0.00	12.40	28.43	28.43	0.00	0.00
12.50	0.00	0.00	0.00	0.00	12.50	64.98	64.98	0.00	0.00
12.60	0.00	0.00	0.00	0.00	12.60	17.26	17.26	0.00	0.00
12.70	0.00	0.00	0.00	0.00	12.70	13.20	13.20	0.00	0.00
12.80	0.00	0.00	0.00	0.00	12.80	13.20	13.20	0.00	0.00
12.90	0.00	0.00	0.00	0.00	12.90	13.20	13.20	0.00	0.00
13.00	17.27	17.27	0.00	19.34	13.00	59.92	59.92	0.00	39.00

Scenario 4a, 4b - t_{50}

Scenario 4a - Theta					Scenario 4b - M				
Step	**F1**	**F2**	**F3**	**F4 = F5**	**Step**	**F1**	**F2**	**F3**	**F4 = F5**
0.00	0.00	0.00	0.00	0.00	0.00	0.00	0.00	0.00	0.00
1.00	0.00	0.00	0.00	0.00	1.00	17.27	17.27	0.00	0.00
2.00	0.00	0.00	0.00	0.00	2.00	34.53	34.53	0.00	19.34
3.00	34.53	34.53	0.00	19.34	3.00	51.80	51.80	0.00	39.00
4.00	34.53	34.53	0.00	39.00	4.00	69.06	69.06	0.00	39.00
5.00	34.53	34.53	0.00	39.00	5.00	71.09	71.09	0.00	39.00
6.00	34.53	34.53	0.00	39.00	6.00	133.54	133.54	0.00	76.96
7.00	51.80	51.80	0.00	39.00	7.00	175.16	175.16	0.00	97.92
8.00	51.80	51.80	0.00	56.39	8.00	233.29	233.29	0.00	98.89
9.00	62.97	62.97	0.00	76.96	9.00	263.75	263.75	0.00	117.49
10.00	80.23	80.23	0.00	97.92	10.00	276.45	276.45	0.00	161.54
11.00	32.50	32.50	0.00	37.96	11.00	159.41	159.41	0.00	90.47
12.00	42.66	42.66	0.00	58.31	12.00	120.83	120.83	0.00	39.00
12.10	32.50	32.50	0.00	38.65	12.10	105.60	105.60	0.00	40.04
12.20	17.27	17.27	0.00	21.24	12.20	88.33	88.33	0.00	1.04
12.30	24.38	24.38	0.00	37.96	12.30	88.33	88.33	0.00	17.50
12.40	28.44	28.44	0.00	37.96	12.40	124.89	124.89	0.00	19.44
12.50	32.50	32.50	0.00	37.96	12.50	124.89	124.89	0.00	73.97
12.60	28.44	28.44	0.00	37.96	12.60	122.86	122.86	0.00	19.44
12.70	24.38	24.38	0.00	37.96	12.70	88.33	88.33	0.00	17.50
12.80	17.27	17.27	0.00	21.24	12.80	88.33	88.33	0.00	1.04
12.90	32.50	32.50	0.00	38.65	12.90	105.60	105.60	0.00	40.04
13.00	42.66	42.66	0.00	58.31	13.00	120.83	120.83	0.00	39.00

Scenario 5a, 5b - t_a

Scenario 5a - C=0					Scenario 5b - Phi=20 deg				
Step	F1	F2	F3	F4 = F5	Step	F1	F2	F3	F4 = F5
0.00	0.00	0.00	0.00	0.00	0.00	0.00	0.00	0.00	0.00
1.00	0.00	0.00	0.00	0.00	1.00	0.00	0.00	0.00	0.00
2.00	0.00	0.00	0.00	0.00	2.00	0.00	0.00	0.00	0.00
3.00	0.00	0.00	0.00	0.00	3.00	28.44	28.44	0.00	0.00
4.00	17.27	17.27	0.00	0.00	4.00	6.09	6.09	0.00	18.38
5.00	17.27	17.27	0.00	16.45	5.00	0.00	0.00	0.00	20.62
6.00	0.00	0.00	0.00	2.89	6.00	0.00	0.00	0.00	0.00
7.00	0.00	0.00	0.00	19.66	7.00	28.44	28.44	0.00	0.00
8.00	17.27	17.27	0.00	0.00	8.00	17.26	17.26	0.00	0.00
9.00	0.00	0.00	0.00	0.00	9.00	8.12	8.12	0.00	37.00
10.00	2.03	2.03	0.00	0.00	10.00	32.49	32.49	0.00	2.00
11.00	0.00	0.00	0.00	0.00	11.00	0.00	0.00	0.00	0.00
12.00	34.53	34.53	0.00	18.38	12.00	34.53	34.53	0.00	39.00
12.10	0.00	0.00	0.00	0.00	12.10	0.00	0.00	0.00	0.00
12.20	0.00	0.00	0.00	0.00	12.20	0.00	0.00	0.00	0.00
12.30	0.00	0.00	0.00	0.00	12.30	0.00	0.00	0.00	0.00
12.40	0.00	0.00	0.00	0.00	12.40	0.00	0.00	0.00	0.00
12.50	0.00	0.00	0.00	0.00	12.50	0.00	0.00	0.00	0.00
12.60	0.00	0.00	0.00	0.00	12.60	0.00	0.00	0.00	0.00
12.70	0.00	0.00	0.00	0.00	12.70	0.00	0.00	0.00	0.00
12.80	0.00	0.00	0.00	0.00	12.80	0.00	0.00	0.00	0.00
12.90	0.00	0.00	0.00	0.00	12.90	0.00	0.00	0.00	0.00
13.00	0.00	0.00	0.00	0.00	13.00	0.00	0.00	0.00	0.00

Scenario 5a, 5b - t_{80}

Scenario 5a - C=0					Scenario 5b - Phi=20 deg				
Step	F1	F2	F3	F4 = F5	Step	F1	F2	F3	F4 = F5
0.00	0.00	0.00	0.00	0.00	0.00	0.00	0.00	0.00	0.00
1.00	0.00	0.00	0.00	0.00	1.00	0.00	0.00	0.00	0.00
2.00	0.00	0.00	0.00	0.00	2.00	0.00	0.00	0.00	0.00
3.00	17.27	17.27	0.00	0.00	3.00	34.53	34.53	0.00	16.45
4.00	34.53	34.53	0.00	18.38	4.00	34.53	34.53	0.00	39.00
5.00	34.53	34.53	0.00	37.96	5.00	34.53	34.53	0.00	39.00
6.00	34.53	34.53	0.00	39.00	6.00	65.00	65.00	0.00	39.00
7.00	51.80	51.80	0.00	39.00	7.00	82.26	82.26	0.00	39.00
8.00	51.80	51.80	0.00	39.00	8.00	88.35	88.35	0.00	76.96
9.00	67.03	67.03	0.00	39.00	9.00	120.84	120.84	0.00	85.50
10.00	73.12	73.12	0.00	57.35	10.00	140.13	140.13	0.00	96.40
11.00	34.53	34.53	0.00	17.39	11.00	93.42	93.42	0.00	35.84
12.00	34.53	34.53	0.00	19.34	12.00	34.53	34.53	0.00	39.00
12.10	0.00	0.00	0.00	0.00	12.10	0.00	0.00	0.00	0.00
12.20	0.00	0.00	0.00	0.00	12.20	0.00	0.00	0.00	0.00
12.30	0.00	0.00	0.00	0.00	12.30	0.00	0.00	0.00	0.00
12.40	0.00	0.00	0.00	0.00	12.40	9.14	9.14	0.00	0.00
12.50	0.00	0.00	0.00	0.00	12.50	45.69	45.69	0.00	0.00
12.60	0.00	0.00	0.00	0.00	12.60	9.14	9.14	0.00	0.00
12.70	0.00	0.00	0.00	0.00	12.70	0.00	0.00	0.00	0.00
12.80	0.00	0.00	0.00	0.00	12.80	0.00	0.00	0.00	0.00
12.90	0.00	0.00	0.00	0.00	12.90	0.00	0.00	0.00	0.00
13.00	34.53	34.53	0.00	19.34	13.00	34.53	34.53	0.00	39.00

Scenario 5a, 5b - t_{50}

Scenario 5a - C=0					Scenario 5b - Phi=20 deg				
Step	**F1**	**F2**	**F3**	**F4 = F5**	**Step**	**F1**	**F2**	**F3**	**F4 = F5**
0.00	0.00	0.00	0.00	0.00	0.00	0.00	0.00	0.00	0.00
1.00	0.00	0.00	0.00	0.00	1.00	0.00	0.00	0.00	0.00
2.00	34.53	34.53	0.00	0.00	2.00	34.53	34.53	0.00	19.34
3.00	34.53	34.53	0.00	37.96	3.00	34.53	34.53	0.00	39.00
4.00	34.53	34.53	0.00	39.00	4.00	34.53	34.53	0.00	39.00
5.00	34.53	34.53	0.00	39.00	5.00	86.32	86.32	0.00	39.00
6.00	51.80	51.80	0.00	39.00	6.00	86.32	86.32	0.00	57.35
7.00	71.09	71.09	0.00	39.00	7.00	103.58	103.58	0.00	96.95
8.00	88.35	88.35	0.00	57.35	8.00	136.07	136.07	0.00	98.89
9.00	103.58	103.58	0.00	94.02	9.00	151.29	151.29	0.00	117.49
10.00	120.84	120.84	0.00	97.92	10.00	155.35	155.35	0.00	155.52
11.00	93.42	93.42	0.00	39.00	11.00	138.09	138.09	0.00	58.37
12.00	51.80	51.80	0.00	58.31	12.00	86.31	86.31	0.00	40.04
12.10	53.83	53.83	0.00	57.30	12.10	79.20	79.20	0.00	40.04
12.20	49.75	49.75	0.00	37.96	12.20	58.89	58.89	0.00	3.12
12.30	51.78	51.78	0.00	37.96	12.30	64.98	64.98	0.00	27.19
12.40	51.78	51.78	0.00	39.00	12.40	91.39	91.39	0.00	38.09
12.50	69.05	69.05	0.00	39.00	12.50	103.57	103.57	0.00	38.09
12.60	51.78	51.78	0.00	39.00	12.60	91.39	91.39	0.00	38.09
12.70	51.78	51.78	0.00	37.96	12.70	64.98	64.98	0.00	27.19
12.80	49.75	49.75	0.00	37.96	12.80	58.89	58.89	0.00	3.12
12.90	53.83	53.83	0.00	57.30	12.90	79.20	79.20	0.00	40.04
13.00	51.80	51.80	0.00	58.31	13.00	86.31	86.31	0.00	40.04

Scenario 5c, 5d - t_a

Scenario 5c - Weak A					Scenario 5b - Weak B				
Step	**F1**	**F2**	**F3**	**F4 = F5**	**Step**	**F1**	**F2**	**F3**	**F4 = F5**
0.00	0.00	0.00	0.00	0.00	0.00	0.00	0.00	0.00	0.00
1.00	0.00	0.00	0.00	0.00	1.00	0.00	0.00	0.00	0.00
2.00	0.00	0.00	0.00	0.00	2.00	0.00	0.00	0.00	0.00
3.00	0.00	0.00	0.00	0.00	3.00	0.00	0.00	0.00	0.00
4.00	2.03	2.03	0.00	0.00	4.00	2.03	2.03	0.00	0.00
5.00	15.23	15.23	0.00	0.00	5.00	15.23	15.23	0.00	0.00
6.00	17.27	17.27	0.00	18.38	6.00	17.27	17.27	0.00	18.38
7.00	17.27	17.27	0.00	0.00	7.00	0.00	0.00	0.00	0.96
8.00	9.14	9.14	0.00	20.62	8.00	0.00	0.00	0.00	19.66
9.00	19.29	19.29	0.00	0.00	9.00	17.27	17.27	0.00	0.00
10.00	43.65	43.65	0.00	35.96	10.00	0.00	0.00	0.00	0.00
11.00	0.00	0.00	0.00	0.00	11.00	0.00	0.00	0.00	0.00
12.00	58.90	58.90	0.00	37.06	12.00	34.53	34.53	0.00	19.34
12.10	9.14	9.14	0.00	0.00	12.10	0.00	0.00	0.00	0.00
12.20	0.00	0.00	0.00	0.00	12.20	0.00	0.00	0.00	0.00
12.30	18.27	18.27	0.00	0.00	12.30	0.00	0.00	0.00	0.00
12.40	19.30	19.30	0.00	0.00	12.40	0.00	0.00	0.00	0.00
12.50	33.51	33.51	0.00	19.34	12.50	0.00	0.00	0.00	0.00
12.60	0.00	0.00	0.00	0.00	12.60	0.00	0.00	0.00	0.00
12.70	0.00	0.00	0.00	0.00	12.70	0.00	0.00	0.00	0.00
12.80	0.00	0.00	0.00	0.00	12.80	0.00	0.00	0.00	0.00
12.90	34.53	34.53	0.00	0.00	12.90	0.00	0.00	0.00	0.00
13.00	26.40	26.40	0.00	19.34	13.00	0.00	0.00	0.00	0.00

Scenario 5c, 5d - t_{80}

Scenario 5c - Weak A					Scenario 5b - Weak B				
Step	**F1**	**F2**	**F3**	**F4 = F5**	**Step**	**F1**	**F2**	**F3**	**F4 = F5**
0.00	0.00	0.00	0.00	0.00	0.00	0.00	0.00	0.00	0.00
1.00	0.00	0.00	0.00	0.00	1.00	0.00	0.00	0.00	0.00
2.00	0.00	0.00	0.00	0.00	2.00	0.00	0.00	0.00	0.00
3.00	0.00	0.00	0.00	0.00	3.00	0.00	0.00	0.00	0.00
4.00	34.53	34.53	0.00	0.00	4.00	34.53	34.53	0.00	0.00
5.00	34.53	34.53	0.00	19.34	5.00	34.53	34.53	0.00	19.34
6.00	51.80	51.80	0.00	39.00	6.00	34.53	34.53	0.00	39.00
7.00	69.06	69.06	0.00	39.00	7.00	34.53	34.53	0.00	39.00
8.00	82.26	82.26	0.00	57.35	8.00	51.80	51.80	0.00	39.00
9.00	118.81	118.81	0.00	76.96	9.00	52.81	52.81	0.00	39.00
10.00	171.60	171.60	0.00	95.43	10.00	73.12	73.12	0.00	52.50
11.00	64.99	64.99	0.00	22.88	11.00	32.50	32.50	0.00	0.00
12.00	117.79	117.79	0.00	74.96	12.00	34.53	34.53	0.00	19.34
12.10	85.30	85.30	0.00	18.35	12.10	0.00	0.00	0.00	0.00
12.20	70.06	70.06	0.00	18.35	12.20	0.00	0.00	0.00	0.00
12.30	78.19	78.19	0.00	18.35	12.30	0.00	0.00	0.00	0.00
12.40	42.65	42.65	0.00	36.73	12.40	0.00	0.00	0.00	0.00
12.50	66.00	66.00	0.00	37.96	12.50	0.00	0.00	0.00	0.00
12.60	20.30	20.30	0.00	0.00	12.60	0.00	0.00	0.00	0.00
12.70	20.30	20.30	0.00	0.00	12.70	0.00	0.00	0.00	0.00
12.80	37.57	37.57	0.00	0.00	12.80	0.00	0.00	0.00	0.00
12.90	81.24	81.24	0.00	18.38	12.90	0.00	0.00	0.00	0.00
13.00	86.32	86.32	0.00	74.96	13.00	34.53	34.53	0.00	19.34

Scenario 5c, 5d - t_{50}

Scenario 5c - Weak A					Scenario 5b - Weak B				
Step	**F1**	**F2**	**F3**	**F4 = F5**	**Step**	**F1**	**F2**	**F3**	**F4 = F5**
0.00	0.00	0.00	0.00	0.00	0.00	0.00	0.00	0.00	0.00
1.00	0.00	0.00	0.00	0.00	1.00	0.00	0.00	0.00	0.00
2.00	13.20	13.20	0.00	0.00	2.00	13.20	13.20	0.00	0.00
3.00	34.53	34.53	0.00	19.34	3.00	34.53	34.53	0.00	19.34
4.00	34.53	34.53	0.00	39.00	4.00	34.53	34.53	0.00	39.00
5.00	51.80	51.80	0.00	39.00	5.00	34.53	34.53	0.00	39.00
6.00	86.32	86.32	0.00	57.35	6.00	34.53	34.53	0.00	39.00
7.00	97.49	97.49	0.00	57.35	7.00	60.94	60.94	0.00	39.00
8.00	129.97	129.97	0.00	95.43	8.00	84.29	84.29	0.00	53.50
9.00	151.29	151.29	0.00	97.37	9.00	88.35	88.35	0.00	75.92
10.00	187.84	187.84	0.00	150.89	10.00	118.81	118.81	0.00	95.43
11.00	147.22	147.22	0.00	133.32	11.00	86.31	86.31	0.00	37.96
12.00	171.60	171.60	0.00	93.29	12.00	42.66	42.66	0.00	58.31
12.10	148.24	148.24	0.00	93.50	12.10	38.59	38.59	0.00	38.65
12.20	130.98	130.98	0.00	71.91	12.20	17.27	17.27	0.00	19.31
12.30	148.24	148.24	0.00	71.91	12.30	17.27	17.27	0.00	19.31
12.40	127.94	127.94	0.00	108.84	12.40	17.27	17.27	0.00	36.92
12.50	108.65	108.65	0.00	94.35	12.50	37.58	37.58	0.00	37.96
12.60	82.24	82.24	0.00	108.84	12.60	17.27	17.27	0.00	36.92
12.70	96.45	96.45	0.00	71.91	12.70	17.27	17.27	0.00	19.31
12.80	137.07	137.07	0.00	71.91	12.80	17.27	17.27	0.00	19.31
12.90	152.30	152.30	0.00	110.91	12.90	38.59	38.59	0.00	38.65
13.00	156.37	156.37	0.00	93.29	13.00	42.66	42.66	0.00	58.31

Scenario 6a, 6b - t_a

Scenario 6a - E = 8 GPa					Scenario 6b - E = 20 GPa				
Step	**F1**	**F2**	**F3**	**F4 = F5**	**Step**	**F1**	**F2**	**F3**	**F4 = F5**
0.00	0.00	0.00	0.00	0.00	0.00	0.00	0.00	0.00	0.00
1.00	0.00	0.00	0.00	0.00	1.00	0.00	0.00	0.00	0.00
2.00	0.00	0.00	0.00	0.00	2.00	0.00	0.00	0.00	0.00
3.00	0.00	0.00	0.00	0.00	3.00	0.00	0.00	0.00	0.00
4.00	17.27	17.27	0.00	0.00	4.00	0.00	0.00	0.00	0.00
5.00	17.27	17.27	0.00	15.48	5.00	2.03	2.03	0.00	0.00
6.00	0.00	0.00	0.00	3.86	6.00	15.23	15.23	0.00	0.00
7.00	0.00	0.00	0.00	18.62	7.00	0.00	0.00	0.00	0.00
8.00	17.27	17.27	0.00	1.04	8.00	17.27	17.27	0.00	16.45
9.00	0.00	0.00	0.00	0.00	9.00	0.00	0.00	0.00	21.52
10.00	0.00	0.00	0.00	0.00	10.00	0.00	0.00	0.00	1.04
11.00	0.00	0.00	0.00	0.00	11.00	0.00	0.00	0.00	0.00
12.00	34.53	34.53	0.00	18.38	12.00	13.20	13.20	0.00	0.00
12.10	0.00	0.00	0.00	0.00	12.10	0.00	0.00	0.00	0.00
12.20	0.00	0.00	0.00	0.00	12.20	0.00	0.00	0.00	0.00
12.30	0.00	0.00	0.00	0.00	12.30	0.00	0.00	0.00	0.00
12.40	0.00	0.00	0.00	0.00	12.40	0.00	0.00	0.00	0.00
12.50	0.00	0.00	0.00	0.00	12.50	0.00	0.00	0.00	0.00
12.60	0.00	0.00	0.00	0.00	12.60	0.00	0.00	0.00	0.00
12.70	0.00	0.00	0.00	0.00	12.70	0.00	0.00	0.00	0.00
12.80	0.00	0.00	0.00	0.00	12.80	0.00	0.00	0.00	0.00
12.90	0.00	0.00	0.00	0.00	12.90	0.00	0.00	0.00	0.00
13.00	0.00	0.00	0.00	0.00	13.00	0.00	0.00	0.00	0.00

Scenario 6a, 6b - t_{80}

Scenario 6a - E = 8 GPa					Scenario 6b - E = 20 GPa				
Step	**F1**	**F2**	**F3**	**F4 = F5**	**Step**	**F1**	**F2**	**F3**	**F4 = F5**
0.00	0.00	0.00	0.00	0.00	0.00	0.00	0.00	0.00	0.00
1.00	0.00	0.00	0.00	0.00	1.00	0.00	0.00	0.00	0.00
2.00	0.00	0.00	0.00	0.00	2.00	0.00	0.00	0.00	0.00
3.00	17.27	17.27	0.00	0.00	3.00	0.00	0.00	0.00	0.00
4.00	34.53	34.53	0.00	17.41	4.00	0.00	0.00	0.00	0.00
5.00	34.53	34.53	0.00	19.34	5.00	2.03	2.03	0.00	0.00
6.00	34.53	34.53	0.00	39.00	6.00	15.23	15.23	0.00	0.00
7.00	51.80	51.80	0.00	39.00	7.00	0.00	0.00	0.00	0.00
8.00	51.80	51.80	0.00	39.00	8.00	17.27	17.27	0.00	16.45
9.00	62.97	62.97	0.00	39.00	9.00	0.00	0.00	0.00	21.52
10.00	71.09	71.09	0.00	57.35	10.00	0.00	0.00	0.00	1.04
11.00	34.53	34.53	0.00	17.39	11.00	0.00	0.00	0.00	0.00
12.00	34.53	34.53	0.00	19.34	12.00	13.20	13.20	0.00	0.00
12.10	0.00	0.00	0.00	0.00	12.10	0.00	0.00	0.00	0.00
12.20	0.00	0.00	0.00	0.00	12.20	0.00	0.00	0.00	0.00
12.30	0.00	0.00	0.00	0.00	12.30	0.00	0.00	0.00	0.00
12.40	0.00	0.00	0.00	0.00	12.40	0.00	0.00	0.00	0.00
12.50	0.00	0.00	0.00	0.00	12.50	0.00	0.00	0.00	0.00
12.60	0.00	0.00	0.00	0.00	12.60	0.00	0.00	0.00	0.00
12.70	0.00	0.00	0.00	0.00	12.70	0.00	0.00	0.00	0.00
12.80	0.00	0.00	0.00	0.00	12.80	0.00	0.00	0.00	0.00
12.90	0.00	0.00	0.00	0.00	12.90	0.00	0.00	0.00	0.00
13.00	34.53	34.53	0.00	19.34	13.00	0.00	0.00	0.00	0.00

Scenario 6a, 6b - t_{50}

Scenario 6a - E = 8 GPa					Scenario 6b - E = 20 GPa				
Step	**F1**	**F2**	**F3**	**F4 = F5**	**Step**	**F1**	**F2**	**F3**	**F4 = F5**
0.00	0.00	0.00	0.00	0.00	0.00	0.00	0.00	0.00	0.00
1.00	0.00	0.00	0.00	0.00	1.00	0.00	0.00	0.00	0.00
2.00	34.53	34.53	0.00	0.00	2.00	0.00	0.00	0.00	0.00
3.00	34.53	34.53	0.00	24.84	3.00	34.53	34.53	0.00	0.00
4.00	34.53	34.53	0.00	39.00	4.00	34.53	34.53	0.00	18.38
5.00	34.53	34.53	0.00	39.00	5.00	34.53	34.53	0.00	39.00
6.00	51.80	51.80	0.00	39.00	6.00	34.53	34.53	0.00	39.00
7.00	69.06	69.06	0.00	39.00	7.00	34.53	34.53	0.00	39.00
8.00	82.26	82.26	0.00	57.35	8.00	34.53	34.53	0.00	39.00
9.00	88.35	88.35	0.00	76.96	9.00	51.80	51.80	0.00	39.00
10.00	120.84	120.84	0.00	97.92	10.00	53.83	53.83	0.00	39.00
11.00	86.31	86.31	0.00	37.96	11.00	17.27	17.27	0.00	0.00
12.00	51.80	51.80	0.00	57.27	12.00	34.53	34.53	0.00	0.00
12.10	51.80	51.80	0.00	38.65	12.10	34.53	34.53	0.00	0.00
12.20	28.43	28.43	0.00	35.87	12.20	34.53	34.53	0.00	0.00
12.30	34.52	34.52	0.00	37.96	12.30	17.27	17.27	0.00	0.00
12.40	34.52	34.52	0.00	37.96	12.40	17.27	17.27	0.00	0.00
12.50	47.73	47.73	0.00	37.96	12.50	17.27	17.27	0.00	0.00
12.60	34.52	34.52	0.00	37.96	12.60	17.27	17.27	0.00	0.00
12.70	34.52	34.52	0.00	37.96	12.70	17.27	17.27	0.00	0.00
12.80	28.43	28.43	0.00	35.87	12.80	34.53	34.53	0.00	0.00
12.90	51.80	51.80	0.00	38.65	12.90	34.53	34.53	0.00	0.00
13.00	51.80	51.80	0.00	57.27	13.00	34.53	34.53	0.00	0.00

Scenario 7a, 7b - t_a

Scenario 7a - Diff.P 100/0					Scenario 7b - Diff.P 100/200				
Step	**F1**	**F2**	**F3**	**F4 = F5**	**Step**	**F1**	**F2**	**F3**	**F4 = F5**
0.00	0.00	0.00	0.00	0.00	0.00	0.00	0.00	0.00	0.00
1.00	0.00	0.00	0.00	0.00	1.00	0.00	0.00	0.00	0.00
2.00	0.00	0.00	0.00	0.00	2.00	0.00	0.00	0.00	0.00
3.00	0.00	0.00	0.00	0.00	3.00	0.00	0.00	0.00	0.00
4.00	2.03	2.03	0.00	0.00	4.00	2.03	2.03	0.00	0.00
5.00	15.23	15.23	0.00	0.00	5.00	15.23	15.23	0.00	0.00
6.00	17.27	17.27	0.00	18.38	6.00	17.27	17.27	0.00	18.38
7.00	0.00	0.00	0.00	0.96	7.00	0.00	0.00	0.00	0.96
8.00	0.00	0.00	0.00	19.66	8.00	0.00	0.00	0.00	19.66
9.00	17.27	17.27	0.00	0.00	9.00	17.27	17.27	0.00	0.00
10.00	0.00	0.00	0.00	0.00	10.00	0.00	0.00	0.00	0.00
11.00	0.00	0.00	0.00	0.00	11.00	0.00	0.00	0.00	0.00
12.00	17.27	17.27	0.00	0.00	12.00	17.27	17.27	0.00	0.00
12.10	0.00	0.00	0.00	0.00	12.10	0.00	0.00	0.00	0.00
12.20	0.00	0.00	0.00	0.00	12.20	0.00	0.00	0.00	0.00
12.30	0.00	0.00	0.00	0.00	12.30	0.00	0.00	0.00	0.00
12.40	0.00	0.00	0.00	0.00	12.40	0.00	17.27	0.00	0.00
12.50	0.00	0.00	0.00	0.00	12.50	0.00	0.00	0.00	0.00
12.60	0.00	0.00	0.00	0.00	12.60	0.00	0.00	0.00	0.00
12.70	0.00	0.00	0.00	0.00	12.70	0.00	0.00	0.00	0.00
12.80	0.00	0.00	0.00	0.00	12.80	0.00	0.00	0.00	0.00
12.90	0.00	0.00	0.00	0.00	12.90	0.00	15.23	0.00	0.00
13.00	0.00	0.00	0.00	0.00	13.00	0.00	2.03	0.00	0.00

Scenario 7a, 7b - t_{80}

Scenario 7a - Diff.P 100/0					Scenario 7b - Diff.P 100/200				
Step	**F1**	**F2**	**F3**	**F4 = F5**	**Step**	**F1**	**F2**	**F3**	**F4 = F5**
0.00	0.00	0.00	0.00	0.00	0.00	0.00	0.00	0.00	0.00
1.00	0.00	0.00	0.00	0.00	1.00	0.00	0.00	0.00	0.00
2.00	0.00	0.00	0.00	0.00	2.00	0.00	0.00	0.00	0.00
3.00	0.00	0.00	0.00	0.00	3.00	0.00	0.00	0.00	0.00
4.00	34.53	34.53	0.00	0.00	4.00	34.53	34.53	0.00	0.00
5.00	34.53	34.53	0.00	19.34	5.00	34.53	34.53	0.00	19.34
6.00	34.53	34.53	0.00	39.00	6.00	34.53	34.53	0.00	39.00
7.00	34.53	34.53	0.00	39.00	7.00	34.53	34.53	0.00	39.00
8.00	51.80	51.80	0.00	39.00	8.00	51.80	51.80	0.00	39.00
9.00	51.80	51.80	0.00	39.00	9.00	51.80	51.80	0.00	39.00
10.00	51.80	51.80	0.00	39.00	10.00	51.80	51.80	0.00	39.00
11.00	17.27	17.27	0.00	0.00	11.00	17.27	17.27	0.00	0.00
12.00	34.53	34.53	0.00	16.45	12.00	34.53	34.53	0.00	16.45
12.10	0.00	34.53	0.00	7.97	12.10	0.00	0.00	0.00	0.00
12.20	0.00	34.53	0.00	7.97	12.20	0.00	0.00	0.00	0.00
12.30	0.00	34.53	0.00	7.47	12.30	0.00	0.00	0.00	0.00
12.40	0.00	34.53	0.00	7.47	12.40	0.00	17.27	0.00	0.00
12.50	0.00	34.53	17.00	7.47	12.50	0.00	51.80	17.00	19.00
12.60	0.00	34.53	0.00	7.47	12.60	0.00	17.27	0.00	0.00
12.70	0.00	34.53	0.00	7.47	12.70	0.00	17.27	0.00	0.00
12.80	0.00	34.53	0.00	7.97	12.80	0.00	17.27	0.00	0.00
12.90	0.00	34.53	0.00	7.97	12.90	0.00	32.50	0.00	0.00
13.00	34.53	34.53	0.00	16.45	13.00	34.53	34.53	0.00	16.45

Scenario 7a, 7b - t_{50}

Scenario 7a - Diff.P 100/0					Scenario 7b - Diff.P 100/200				
Step	**F1**	**F2**	**F3**	**F4 = F5**	**Step**	**F1**	**F2**	**F3**	**F4 = F5**
0.00	0.00	0.00	0.00	0.00	0.00	0.00	0.00	0.00	0.00
1.00	0.00	0.00	0.00	0.00	1.00	0.00	0.00	0.00	0.00
2.00	13.20	13.20	0.00	0.00	2.00	13.20	13.20	0.00	0.00
3.00	34.53	34.53	0.00	19.34	3.00	34.53	34.53	0.00	19.34
4.00	34.53	34.53	0.00	39.00	4.00	34.53	34.53	0.00	39.00
5.00	34.53	34.53	0.00	39.00	5.00	34.53	34.53	0.00	39.00
6.00	34.53	34.53	0.00	39.00	6.00	34.53	34.53	0.00	39.00
7.00	51.80	51.80	0.00	39.00	7.00	51.80	51.80	0.00	39.00
8.00	71.09	71.09	0.00	39.00	8.00	71.09	71.09	0.00	39.00
9.00	86.32	86.32	0.00	57.35	9.00	86.32	86.32	0.00	57.35
10.00	103.58	103.58	0.00	76.96	10.00	103.58	103.58	0.00	76.96
11.00	51.79	51.79	0.00	19.31	11.00	51.79	51.79	0.00	19.31
12.00	51.80	51.80	0.00	37.69	12.00	51.80	51.80	0.00	37.69
12.10	51.80	51.80	0.00	37.21	12.10	51.80	17.27	0.00	27.79
12.20	17.27	51.80	0.00	28.27	12.20	17.27	30.46	0.00	18.35
12.30	19.30	51.80	17.00	28.27	12.30	19.30	51.79	17.00	18.83
12.40	30.46	51.80	34.00	27.77	12.40	30.46	86.32	19.00	46.90
12.50	32.49	51.80	34.00	28.25	12.50	32.49	103.58	34.00	48.88
12.60	30.46	51.80	34.00	27.77	12.60	30.46	86.31	19.00	46.90
12.70	19.30	51.80	17.00	28.27	12.70	19.30	53.82	17.00	18.83
12.80	17.27	51.80	0.00	28.27	12.80	17.27	67.03	0.00	18.35
12.90	51.80	51.80	0.00	37.21	12.90	51.80	51.80	0.00	27.79
13.00	51.80	51.80	0.00	37.69	13.00	51.80	51.80	0.00	37.69

Scenario 8 - t_a

Scenario 8 - 04_MECH				
Step	**F1**	**F2**	**F3**	**F4 = F5**
0.00	0.00	0.00	0.00	0.00
1.00	0.00	0.00	0.00	0.00
2.00	0.00	0.00	0.00	0.00
3.00	0.00	0.00	0.00	0.00
4.00	2.03	2.03	0.00	0.00
5.00	15.23	15.23	0.00	0.00
6.00	17.27	17.27	0.00	18.38
7.00	0.00	0.00	0.00	0.96
8.00	0.00	0.00	0.00	19.66
9.00	17.27	17.27	0.00	0.00
10.00	0.00	0.00	0.00	0.00
11.00	0.00	0.00	0.00	0.00
12.00	17.27	17.27	0.00	0.00
12.10	0.00	0.00	0.00	0.00
12.20	0.00	0.00	0.00	0.00
12.30	0.00	0.00	0.00	0.00
12.40	0.00	0.00	0.00	0.00
12.50	0.00	0.00	0.00	0.00
12.60	0.00	0.00	0.00	0.00
12.70	0.00	0.00	0.00	0.00
12.80	0.00	0.00	0.00	0.00
12.90	0.00	0.00	0.00	0.00
13.00	0.00	0.00	0.00	0.00

Scenario 8 - t_{80}

Scenario 8 - 04_MECH				
Step	**F1**	**F2**	**F3**	**F4 = F5**
0.00	0.00	0.00	0.00	0.00
1.00	0.00	0.00	0.00	0.00
2.00	0.00	0.00	0.00	0.00
3.00	0.00	0.00	0.00	0.00
4.00	34.53	34.53	0.00	0.00
5.00	34.53	34.53	0.00	19.34
6.00	34.53	34.53	0.00	39.00
7.00	34.53	34.53	0.00	39.00
8.00	51.80	51.80	0.00	39.00
9.00	51.80	51.80	0.00	39.00
10.00	51.80	51.80	0.00	39.00
11.00	17.27	17.27	0.00	0.00
12.00	34.53	34.53	0.00	16.45
12.10	0.00	0.00	0.00	0.00
12.20	0.00	0.00	0.00	0.00
12.30	0.00	0.00	0.00	0.00
12.40	0.00	0.00	0.00	0.00
12.50	17.27	17.27	0.00	0.00
12.60	0.00	0.00	0.00	0.00
12.70	0.00	0.00	0.00	0.00
12.80	0.00	0.00	0.00	0.00
12.90	0.00	0.00	0.00	0.00
13.00	34.53	34.53	0.00	16.45

Scenario 8 - t_{50}

Scenario 8 - 04_MECH				
Step	**F1**	**F2**	**F3**	**F4 = F5**
0.00	0.00	0.00	0.00	0.00
1.00	0.00	0.00	0.00	0.00
2.00	13.20	13.20	0.00	0.00
3.00	34.53	34.53	0.00	19.34
4.00	34.53	34.53	0.00	39.00
5.00	34.53	34.53	0.00	39.00
6.00	34.53	34.53	0.00	39.00
7.00	51.80	51.80	0.00	39.00
8.00	71.09	71.09	0.00	39.00
9.00	86.32	86.32	0.00	57.35
10.00	103.58	103.58	0.00	76.96
11.00	51.79	51.79	0.00	19.31
12.00	51.80	51.80	0.00	37.69
12.10	34.53	34.53	0.00	33.83
12.20	19.30	19.30	0.00	18.35
12.30	32.49	32.49	0.00	18.35
12.40	51.79	51.79	0.00	19.31
12.50	69.06	69.06	0.00	76.96
12.60	51.79	51.79	0.00	19.31
12.70	32.49	32.49	0.00	18.35
12.80	19.30	19.30	0.00	18.35
12.90	34.53	34.53	0.00	33.83
13.00	51.80	51.80	0.00	37.69

Scenario 9 - t_a

Scenario 9 - 05_MECH				
Step	**F1**	**F2**	**F3**	**F4 = F5**
0.00	0.00	0.00	0.00	0.00
1.00	0.00	0.00	0.00	0.00
2.00	0.00	0.00	0.00	0.00
3.00	0.00	0.00	0.00	0.00
4.00	17.27	17.27	0.00	0.00
5.00	0.00	0.00	0.00	0.00
6.00	0.00	0.00	0.00	19.34
7.00	0.00	0.00	0.00	0.00
8.00	2.03	2.03	0.00	0.00
9.00	15.23	15.23	0.00	19.66
10.00	0.00	0.00	0.00	0.00
11.00	0.00	0.00	0.00	0.00
12.00	34.53	34.53	0.00	19.34
12.10	0.00	0.00	0.00	0.00
12.20	0.00	0.00	0.00	0.00
12.30	0.00	0.00	0.00	0.00
12.40	0.00	0.00	0.00	0.00
12.50	7.11	7.11	0.00	0.00
12.60	0.00	0.00	0.00	0.00
12.70	0.00	0.00	0.00	0.00
12.80	0.00	0.00	0.00	0.00
12.90	0.00	0.00	0.00	0.00
13.00	0.00	0.00	0.00	0.00

Scenario 9 - t_{80}

Scenario 9 - 05_MECH				
Step	**F1**	**F2**	**F3**	**F4 = F5**
0.00	0.00	0.00	0.00	0.00
1.00	0.00	0.00	0.00	0.00
2.00	0.00	0.00	0.00	0.00
3.00	17.27	17.27	0.00	0.00
4.00	17.27	17.27	0.00	0.00
5.00	17.27	17.27	0.00	19.34
6.00	19.30	19.30	0.00	19.34
7.00	34.53	34.53	0.00	39.00
8.00	34.53	34.53	0.00	39.00
9.00	44.69	44.69	0.00	39.00
10.00	51.80	51.80	0.00	39.00
11.00	17.27	17.27	0.00	0.00
12.00	34.53	34.53	0.00	19.34
12.10	0.00	0.00	0.00	0.00
12.20	0.00	0.00	0.00	0.00
12.30	0.00	0.00	0.00	0.00
12.40	9.14	9.14	0.00	0.00
12.50	15.23	15.23	0.00	0.00
12.60	0.00	0.00	0.00	0.00
12.70	0.00	0.00	0.00	0.00
12.80	0.00	0.00	0.00	0.00
12.90	0.00	0.00	0.00	0.00
13.00	17.27	17.27	0.00	19.34

Scenario 9 - t_{50}

Scenario 9 - 05_MECH				
Step	**F1**	**F2**	**F3**	**F4 = F5**
0.00	0.00	0.00	0.00	0.00
1.00	0.00	0.00	0.00	0.00
2.00	17.27	17.27	0.00	0.00
3.00	17.27	17.27	0.00	19.34
4.00	34.53	34.53	0.00	32.84
5.00	34.53	34.53	0.00	39.00
6.00	34.53	34.53	0.00	39.00
7.00	38.59	38.59	0.00	39.00
8.00	51.80	51.80	0.00	39.00
9.00	53.83	53.83	0.00	58.31
10.00	69.06	69.06	0.00	58.31
11.00	57.88	57.88	0.00	19.31
12.00	34.53	34.53	0.00	19.34
12.10	17.27	17.27	0.00	19.34
12.20	0.00	0.00	0.00	0.00
12.30	13.20	13.20	0.00	0.00
12.40	17.27	17.27	0.00	0.00
12.50	17.27	17.27	0.00	0.00
12.60	17.27	17.27	0.00	0.00
12.70	0.00	0.00	0.00	0.00
12.80	0.00	0.00	0.00	0.00
12.90	17.27	17.27	0.00	19.34
13.00	34.53	34.53	0.00	19.34

Scenario 10 - t_a

Scenario 10 - COMB_01				
Step	**F1**	**F2**	**F3**	**F4 = F5**
0.00	0.00	0.00	0.00	0.00
1.00	0.00	0.00	0.00	0.00
2.00	0.00	0.00	0.00	0.00
3.00	0.00	0.00	0.00	0.00
4.00	17.27	17.27	0.00	0.00
5.00	17.27	17.26	0.00	17.51
6.00	0.00	0.00	16.55	1.46
7.00	0.00	15.23	2.21	18.31
8.00	17.27	2.03	4.41	1.00
9.00	0.00	0.00	16.55	0.00
10.00	2.03	19.30	33.10	0.00
11.00	0.00	0.00	0.00	0.00
12.00	34.53	34.52	0.00	18.48
12.10	0.00	0.00	0.00	0.00
12.20	0.00	0.00	0.00	0.00
12.30	0.00	0.00	0.00	0.00
12.40	0.00	0.00	0.00	0.00
12.50	0.00	0.00	0.00	0.00
12.60	0.00	0.00	0.00	0.00
12.70	0.00	0.00	0.00	0.00
12.80	0.00	0.00	0.00	0.00
12.90	0.00	0.00	0.00	0.00
13.00	0.00	0.00	0.00	0.00

Scenario 10 - t_{80}

Scenario 10 - COMB_01				
Step	**F1**	**F2**	**F3**	**F4 = F5**
0.00	0.00	0.00	0.00	0.00
1.00	0.00	0.00	0.00	0.00
2.00	0.00	0.00	0.00	0.00
3.00	17.27	17.27	0.00	0.00
4.00	34.53	34.52	18.76	18.48
5.00	34.53	34.52	18.76	35.77
6.00	34.53	34.52	35.31	38.28
7.00	51.80	51.78	41.93	38.28
8.00	51.80	62.95	72.82	38.28
9.00	67.03	71.08	75.03	46.10
10.00	73.12	105.60	75.03	57.75
11.00	34.53	34.52	0.00	17.48
12.00	34.53	34.52	9.93	18.97
12.10	0.00	0.00	0.00	0.00
12.20	0.00	0.00	0.00	0.00
12.30	0.00	0.00	0.00	0.00
12.40	0.00	0.00	0.00	0.00
12.50	0.00	2.03	0.00	0.00
12.60	0.00	0.00	0.00	0.00
12.70	0.00	0.00	0.00	0.00
12.80	0.00	0.00	0.00	0.00
12.90	0.00	0.00	0.00	0.00
13.00	34.53	34.52	9.93	18.97

Scenario 10 - t_{50}

Scenario 10 - COMB_01				
Step	**F1**	**F2**	**F3**	**F4 = F5**
0.00	0.00	0.00	0.00	0.00
1.00	0.00	0.00	0.00	0.00
2.00	34.53	34.52	18.76	0.00
3.00	34.53	34.52	37.52	36.77
4.00	34.53	34.52	37.52	38.28
5.00	34.53	34.52	41.93	39.78
6.00	51.80	64.99	75.03	39.78
7.00	71.09	71.08	75.03	45.68
8.00	88.35	99.52	77.24	60.31
9.00	114.75	120.84	89.37	93.63
10.00	120.84	120.84	114.75	98.07
11.00	101.54	103.58	45.24	45.05
12.00	53.83	69.05	41.93	58.82
12.10	64.99	69.05	23.17	46.73
12.20	36.55	34.52	20.96	28.79
12.30	51.78	34.52	20.96	29.28
12.40	51.78	36.56	37.51	33.76
12.50	69.05	64.99	45.24	36.27
12.60	51.78	36.56	37.51	33.76
12.70	51.78	34.52	20.96	29.28
12.80	36.55	34.52	20.96	28.79
12.90	64.99	69.05	23.17	46.73
13.00	53.83	69.05	41.93	58.82

Scenario 11 - t_a

Scenario 11 - COMB_02				
Step	**F1**	**F2**	**F3**	**F4 = F5**
0.00	0.00	0.00	0.00	0.00
1.00	0.00	0.00	0.00	0.00
2.00	0.00	0.00	0.00	0.00
3.00	17.27	17.27	0.00	0.00
4.00	0.00	0.00	0.00	18.97
5.00	2.03	17.26	20.96	0.00
6.00	15.23	0.00	16.55	19.31
7.00	17.27	17.26	2.21	0.00
8.00	0.00	2.03	18.76	1.99
9.00	2.03	4.06	0.00	16.47
10.00	15.23	28.44	2.21	2.00
11.00	0.00	0.00	0.00	0.00
12.00	12.19	17.26	18.76	1.93
12.10	0.00	0.00	0.00	0.00
12.20	0.00	0.00	0.00	0.00
12.30	9.14	0.00	0.00	0.00
12.40	8.13	0.00	0.00	0.00
12.50	0.00	0.00	0.00	0.00
12.60	0.00	0.00	0.00	0.00
12.70	0.00	0.00	0.00	0.00
12.80	0.00	0.00	0.00	0.00
12.90	11.17	0.00	0.00	0.00
13.00	23.36	17.27	18.76	0.00

Scenario 11 - t_{80}

Scenario 11 - COMB_02				
Step	**F1**	**F2**	**F3**	**F4 = F5**
0.00	0.00	0.00	0.00	0.00
1.00	0.00	0.00	0.00	0.00
2.00	17.27	17.27	0.00	0.00
3.00	17.27	17.27	0.00	9.23
4.00	27.42	34.52	37.52	18.97
5.00	34.53	34.52	37.52	38.28
6.00	40.63	51.78	41.93	38.28
7.00	51.80	51.78	58.48	38.28
8.00	55.86	63.97	62.89	57.24
9.00	69.06	86.31	77.24	63.94
10.00	75.15	86.31	104.82	89.74
11.00	45.70	60.94	18.76	38.68
12.00	34.53	41.63	29.79	36.77
12.10	0.00	0.00	11.03	0.00
12.20	0.00	0.00	11.03	0.00
12.30	15.23	0.00	15.45	0.00
12.40	17.27	0.00	18.76	0.00
12.50	30.47	17.27	18.76	20.73
12.60	0.00	0.00	18.76	0.00
12.70	0.00	0.00	13.24	0.00
12.80	0.00	0.00	11.03	0.00
12.90	17.27	0.00	15.45	0.00
13.00	34.53	34.52	29.79	36.77

Scenario 11 - t_{50}

Scenario 11 - COMB_02				
Step	**F1**	**F2**	**F3**	**F4 = F5**
0.00	0.00	0.00	0.00	0.00
1.00	0.00	0.00	0.00	0.00
2.00	17.27	34.52	18.76	18.97
3.00	34.53	34.52	37.52	38.28
4.00	34.53	34.52	39.72	38.78
5.00	51.80	51.78	75.03	39.78
6.00	53.83	57.88	93.79	51.06
7.00	69.06	86.31	112.55	61.24
8.00	86.32	86.31	112.55	98.08
9.00	88.35	89.36	114.75	100.57
10.00	92.41	99.52	116.96	110.14
11.00	86.32	86.32	37.51	76.25
12.00	51.80	69.05	112.55	57.61
12.10	28.44	68.03	72.82	44.03
12.20	13.20	30.46	41.93	22.46
12.30	25.39	18.28	37.51	19.34
12.40	39.60	18.28	37.51	35.34
12.50	49.76	34.52	37.51	39.78
12.60	39.60	16.25	37.51	36.37
12.70	15.23	20.31	37.51	19.34
12.80	4.06	22.34	41.93	21.93
12.90	34.53	43.67	60.69	40.09
13.00	34.53	69.05	112.55	57.61

Scenario 12 - t_a

Scenario 12 - COMB_04				
Step	**F1**	**F2**	**F3**	**F4 = F5**
0.00	0.00	0.00	0.00	0.00
1.00	0.00	0.00	0.00	0.00
2.00	0.00	0.00	0.00	0.00
3.00	12.19	17.27	0.00	0.00
4.00	5.08	0.00	0.00	0.00
5.00	0.00	0.00	0.00	18.49
6.00	0.00	0.00	4.41	0.48
7.00	2.03	17.26	14.34	0.00
8.00	17.27	17.26	4.41	11.31
9.00	15.23	0.00	2.21	8.00
10.00	0.00	2.03	30.89	10.78
11.00	0.00	0.00	0.00	0.00
12.00	34.53	32.49	3.31	17.88
12.10	0.00	0.00	0.00	0.00
12.20	0.00	0.00	0.00	0.00
12.30	0.00	0.00	0.00	0.00
12.40	11.17	0.00	0.00	0.00
12.50	6.09	0.00	0.00	0.00
12.60	0.00	0.00	0.00	0.00
12.70	0.00	0.00	0.00	0.00
12.80	0.00	0.00	0.00	0.00
12.90	0.00	0.00	0.00	0.00
13.00	21.33	17.27	2.21	0.00

Scenario 12 - t_{80}

Scenario 12 - COMB_04				
Step	**F1**	**F2**	**F3**	**F4 = F5**
0.00	0.00	0.00	0.00	0.00
1.00	0.00	0.00	0.00	0.00
2.00	0.00	0.00	0.00	0.00
3.00	17.27	17.27	0.00	0.00
4.00	17.27	17.27	0.00	18.02
5.00	17.27	19.30	18.76	18.97
6.00	34.53	34.52	37.52	29.76
7.00	36.56	42.65	41.93	38.28
8.00	51.80	51.78	56.27	38.28
9.00	51.80	53.81	58.48	50.04
10.00	53.83	59.91	62.89	57.21
11.00	34.53	35.54	0.00	34.54
12.00	34.53	34.52	18.76	18.97
12.10	0.00	0.00	0.00	0.00
12.20	0.00	0.00	0.00	0.00
12.30	11.17	0.00	0.00	0.00
12.40	17.27	0.00	0.00	0.00
12.50	17.27	0.00	0.00	0.00
12.60	0.00	0.00	0.00	0.00
12.70	0.00	0.00	0.00	0.00
12.80	0.00	0.00	0.00	0.00
12.90	0.00	0.00	0.00	0.00
13.00	34.53	34.52	18.76	13.12

Scenario 12 - t_{50}

Scenario 12 - COMB_04				
Step	**F1**	**F2**	**F3**	**F4 = F5**
0.00	0.00	0.00	0.00	0.00
1.00	0.00	0.00	0.00	0.00
2.00	17.27	17.27	0.00	0.00
3.00	17.27	34.52	37.52	18.97
4.00	34.53	34.52	37.52	38.28
5.00	34.53	34.52	41.93	38.78
6.00	40.63	51.78	77.24	39.28
7.00	51.80	53.81	75.03	42.25
8.00	55.86	69.05	75.03	58.74
9.00	69.06	69.05	77.24	63.21
10.00	71.09	74.13	77.24	85.55
11.00	51.79	69.06	18.76	43.37
12.00	34.53	49.76	39.72	18.97
12.10	19.30	47.73	20.96	14.60
12.20	13.20	2.03	0.00	0.00
12.30	21.33	6.09	0.00	0.00
12.40	21.33	8.13	16.55	0.00
12.50	28.44	27.42	18.76	17.52
12.60	21.33	8.13	16.55	0.00
12.70	4.06	6.09	0.00	0.00
12.80	4.06	9.14	0.00	0.00
12.90	30.47	45.70	20.96	1.94
13.00	34.53	45.70	23.17	18.97

Scenario 13 - t_a

Scenario 13 - COMB_05				
Step	**F1**	**F2**	**F3**	**F4 = F5**
0.00	0.00	0.00	0.00	0.00
1.00	0.00	0.00	0.00	0.00
2.00	0.00	0.00	0.00	0.00
3.00	0.00	0.00	0.00	0.00
4.00	0.00	2.03	0.00	0.00
5.00	17.27	15.23	0.00	0.00
6.00	2.03	17.26	0.00	0.00
7.00	15.23	0.00	2.21	18.48
8.00	0.00	0.00	16.55	10.30
9.00	0.00	0.00	2.21	7.00
10.00	15.23	17.26	2.21	2.50
11.00	0.00	0.00	0.00	0.00
12.00	17.27	17.27	0.00	0.00
12.10	0.00	0.00	0.00	0.00
12.20	0.00	0.00	0.00	0.00
12.30	0.00	0.00	0.00	0.00
12.40	0.00	0.00	0.00	0.00
12.50	0.00	0.00	0.00	0.00
12.60	0.00	0.00	0.00	0.00
12.70	0.00	0.00	0.00	0.00
12.80	0.00	0.00	0.00	0.00
12.90	0.00	0.00	0.00	0.00
13.00	0.00	0.00	0.00	0.00

Scenario 13 - t_{80}

Scenario 13 - COMB_05				
Step	**F1**	**F2**	**F3**	**F4 = F5**
0.00	0.00	0.00	0.00	0.00
1.00	0.00	0.00	0.00	0.00
2.00	0.00	0.00	0.00	0.00
3.00	0.00	0.00	0.00	0.00
4.00	17.27	17.27	0.00	0.00
5.00	34.53	34.52	2.21	0.00
6.00	34.53	34.52	18.76	21.06
7.00	34.53	34.52	20.96	37.28
8.00	34.53	34.52	39.72	38.28
9.00	44.69	51.78	41.93	38.28
10.00	51.80	51.78	41.93	38.28
11.00	17.27	17.26	0.00	0.00
12.00	17.27	19.30	0.00	0.00
12.10	0.00	0.00	0.00	0.00
12.20	0.00	0.00	0.00	0.00
12.30	0.00	0.00	0.00	0.00
12.40	0.00	0.00	0.00	0.00
12.50	0.00	0.00	0.00	0.00
12.60	0.00	0.00	0.00	0.00
12.70	0.00	0.00	0.00	0.00
12.80	0.00	0.00	0.00	0.00
12.90	0.00	0.00	0.00	0.00
13.00	17.27	19.30	0.00	0.00

Scenario 13 - t_{50}

Scenario 13 - COMB_05				
Step	**F1**	**F2**	**F3**	**F4 = F5**
0.00	0.00	0.00	0.00	0.00
1.00	0.00	0.00	0.00	0.00
2.00	0.00	0.00	0.00	0.00
3.00	34.53	34.52	18.76	0.00
4.00	34.53	34.52	37.52	36.28
5.00	34.53	34.52	37.52	38.28
6.00	34.53	34.52	39.72	38.28
7.00	34.53	36.55	41.93	39.78
8.00	51.80	71.08	75.03	40.28
9.00	62.97	73.11	75.03	40.28
10.00	88.35	103.58	77.24	51.66
11.00	23.36	53.82	35.31	0.00
12.00	49.77	51.79	2.21	18.48
12.10	32.50	45.70	0.00	0.00
12.20	32.50	19.30	0.00	0.00
12.30	17.26	17.27	0.00	0.00
12.40	17.26	19.30	18.76	0.00
12.50	19.30	19.30	35.31	0.00
12.60	17.26	19.30	18.76	0.00
12.70	17.26	17.27	0.00	0.00
12.80	32.50	19.30	0.00	0.00
12.90	32.50	45.70	0.00	0.00
13.00	49.77	51.79	2.21	18.48

Scenario 14 - t_a

Scenario 14 - COMB_06				
Step	**F1**	**F2**	**F3**	**F4 = F5**
0.00	0.00	0.00	0.00	0.00
1.00	0.00	0.00	0.00	0.00
2.00	0.00	0.00	0.00	0.00
3.00	0.00	0.00	0.00	0.00
4.00	17.27	17.27	0.00	0.00
5.00	0.00	0.00	0.00	2.96
6.00	0.00	17.26	13.24	16.01
7.00	4.06	0.00	24.27	9.81
8.00	13.20	0.00	0.00	9.50
9.00	0.00	0.00	2.21	0.00
10.00	0.00	0.00	2.21	0.00
11.00	0.00	0.00	0.00	0.00
12.00	34.53	34.52	2.21	18.97
12.10	0.00	0.00	0.00	0.00
12.20	0.00	0.00	0.00	0.00
12.30	0.00	0.00	0.00	0.00
12.40	0.00	0.00	0.00	0.00
12.50	0.00	0.00	0.00	0.00
12.60	0.00	0.00	0.00	0.00
12.70	0.00	0.00	0.00	0.00
12.80	0.00	0.00	0.00	0.00
12.90	0.00	0.00	0.00	0.00
13.00	4.06	6.09	2.21	0.00

Scenario 14 - t_{80}

Scenario 14 - COMB_06				
Step	**F1**	**F2**	**F3**	**F4 = F5**
0.00	0.00	0.00	0.00	0.00
1.00	0.00	0.00	0.00	0.00
2.00	0.00	0.00	0.00	0.00
3.00	17.27	17.27	0.00	0.00
4.00	17.27	17.27	0.00	0.96
5.00	17.27	34.52	37.52	18.97
6.00	34.53	34.52	37.52	35.78
7.00	34.53	34.52	37.52	38.28
8.00	34.53	34.52	39.72	38.28
9.00	34.53	36.56	41.93	38.28
10.00	36.56	40.62	60.69	38.78
11.00	2.03	2.03	0.00	0.00
12.00	34.53	34.52	18.76	18.97
12.10	0.00	0.00	0.00	0.00
12.20	0.00	0.00	0.00	0.00
12.30	0.00	0.00	0.00	0.00
12.40	0.00	0.00	0.00	0.00
12.50	1.02	0.00	0.00	0.00
12.60	0.00	0.00	0.00	0.00
12.70	0.00	0.00	0.00	0.00
12.80	0.00	0.00	0.00	0.00
12.90	0.00	0.00	0.00	0.00
13.00	21.33	34.52	18.76	18.97

Scenario 14 - t_{50}

Scenario 14 - COMB_06				
Step	**F1**	**F2**	**F3**	**F4 = F5**
0.00	0.00	0.00	0.00	0.00
1.00	0.00	0.00	0.00	0.00
2.00	17.27	17.27	18.76	0.00
3.00	17.27	34.52	37.52	18.97
4.00	34.53	34.52	37.52	38.28
5.00	34.53	34.52	37.52	38.28
6.00	34.53	34.52	41.93	38.78
7.00	36.56	36.56	60.69	40.28
8.00	50.78	55.85	81.65	40.28
9.00	57.88	66.00	107.03	61.62
10.00	69.06	91.39	112.55	82.80
11.00	50.77	83.27	37.51	21.99
12.00	36.56	49.76	56.27	27.25
12.10	21.33	41.63	39.72	18.97
12.20	4.06	4.06	29.79	0.97
12.30	4.06	6.09	37.51	0.00
12.40	19.29	8.13	37.51	0.53
12.50	25.39	10.16	37.51	1.58
12.60	13.20	8.13	37.51	0.53
12.70	4.06	6.09	37.51	0.00
12.80	6.09	6.09	32.00	0.00
12.90	23.36	38.59	39.72	18.97
13.00	36.56	38.59	37.52	26.74